





L



This is to certify that the  
thesis entitled  
HYDROGEN ATOM GENERATION AND ENERGY BALANCE--  
LITERATURE REVIEW, MODELING, AND  
EXPERIMENTAL APPARATUS DESIGN  
presented by

Reed Winston Snellenberger

has been accepted towards fulfillment  
of the requirements for

Master's degree in Chemical Engineering

*Martin C. Hawley*  
Major professor

Date November, 14, 1980



OVERDUE FINES:  
25¢ per day per item

RETURNING LIBRARY MATERIALS:  
Place in book return to remove  
charge from circulation records

OCT 06 1996

---

---

**HYDROGEN ATOM GENERATION AND ENERGY BALANCE--  
LITERATURE REVIEW, MODELING, AND  
EXPERIMENTAL APPARATUS DESIGN**

**By**

**Reed Winston Snellenberger**

**A THESIS**

**Submitted to  
Michigan State University  
in partial fulfillment of the requirements  
for the degree of**

**MASTER OF SCIENCE**

**Department of Chemical Engineering**

**1980**

## ABSTRACT

### HYDROGEN ATOM GENERATION AND ENERGY BALANCE-- LITERATURE REVIEW, MODELING, AND EXPERIMENTAL APPARATUS DESIGN

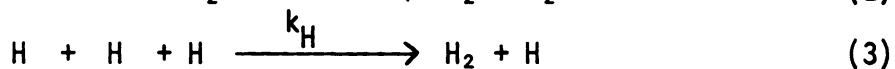
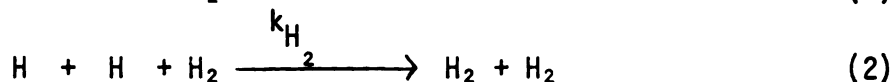
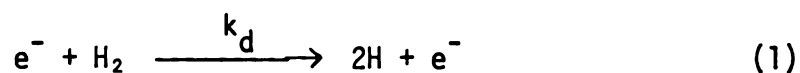
By

Reed Winston Snellenberger

An experimental apparatus was designed to measure the energy balance around a system for the conversion of molecular hydrogen to atoms. A prerequisite for the use of atomic hydrogen in any practical application, such as spacecraft propulsion or large-scale chemical synthesis, is the development of an energy-efficient method for generating the atoms. The design of a hydrogen atom generation system requires basic data on the energy requirements and conversion versus the reaction parameters. These data have not been reported in the literature on hydrogen atom generation for any of the photolysis, thermal dissociation, or electron-impact dissociation techniques for hydrogen atom generation. A microwave plasma system was selected as a promising, energy-efficient method for the generation of hydrogen atoms because of the high conversions reported in the literature, and because of the expected coupling efficiency between the source and the gas. Results of the literature survey of hydrogen atom generation and detection techniques were used for modeling and design of an experimental system to be used for energy balance and kinetics studies of hydrogen atom generation.

The apparatus is composed of: (a) a microwave discharge hydrogen atom generator enclosed in a calorimeter, (b) electron spin resonance (esr) spectrometer and gas-phase titration detection systems, and (c) a spectrometer for measurements of electron temperature and density using the Stark broadening of the  $H_{\beta}$  emission line. The microwave discharge technique was chosen instead of the direct photolysis, mercury photosensitization, electron pulse radiolysis, shock tube, hot tungsten filament, direct-current discharge, and radio-frequency discharge techniques on the basis of its demonstrated ability to achieve outlet conversion greater than 10% in pure hydrogen at pressures above 5 torr. Esr spectroscopy, a non-destructive hydrogen atom detection technique, and gas-phase titration, a destructive technique, were chosen for their relative ease of calibration and species-specificity. The Lyman- $\alpha$  photometric technique is a non-destructive alternative which would have to be calibrated against one of the other two techniques.

Preliminary modeling of the apparatus was used to determine the hydrogen atom concentration versus operating conditions in the discharge and downstream regions to insure that measureable quantities of hydrogen atoms could be expected to exist at distances downstream from the plasma sufficient for locating measurement equipment, and to determine the sensitivities of the apparatus to variations in the experimental parameters. The discharge was modeled as a continuously-stirred tank reactor, using the reactions



The most important parameters in the discharge were found to be the pressure, wall recombination coefficient, and the electron density. The discharge model also showed that there is a pressure-dependent electron density threshold, below which the conversion is negligible. For example, at a pressure of 1.0 torr, the conversion increases rapidly from 20% to 90% as the electron density changes from  $10^{11}$  to  $10^{12} \text{ cm}^{-3}$ . This indicates a need for accurate measurements of the electron density in hydrogen discharge experiments.

The downstream region was modeled as an isothermal, plus-flow reactor, using only reactions (2)-(4) since there is no electron-impact dissociation. The most important parameter in the downstream region, at the low pressures (<5.0 torr) under which kinetics studies are usually carried out, was found to be the wall recombination coefficient. The model demonstrated that hydrogen atoms could be transported for distances of ten meters or more when the wall recombination coefficient was reduced below  $10^{-4}$ .

Experimental and theoretical studies on wall recombination and hydrogen-atom-stabilized gas-phase recombination are recommended because of the lack of reliable data. In addition, development of a discharge model to correctly predict electron density is recommended.

**To Shirley**

## ACKNOWLEDGMENTS

The author gratefully acknowledges the National Aeronautics and Space Administration and the Michigan State University Division of Engineering Research for financial support.

Appreciation is extended to Dr. M. C. Hawley for his support and guidance during the course of this research. Appreciation is also extended to Dr. R. Kerber and Dr. J. Asmussen for many useful discussions.

The patience and understanding of the author's wife, Shirley, is sincerely appreciated, and her assistance in preparation of figures is gratefully acknowledged.

## TABLE OF CONTENTS

LIST OF FIGURES . . . . .	vi
LIST OF TABLES . . . . .	ix
INTRODUCTION . . . . .	1
HYDROGEN ATOM GENERATION METHODS . . . . .	6
Thermodynamics and Reactions . . . . .	9
Photolysis and Electron Pulse Radiolysis . . . . .	19
Thermal Dissociation . . . . .	24
Direct-current Discharge . . . . .	27
Alternating-current Discharges . . . . .	31
Summary--Generation . . . . .	37
METHODS OF HYDROGEN ATOM DETECTION . . . . .	41
Molecular Diffusion . . . . .	43
Catalytic Probe . . . . .	45
Mass Spectrometry . . . . .	47
Lyman- $\alpha$ Photometry . . . . .	49
Titration . . . . .	54
Magnetic Resonance . . . . .	56
Summary--Detection . . . . .	59

KINETIC AND DISCHARGE PARAMETERS . . . . .	63
Gas Phase Recombination . . . . .	63
Wall Recombination . . . . .	71
Discharge Parameters . . . . .	78
MODELING THE MICROWAVE DISCHARGE . . . . .	88
Rationale . . . . .	88
Development of the Discharge Model Equation . . . . .	93
Results of the Discharge Modeling . . . . .	99
MODELING THE DOWNSTREAM REGION . . . . .	121
Rationale and Model Development . . . . .	121
Results of the Downstream Region Modeling . . . . .	126
APPARATUS DESIGN . . . . .	135
Energy Balance Experiment . . . . .	137
Wall Recombination Experiment . . . . .	142
Conclusion . . . . .	144
RESULTS AND CONCLUSIONS . . . . .	145
RECOMMENDATIONS FOR RESEARCH . . . . .	151
APPENDICES	
Appendix A. The computer program used to model the discharge . . . . .	152
Appendix B. The computer program used to model the downstream region. . . . .	155
BIBLIOGRAPHY . . . . .	158

## LIST OF FIGURES

Figure	Page
1. Temperature dependence of equilibrium dissociation at one atmosphere for Br <sub>2</sub> , Cl <sub>2</sub> , O <sub>2</sub> , H <sub>2</sub> , and N <sub>2</sub> . . . .	11
2. Temperature and pressure dependence of equilibrium dissociation for H <sub>2</sub> . . . . .	12
3. Molecular energy diagram for hydrogen . . . . .	13
4. Conceptual diagram for the photolysis methods . . . . .	20
5. Conceptual diagram for thermal dissociation methods . . . . .	25
6. Conceptual diagram of the d.c. discharge dissociation method . . . . .	29
7. Conceptual diagram of the a.c. discharge dissociation methods . . . . .	34
8. Absorption of ultraviolet light by O <sub>2</sub> in the vicinity of the H <sub>2</sub> Lyman-α emission line . . . . .	52
9. Gas-phase recombination of hydrogen atoms: Theoretical rate coefficients for H + H + M → H <sub>2</sub> + M for M = H, Ar, He, and H <sub>2</sub> . . . . .	72
10. Theoretical and experimental values of the wall recombination coefficient . . . . .	79
11. Dependence of electron-impact dissociation rate constant on electron energy . . . . .	81
12. Relationship between discharge parameters E <sub>e</sub> /p and pλ . . . . .	83
13. Comparison of theoretical and experimental electron density as a function of microwave power input . . . . .	86
14. Pressure and flow rate dependence of discharge conversion for γ = 0.1 . . . . .	101
15. Pressure and flow rate dependence of discharge conversion for γ = 10 <sup>-3</sup> . . . . .	102

Figure	Page
16. Pressure and flow rate dependence of discharge conversion for $\gamma = 10^{-6}$ . . . . .	103
17. Dependence of conversion on discharge temperature for pressure of 5.0 torr . . . . .	105
18. Dependence of conversion on discharge temperature for pressure of 20.0 torr . . . . .	106
19. Discharge conversion dependence on wall recombination coefficient at 1.0 torr . . . . .	108
20. Discharge conversion dependence on wall recombination coefficient at 10.0 torr . . . . .	109
21. Discharge conversion dependence on wall recombination coefficient at 20.0 torr . . . . .	110
22. Effects of increasing discharge tube diameter on discharge conversion at 0.5 torr . . . . .	111
23. Effects of increasing discharge tube diameter on discharge conversion at 1.0 torr . . . . .	112
24. Effects of increasing discharge tube diameter on discharge conversion at 10.0 torr . . . . .	113
25. Dependence of discharge conversion on microwave power input using theoretical relations of Bell (12) at 0.5 torr . . . . .	115
26. Dependence of discharge conversion on microwave power input using theoretical relations of Bell (12) at 1.0 torr . . . . .	116
27. Dependence of discharge conversion on microwave power input using theoretical relations of Bell (12) at 10.0 torr . . . . .	117
28. Dependence of the discharge conversion on electron density . . . . .	119
29. Effects on the downstream quenching distance of changing the threshold concentration . . . . .	127
30. Temperature dependence of the downstream quenching distance at two pressures . . . . .	129

Figure	Page
31. Pressure dependence of the downstream quenching distance . . . . .	130
32. Effects of varying tube diameter on quenching distance at pressures of 0.5 and 5.0 torr . . . .	131
33. Dependence of quenching distance on the wall recombination coefficient, $\gamma$ . . . . .	133
34. Diagram of the proposed experimental apparatus . . . .	136

## LIST OF TABLES

Table	Page
1. Results of hydrogen radical generation experiments . . .	32
2. $Q_{at}$ values for O, N, and H for several $O_2$ lines . . .	60
3. Hydrogen gas-phase recombination rate coefficients . . .	65
4. Hydrogen atom recombination coefficients: $M = H$ . . .	67
5. Cross-sections for collision of $MH^*$ with H atoms for $M = H_2$ . . . . .	70
6. Hydrogen atom wall recombination coefficients . . .	74
7. Reactions and rate expressions to be used in the discharge model . . . . .	95
8. Experimental parameters used in the discharge model . .	98
9. Experimental parameters used in the downstream region model . . . . .	125

## INTRODUCTION

Research into the chemistry of hydrogen atoms has been going on for nearly 80 years. During that time, many techniques have been used to generate the hydrogen atoms needed in such research. These techniques have generally been developed to meet the needs of the laboratory experiments, and no attempt has been made to make them efficient in terms of energy use. In any large-scale application of hydrogen atoms, however, the efficiency of generation is of great importance, and any device would need to be optimized with respect to that efficiency. The critical experiment for optimizing the efficiency of an atom generation device is measurement of the energy balance around the device. It is the objective of this research to develop an apparatus in which the energy balance around a microwave discharge can be measured.

The complete lack of previous research in this area is a major motivation for wanting to do this type of experiment. The only previous attempt to measure energy efficiencies in a discharge is by Poole (76-78), who, in 1937, measured the energy efficiency of a d.c. electrical discharge. He did this by comparing the power consumed by the discharge to the quantity of hydrogen atoms produced, measured by a catalytic probe detector. Although this was an important effort, it suffered from several flaws. Poole made no attempt to perform a complete energy balance around the discharge, and neglected

such energy loss mechanisms as radiated light, recombination on the walls of the discharge tube, and heat losses to the outside environment from the discharge tube. Poole also made the then-common mistake of saturating the feed hydrogen with water to increase the production of hydrogen atoms, a practice which has been criticized (79) and ultimately abandoned.

Another important motivation for measuring energy balances around hydrogen atom generation methods is the need for such information when designing a large-scale application of the technology. Any industrial use of hydrogen atom chemistry, for example, would be dependent on the energy requirements of the generation method for the purpose of economic analysis. Also, the information gained in such an experiment could be useful for increasing the scale of the generator.

Another application in which hydrogen atoms could be used, and the one which originally prompted this research, is in the field of spacecraft propulsion. The recombination of hydrogen atoms to give molecular hydrogen is a very exothermic reaction, yielding 51.6 kcal for every gram of reactant (propellant). In contrast, the combustion of hydrogen and oxygen (a propellant combination used in some of the Apollo boosters) only produces 3.2 kcal per gram of propellant. Although the difference in energies implies that a recombination engine would be superior to the  $H_2/O_2$  engine, the values themselves are obtained under the assumption that the atomic hydrogen has already been generated. It is in generating the atoms that the energy-efficiency is most important, particularly since the size

(weight) of the energy storage/generation devices would be limited in a spacecraft.

The design of the proposed experimental apparatus was formulated in three steps. First, the atomic hydrogen literature was reviewed to determine the most suitable techniques for atom generation and detection. A microwave discharge was chosen as the atom generator, primarily because of the availability of high power microwave devices (which allow operation at pressures in the range of 10-100 torr) and because of the high conversions (>90%) which have been reported in the literature (84). Both gas-phase titration and electron spin resonance (esr) spectroscopy were chosen to be the atomic hydrogen detection methods, primarily because of their shared properties of species-specificity (which will make it possible to measure atom concentrations in complex gas mixtures in later experiments) and the ease with which they can be calibrated.

The second step in the development of the apparatus consisted of some simple modeling of the microwave discharge and the region downstream from the discharge. This modeling was preceded by a review of the literature on hydrogen atom dissociation (by electron impact) and recombination. This review provided the kinetic rate coefficients subsequently used in the models.

The discharge model, a constant volume reactor with uniform temperature and concentrations, was used to determine which experimental parameters (electron density, pressure, tube diameter, etc.) were the most important in determining the conversion of molecules

to atoms in the discharge. It was found that there was a pressure-dependent, threshold-like dependence of the conversion on the electron density, indicating that any modeling of experimental discharges would require an experimental measurement of the electron density to be accurate. It was also found that decreasing the wall recombination coefficient (the fraction of atoms striking the wall which recombine) to  $10^{-3}$  would be sufficient to nearly eliminate wall recombination, except possibly at low pressures.

The purpose of the plug-flow reactor model used in the downstream region was to determine how the experimental parameters could affect the distance downstream from the discharge in which the atom concentrations would remain measurable. This model showed that the most important factor in determining this downstream distance (called the quenching distance) was the wall recombination coefficient. Although a coefficient of 0.1 was found to quench the atom concentration within a few centimeters of the discharge, decreasing the coefficient to  $10^{-4}$  made the quenching distance effectively infinite.

The third, and final, step in the design of the hydrogen discharge apparatus was the incorporation of the hydrogen atom generator (microwave discharge) and detectors (esr spectrometer and titration) determined in step one, along with the modeling results from step two, into an overall design for the experimental apparatus. This also required the specification of all components of the apparatus which were necessary to perform the planned experiments.

The experiment for which this apparatus was designed, the energy-balance experiment, requires the measurement of all energy inputs to

and losses from the discharge. This is made possible in the present design by surrounding the discharge with a calorimeter housing which converts difficult-to-measure losses like microwave radiation leakage and light emission into heat, which can be measured using strategically placed thermocouples. Another addition to the apparatus is a monochromator system for the purpose of measuring electron densities in the discharge, using the Stark line-broadening of the atom hydrogen Balmer- $\beta$  emission (36).

Once the generation and detection devices are in place, the apparatus can also be used in several other experiments for measuring the kinetics of hydrogen atom reactions. As an example of this, an additional experiment is suggested in which the wall recombination coefficient can be measured over a wide range of temperatures. The primary change in the apparatus which this experiment requires is the addition of a jacketed section of tubing in the downstream region in which the recombination occurs. The wall recombination coefficient is determined from the difference in atom concentration at the entrance and exit of the jacketed section.

## HYDROGEN ATOM GENERATION METHODS

The history of research into the chemistry of hydrogen atoms dates back to the early part of the century. The first generation method was the d.c. glow discharge, in which Kirkby (46) observed that the amount of "chemical action" was proportional to the distance between the electrodes and postulated that "swiftly moving ions dissociate the gas molecules, which are then able to combine to form water." The species actually responsible for dissociation in glow discharges are electrons which have been accelerated in the electric field to a velocity which is high enough that, when an electron collides with a molecule of hydrogen, enough energy can be transferred from the electron to the hydrogen to cause the molecule to dissociate.

The next dissociation method to be used experimentally was thermal dissociation on a hot tungsten filament. This phenomenon was first observed in 1912 by Langmuir (50), who was studying the thermal properties of gases. Although the energy losses from a wire suspended in nitrogen, air, carbon dioxide, or mercury vapor could be predicted theoretically, the energy loss from a wire heated to 3300 °K in hydrogen was four to five times the expected value. That energy was expended to dissociate the hydrogen molecules which adsorb on the hot metal surface. When the atoms which had been formed desorbed from

the surface, the dissociated atoms would remain apart, and the net result was the dissociation of the hydrogen on the surface.

Mercury photosensitization was the next hydrogen atom generation method to be developed. Beginning in 1924 with an article by Duffendack and Compton (31), this technique immediately saw a great deal of use, principally in experiments studying the kinetics of hydrogen atom addition reactions (11, 25-6, 29, 60-1, 71, 74, 93-4, 119). In this technique, the energy of an excited atom of mercury is transferred to the hydrogen molecule during a collision. Because the energy available (4.89 electron volts) is very similar to that which is required to dissociate hydrogen in its ground electronic state (~4.5 electron volts), the result is an efficient transfer of energy from the mercury excitation source to the hydrogen molecules, followed by dissociation.

These three methods remained the only hydrogen atom generation techniques for approximately the next 30 years (1924-1954). The greatest amount of research occurred during the 1930s, when Amdur and his co-workers (2, 4, 5) studied the reactions of hydrogen produced in a d.c. discharge, and Poole (76-8) measured the efficiencies of hydrogen atom production. Additional work was done by Smith in 1943 (89), when he studied the recombination rates of hydrogen on several different surfaces.

The 1950s and 1960s saw the development of two new generation techniques using alternating-current electrical fields to dissociate the hydrogen molecules. The oldest of these two methods was the radio-frequency discharge, which had first been used in 1922 (41).

Although this technique was used quite frequently during the 1960s (21-4, 43), it apparently never quite caught on, probably because of the appearance during the same time-period of the microwave discharge apparatus.

The most recent atom generation method is the microwave discharge. It was first used in 1954 by McCarthy (63) to dissociate several gases, including oxygen, nitrogen, and hydrogen. The necessity for using modified radar transmitters as microwave radiation sources during the first years of development apparently slowed the acceptance of the technique, but the commercial availability of both low power devices (in the form of therapeutic diathermy devices) and high power devices (microwave ovens with power outputs of up to 1500 watts) has made this technique since 1960 the most commonly used method for generating hydrogen atoms.

The objective of this literature survey was to select from amongst the various generation methods the one method which could be developed into the most efficient hydrogen atom generator. This generator could then be used as the basis for any application of hydrogen atom chemistry, either to industrial uses or spacecraft propulsion. The criteria used to select the generation technique were chosen to reflect these objectives. The primary criterion was the technique's ability to achieve high conversions of molecules to atoms. The application of this criterion to the selection of a generation method appeared to work in either of two ways--either the method was incapable of achieving conversions much in excess of 5% (the case with electron pulse radiolysis), or the method was unable

to achieve a large conversion at pressures in excess of a few torr (as in the case with d.c. discharges).

The secondary criterion which was used to select the generation method for this apparatus was its suitability for use with a recombination rocket engine. Methods which require a static gas mixture, such as shock tubes or furnace-heating of the gas, were eliminated because of their obvious unsuitability for inclusion into a flow system.

### Thermodynamics and Reactions

There are really only two approaches which can be employed to dissociate hydrogen molecules into atoms. The most commonly used strategy takes advantage of the decreased stability of the hydrogen molecule's excited states to increase the frequency (and thereby the overall rate) of the molecules' dissociation. The alternative strategy takes advantage of the dissociation thermodynamics to increase the concentration of hydrogen atoms in equilibrium with hydrogen molecules. An understanding of these two approaches is necessary to understand the differences and similarities between the generation methods which will be reviewed in the subsequent sections.

The dissociation of hydrogen into atoms is a thermodynamically unfavorable reaction. Its enthalpy of dissociation (103.2 kcal/mole) is exceeded among the diatomic gases only by oxygen (118.0 kcal/mole) and nitrogen (225.1 kcal/mole), both of which contain multiple bonds. Furthermore, the equilibrium constant  $K_p = (p_H)^2 / p_{H_2}$  at room temperature (298 °K) is equal to  $5 \times 10^{-69}$  torr (64). The entropy of reaction is

positive ( $\Delta S_{298}^{\circ} = +23.57$  cal/°K mole), however, which makes it possible to increase the equilibrium constant by increasing the temperature in accordance with the thermodynamic equation

$$\Delta G^{\circ} = -RT \ln K_p = \Delta H^{\circ} - T \Delta S^{\circ} \quad (1)$$

(constant T, closed system)

The equilibrium conversion of molecules to atoms, calculated from spectroscopically determined equilibrium constants (56), is shown in Figures 1 and 2. In Figure 1, the conversion of Br<sub>2</sub>, Cl<sub>2</sub>, H<sub>2</sub>, O<sub>2</sub>, and N<sub>2</sub> as functions of the gas temperature is compared at a pressure of one atmosphere (760 torr). Although this pressure is quite high (typical operating pressures in atomic hydrogen research are in the range 0.5 torr < P < 100 torr), the figure shows the high temperatures required for dissociation of the latter three gases, as well as the relatively steep temperature dependence. Figure 2 shows the same information plotted for H<sub>2</sub> at pressures between 0.5 torr and 760 torr. This figure again shows the high (>2000 °K) temperatures which are required for high conversions to occur. In addition, the close spacing of the curves indicates that the conversion depends less strongly on pressure than it does on temperature.

The stability of a hydrogen molecule is determined primarily by the potential energy it possesses. The potential energy of a molecule can be specified by its electronic "state" and by the separation between the nuclei. This information is usually expressed in a molecular energy diagram, such as that shown for H<sub>2</sub> in Figure 3, in which the potential energy of each state is plotted vs. the inter-nuclear separation. Each state, represented by "term symbols" such

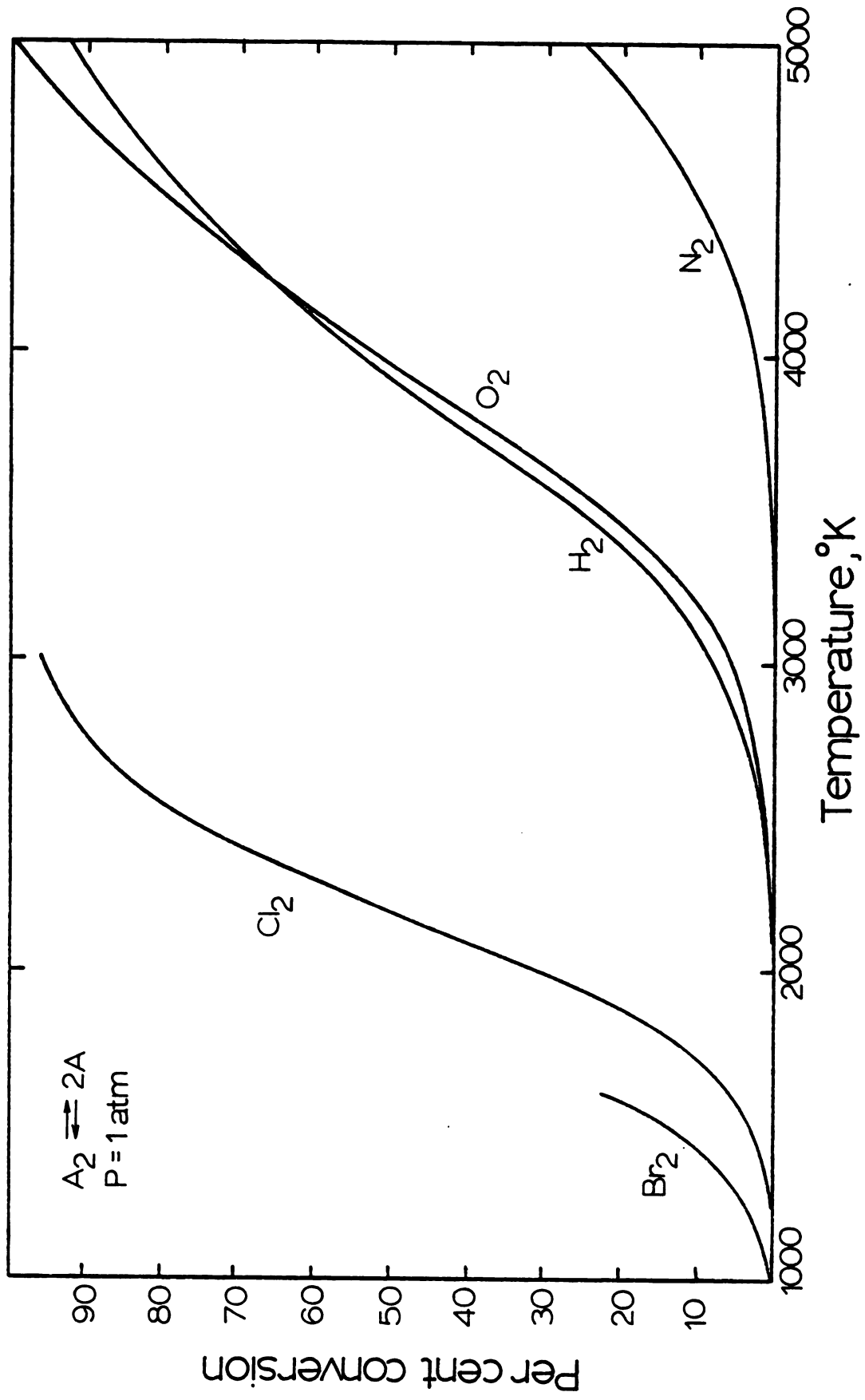


Figure 1.--Temperature dependence of equilibrium dissociation at one atmosphere for Br<sub>2</sub>, Cl<sub>2</sub>, O<sub>2</sub>, H<sub>2</sub>, and N<sub>2</sub>.

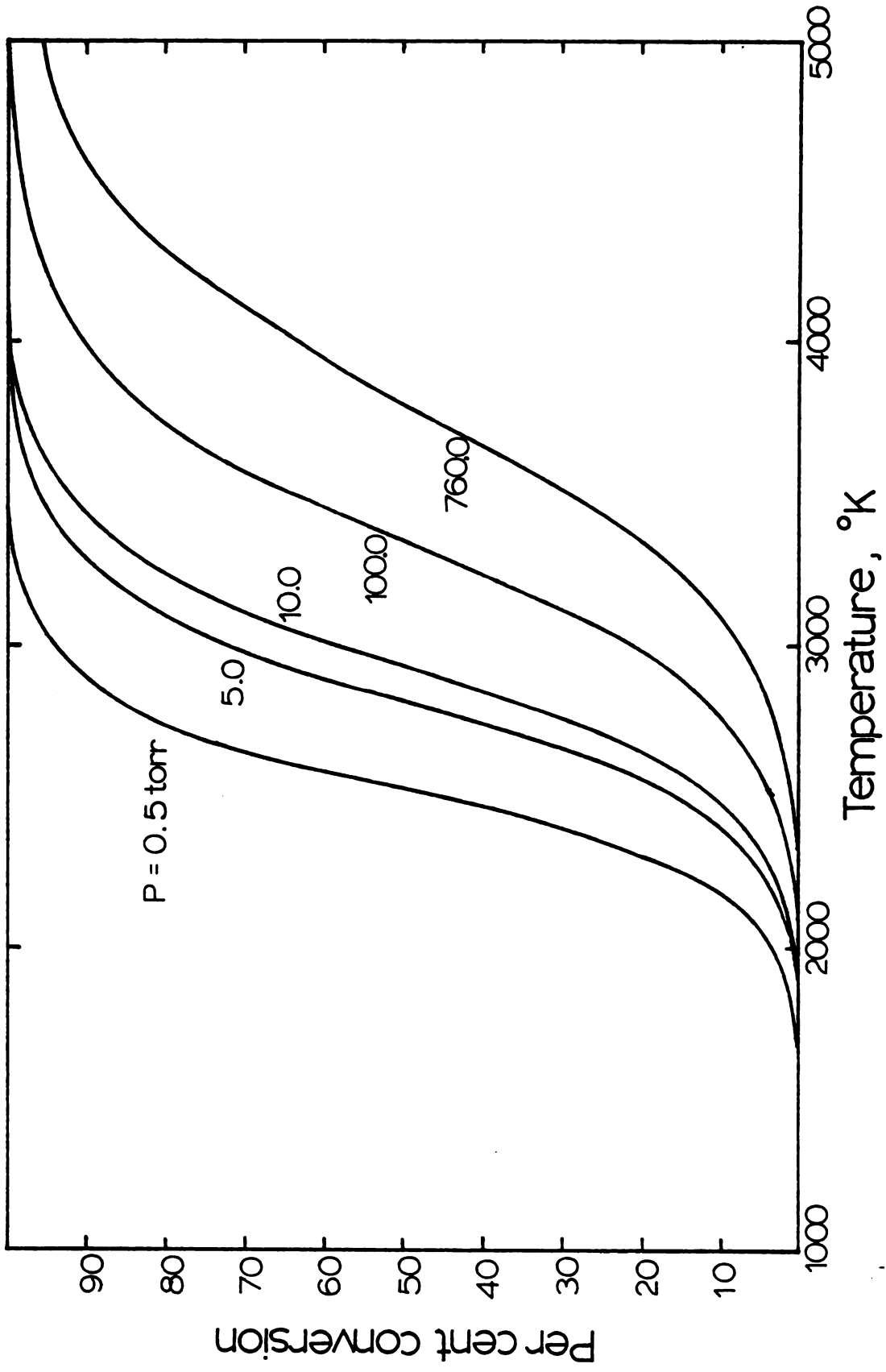


Figure 2.--Temperature and pressure dependence of equilibrium dissociation for H<sub>2</sub>.

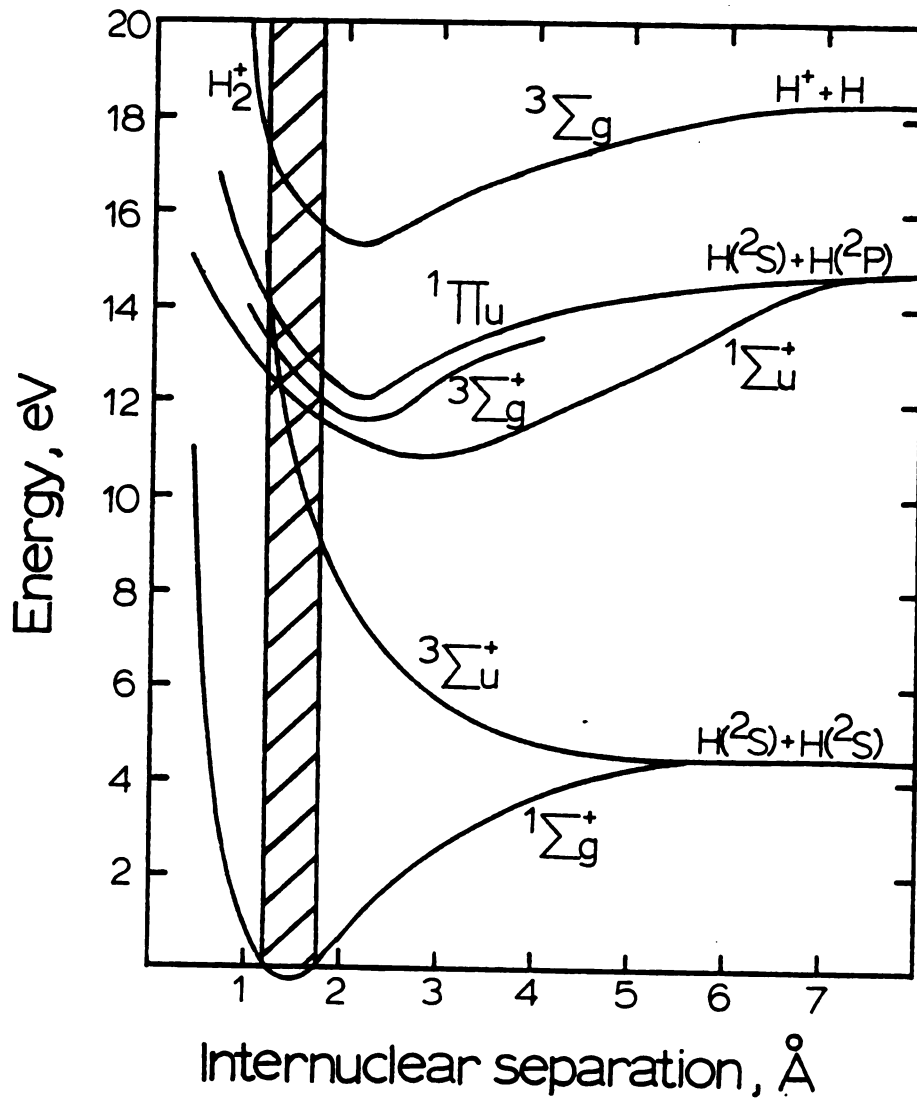


Figure 3.--Molecular energy diagram for hydrogen (13).

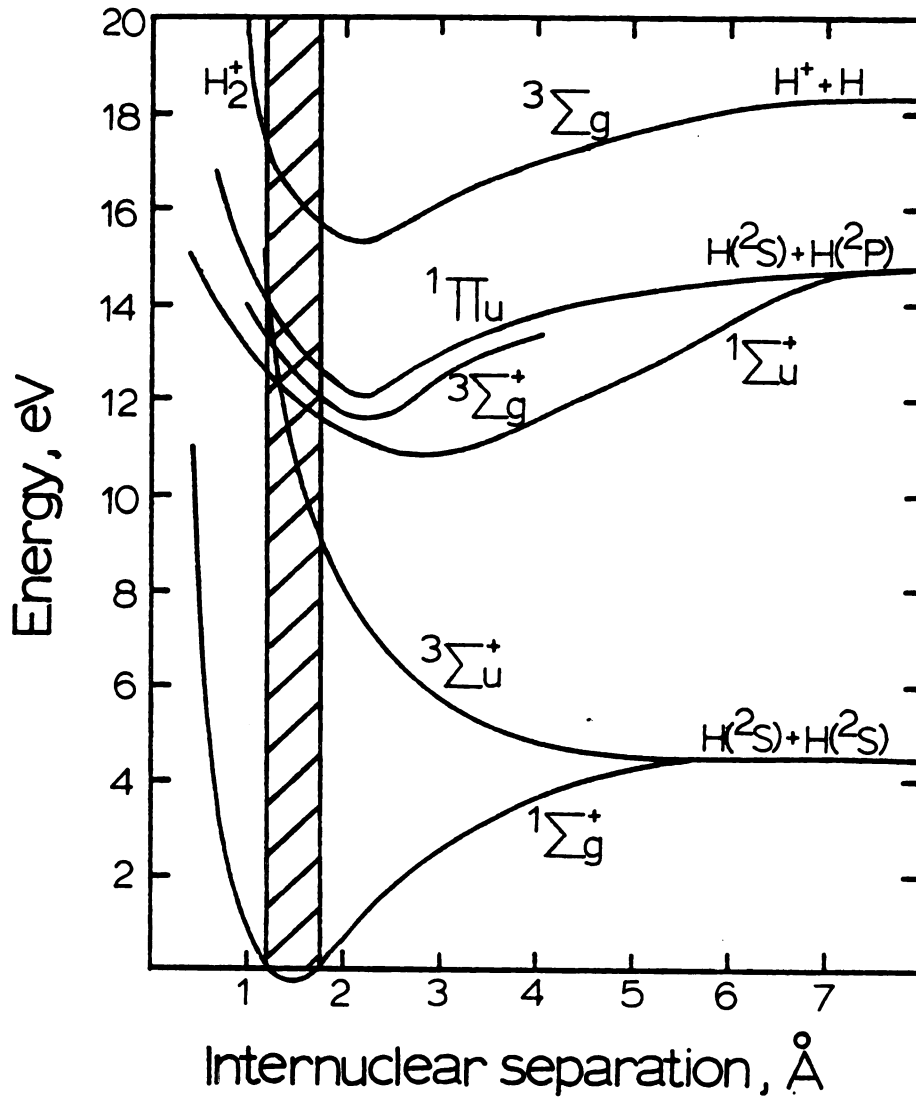


Figure 3.--Molecular energy diagram for hydrogen (13).

as  ${}^1\Sigma_g^+$ , corresponds to a particular solution of the quantum-mechanical wave equation for the molecule. This solution is identified by two quantum numbers and, sometimes, by symbols which represent the symmetry possessed by the electronic wave function. The bulk of this discussion is based on information found in Chapters IV and V of Herzberg (40).

The central quantity in a term symbol is the quantum number which corresponds to the component of the electronic orbital angular momentum along the internuclear axis ( $\Lambda$ ). The values which  $\Lambda$  takes on (0, 1, 2, ...) are represented by the Greek letters  $\Sigma$ ,  $\pi$ ,  $\Delta$ , ... in much the same manner as in the case of the atomic angular momentum quantum number  $\ell$ , where  $\ell = 0, 1, 2, \dots$  are represented by the letters s, p, d, and so on.

The second quantum number which is used in a term symbol is the electron spin quantum number,  $S$ . The values which this number takes on depend on the number of electrons in the molecule--if a molecule has  $n$  electrons, then  $S$  can have the values  $n/2, n/2-1, \dots$ , (0 or  $1/2$ ), with the lowest value being 0 if  $n$  is even, or  $1/2$  if  $n$  is odd. Since the spin quantum number represents a vector quantity (the spin orientation vector) which can be either positive or negative, the total number of spin states represented by any value of  $S$  is equal to  $2S+1$ . This number, called the spin multiplicity, is the value which appears in the term symbol as a superscript to the left of the symbol for  $\Lambda$ . The electronic state is usually referred to as being singlet, doublet, triplet, etc., for spin multiplicities of 1, 2, 3, ... .

The symmetry properties of an electronic state describe the behavior of the wave function's sign under the symmetry operations of inversion through the molecular origin (midway between the nuclei) and reflection in a plane passing through the two nuclei. The inversion operation can be formally defined by reversing the sign of all the electron coordinates. The reflection operation can be similarly defined by reversing the sign of the coordinate whose axis is perpendicular to the reflection plane. The symbols for these operations appear in a term symbol to the right of the symbol for  $\Lambda$  (inversion as a subscript, reflection as a superscript). If the result of a symmetry operation is to change the sign of the state's wave function, the state is said to be antisymmetric with respect to that operation (denoted by  $u$  for inversion and  $-$  for reflection). If the sign remains unchanged by the operation, then the state is symmetric with respect to the operation (denoted in the term symbol by a  $g$  for inversion and a  $+$  for reflection). If the result of the operation is anything else, then the state possesses no symmetry with respect to that operation, and the position in the term symbol is left blank.

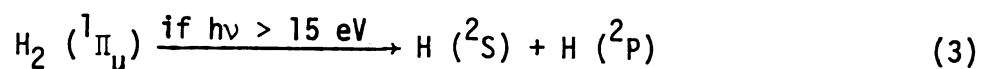
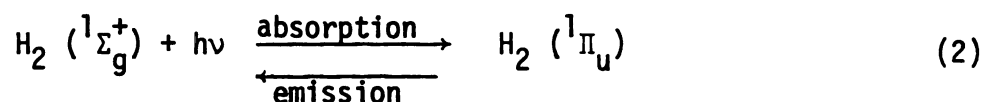
In addition to the potential energy of the hydrogen molecule, the vibrational energy it possesses is also a determining factor in the stability of the molecule. The vibrational energy states of the molecule are usually superimposed over the molecular energy diagram as a series of energy levels placed across the energy minimum, or "well," of the potential function. Although it is possible for a molecule to dissociate solely from vibrational excitation, electronic

transitions play a much more important role in determining the success or failure of a generation method.

The essential difference between dissociation due to collision with energetic particles and dissociation by absorption of light arises from limitations placed by quantum mechanics on light-induced transitions between molecular states. It is possible to show that, for processes involving absorption or emission of light, only certain transitions have a non-zero probability of occurring. These "allowed" transitions are governed by "selection rules" derived from the solution of a wave equation which includes a term for the interaction between the electromagnetic radiation and the molecule's electric dipole moment. For the dissociation of hydrogen, the rules state that a transition between electronic states can take place only between states of the same spin multiplicity and between states with  $\Lambda$  values differing by 0 or  $\pm 1$ . Also, the transition must be between states whose symmetries differ (i.e.,  $g \leftrightarrow u$  and  $+ \leftrightarrow -$  can occur, but not  $g \leftrightarrow g$  or  $+ \leftrightarrow +$ ).

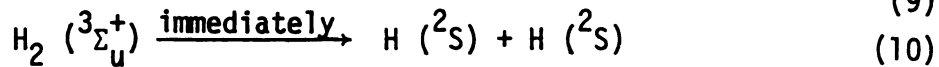
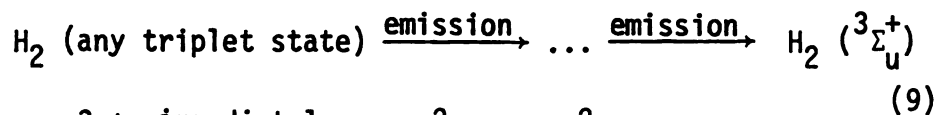
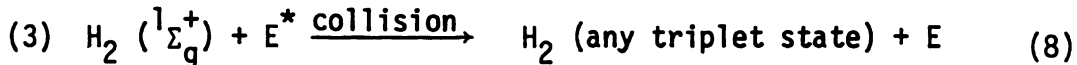
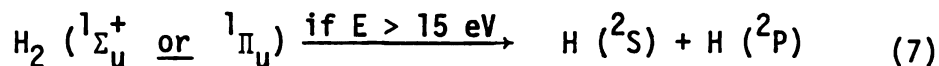
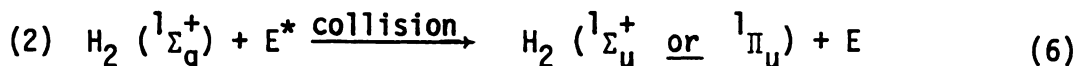
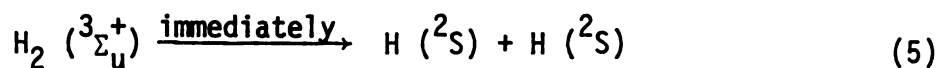
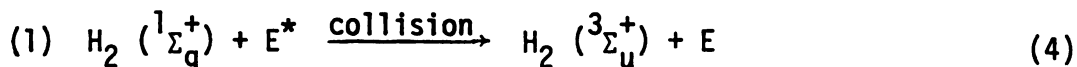
According to the Franck-Condon principle, transitions between electronic states occur vertically on a molecular energy diagram. The principle, first derived by Franck, and later put on a quantum-mechanical basis by Condon, states that electronic transitions are so much faster than the nuclear motions that the internuclear separation remains essentially constant during the transition. Thus, it would appear that the transitions take place vertically on the energy diagram.

As indicated earlier, transition by absorption or emission of light are processes governed by the selection rules. As a result, this dissociation method has a minimum energy requirement of approximately 15 eV, which means that the light must have a wavelength which is less than 83 nanometers. This is the energy required to excite the hydrogen molecule from the singlet ground state,  $^1\Sigma_g^+$ , to the next excited state which has a singlet spin multiplicity,  $^1\Pi_u$ . Dissociation can occur only if the energy possessed by the  $^1\Pi_u$  state is greater than that of the separated atoms to which it dissociates, which gives the 15 eV minimum energy requirement. In contrast to this high minimum energy requirement, the dissociative transition of an oxygen molecule from its triplet ground state,  $^3\Sigma_g^-$ , to the first triplet excited state,  $^3\Sigma_u^+$ , requires only about 7 eV, which can be provided by light whose wavelength is less than 175 nanometers. The transition sequence for the light-induced dissociation of the hydrogen molecule is:



Dissociation of hydrogen molecules by collision with energetic particles differs from light-induced dissociation in that the selection rules do not apply, and transitions may occur between electronic states with different spin multiplicities. The biggest advantage of this characteristic is that the unstable character of the first

excited state ( ${}^3\Sigma_u^+$ ) forces the immediate dissociation of all molecules which enter it. There are three possible transition sequences which can lead to dissociation after collision with the energetic particle  $E^*$  (this particle is either an excited mercury atom or an accelerated electron):



In the first case, the ground state molecule is excited to the repulsive  ${}^3\Sigma_u^+$  state, which dissociates on the next pseudo-vibration (the next time the nuclei move apart, they simply keep moving and dissociate). In the second case, the ground state is excited to the next lowest singlet state. If the energy of the molecule is greater than that of the separated atoms, the molecule will dissociate. This process is identical to that which is followed during light-induced dissociation. In the third case, the transition which follows the

collision leaves the molecule in one of the stable triplet states with less energy than is needed to dissociate from that state. However, since any transitions after the initial collision will be by the emission of light, these transitions will be governed by the selection rules. Although more than one transition may be required, the molecule will eventually make a transition to the unstable ( $^3\Sigma_u^+$ ) state and dissociate.

### Photolysis and Electron Pulse Radiolysis

Photolysis is usually associated with the breaking of bonds by the absorption of electromagnetic radiation near the visible region of the spectrum. Since direct photolysis of hydrogen requires irradiation with vacuum-ultraviolet light with wavelengths below 100 nm (which is experimentally difficult to use), other techniques have had to be developed which allow longer light wavelengths to be used. Two methods commonly used for hydrogen atom generation are direct photolysis of hydrogen-containing molecules (other than  $H_2$ ) and mercury photosensitization. Hydrogen can also be dissociated by using ionizing radiation, a technique called radiolysis. Radiolysis using pulses of high-energy electrons, called pulse radiolysis, is another method used to produce hydrogen atoms. A conceptual diagram of the three techniques discussed here is shown in Figure 4, along with the dissociation pathways followed by each.

As was shown earlier, the direct photolysis of hydrogen requires the use of light with a wavelength less than 83 nanometers. Although it is experimentally feasible to produce light of this wavelength

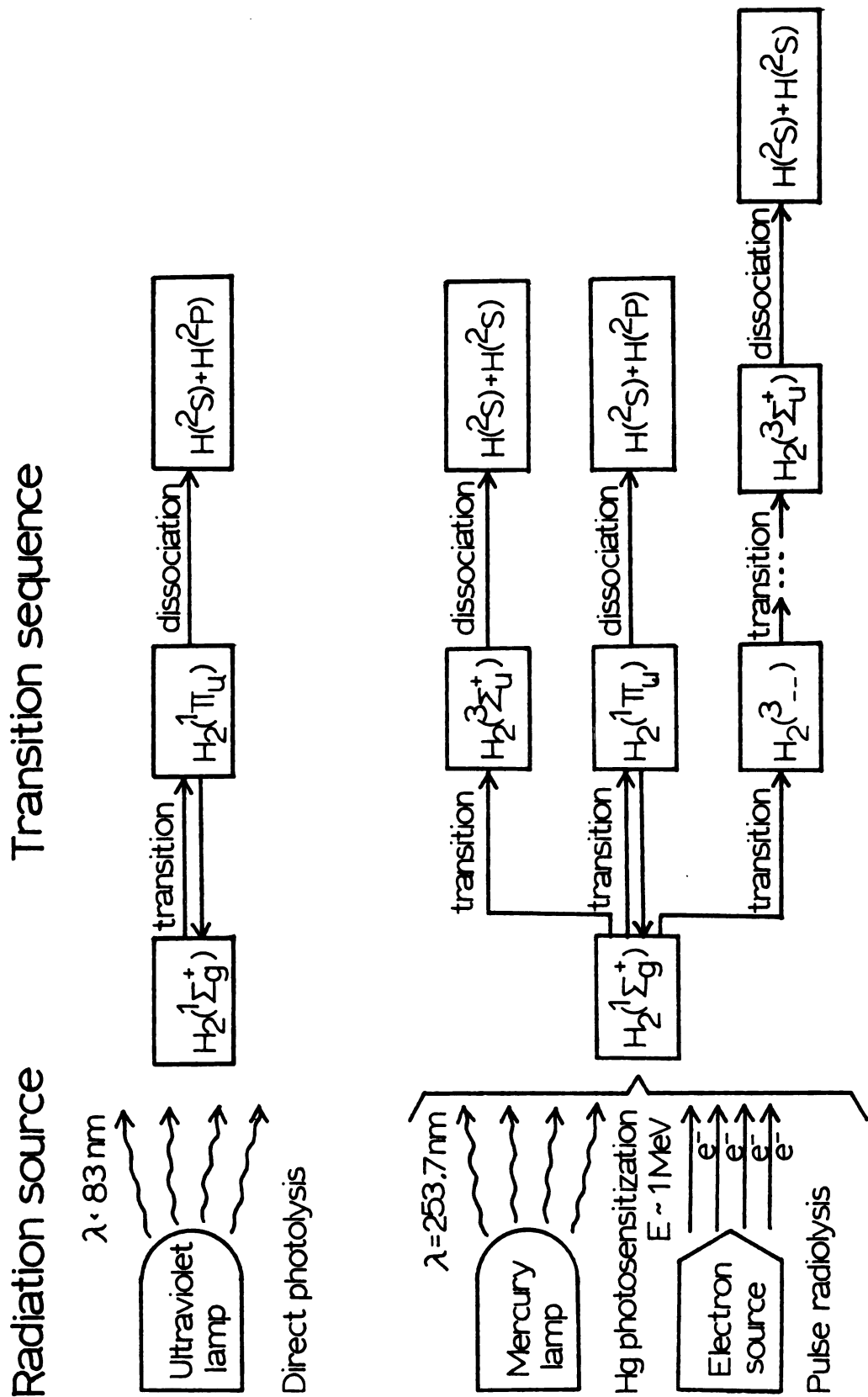


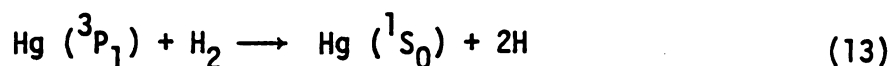
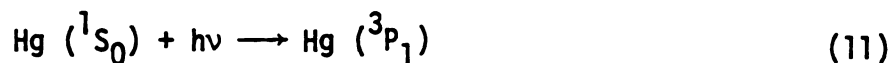
Figure 4.--Conceptual diagram for the photolysis methods.

(sources producing a spark source continuum create light with a wavelength as low as 10 nanometers), the difficulty of working with light which is absorbed by nearly all potential window materials makes direct photolysis a seldom-used dissociation method. The window material having the shortest cutoff wavelength is lithium fluoride (LiF), but even that begins to absorb below 100-110 nm, the lower limit depending on the quality of the window (62). The only reference as yet found in which hydrogen was directly photolyzed circumvented the necessity of windows by connecting the sample cell directly to the exit slit of the evacuated monochromator which was used to select the specific wavelengths desired (66). The application of this apparatus to kinetic studies could be complicated by the fact that the interior of the monochromator is open to the gases in the reaction cell.

Although hydrogen is difficult to photolyse directly, it is considerably simpler to photolyse larger molecules, and the photolysis of hydrocarbons yields hydrogen atoms. As the light required to perform the dissociation is in the range 100-120 nm, LiF can be used for windows, and the apparatus is simplified a great deal. This technique has been applied to various hydrocarbons and  $H_2S$  (16, 117) and to formaldehyde (91). The extent of decomposition is small (in reference 16, approximately 1% of the hydrocarbons were decomposed), allowing the effect of hydrogen atom recombination to be neglected in the kinetic analysis.

The mercury-photosensitized dissociation of hydrogen is the most commonly used photolysis method. Rather than attempting to pass the

vacuum-ultraviolet light necessary for direct photolysis through the walls of the container, the ultraviolet resonance radiation emission of mercury (253.7 nm) is used to excite mercury atoms present in low concentration in the reactant gas. The excited mercury atoms can then collide with the hydrogen molecules and transfer enough energy (4.89 eV) to them to cause dissociation. The mechanism of the reaction is as follows (70):



The experimental procedure itself is quite simple. The basic concepts of a mercury photosensitization apparatus are shown in Figure 4. The mercury vapor which is required can come either from a manometer or from a mercury-containing bulb attached to the reaction vessel. A mercury lamp is used to generate the 253.7 nm radiation needed to excite the mercury. The concentration of mercury vapor in the reaction vessel can be determined by measuring the absorption of the resonance radiation as it passes through the vessel. The operation of the system may either be pulsed, to allow a time-resolved experiment in which the hydrogen atom concentration is continuously monitored (70), or continuous, in which the products are analyzed afterward using various appropriate methods (28, 43).

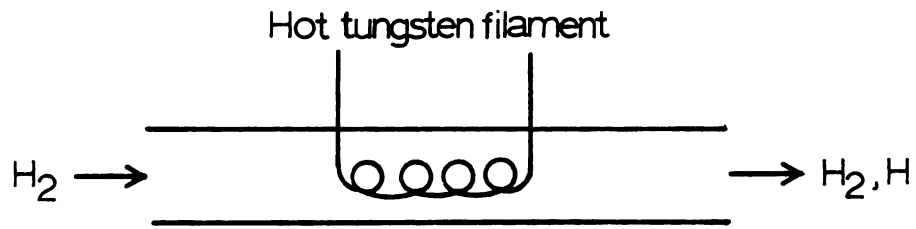
The technique of pulse radiolysis is really a form of electron-impact dissociation, but in actual practice it is most closely related to photolysis, since it is dissociation by a "flash," or pulse, of high-energy electrons. The electron energies used have ranged from a low of 0.5 MeV (14) up to a maximum of 15 MeV. Energies as high as this allow measurements at pressures of up to 61 atmospheres, considerably higher than for any of the other methods reviewed here. One reason for using such extremely high pressures is that high-pressure limiting values for the kinetic constants of hydrogen atom addition can be determined (32). These experiments are also very fast, with the electron pulse taking place over a period of between 10 nsec and 1 microsecond and the reactions being completed within a few hundred milliseconds. Instantaneous atomic concentrations of between  $6 \times 10^{12}$  atoms/cm<sup>3</sup> and  $6 \times 10^{13}$  atoms/cm<sup>3</sup> have been produced in each pulse, but this represents a conversion of molecules to atoms of only a few percent (14).

One advantage which pulse radiolysis does have over the more conventional techniques for atom production, such as electrical discharges and direct photolysis, is that no light is directly generated by the pulse. When photometric techniques are used for measurements with one of the more conventional photolysis methods, the presence of background light from the plasma and from the photolysis source creates a great deal more "noise" in the measurement than is the case for pulse radiolysis, whose electrical disturbance only perturbs the measurement system for a few microseconds after the pulse (14).

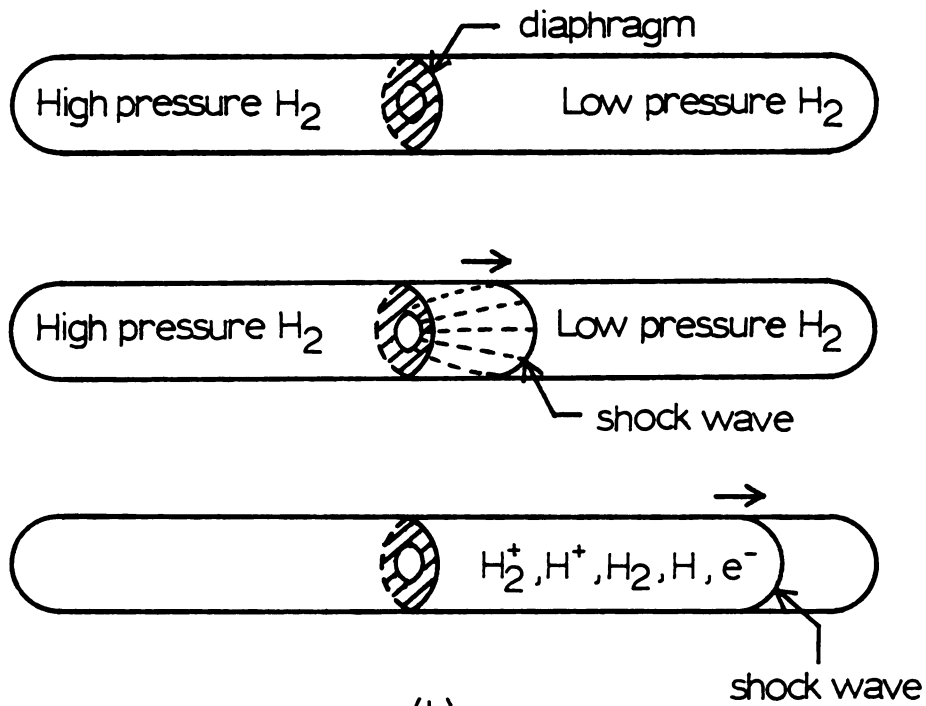
### Thermal Dissociation

The term "thermal dissociation" refers to any process which is brought about due to the application of a high temperature. Two techniques, furnace heating and shock wave heating of static gas mixtures, involve heating the gas itself. Another technique, thermal dissociation on a tungsten filament, relies on the high-temperature equilibria of hydrogen molecules on tungsten. Conceptual diagrams of the hot filament and shock tube dissociation techniques are shown in Figure 5.

It is theoretically possible to heat a flowing gas stream in a furnace to a temperature high enough that significant dissociation can occur. This is made difficult, however, by the temperatures which would be required and the low pressure of the hydrogen. As an example of this, consider hydrogen flowing through an apparatus at a flow-rate of 500 micromoles/sec and a pressure of 10.0 torr. Assuming that the desired conversion is 30%, the gas must be raised to a temperature of 2500 °K (see Figure 2). The length of heated tubing required to cause the temperature rise can be calculated by using the Seider-Tate equation to calculate the heat transfer coefficient from the tube-wall to the gas (75). With a wall temperature of 4000 °K, almost four feet of 5 cm ID tubing would be required. Furthermore, since the melting point of glass or silica tubing is far below 4000 °K, some other material (such as metal or ceramic) will have to be used for the tube, complicating the wall recombination problem (75). It is perhaps for this reason that the only reference to the use of direct heating of hydrogen is a paper in which  $H_2$  and  $Cl_2$  were heated in a



(a)



(b)

Figure 5.--Conceptual diagram for thermal dissociation methods: (a) Hot filament (b) Shock tube.

furnace with  $\text{NO}_2$  to determine the reaction rate of the  $\text{H}_2/\text{Cl}_2$  system relative to that for  $\text{H}_2\text{NO}_2$  (81). In this experiment, the gas was heated to 500 °K before the hydrogen was added, and the reactions were allowed to proceed for a period of several hundred seconds, using light absorbance to measure the changes in product concentration.

Shock-wave heating of hydrogen is used primarily for measurement of high-temperature reaction kinetics. The experiments are performed in a tube which is divided into two sections by a diaphragm. The pressure on one side of the diaphragm is between 1 and 10 atmospheres, while the gas on the other side is at a pressure of about 0.01 atmospheres. The experiment begins when the diaphragm is ruptured. The pV work in the pressurized gas is converted to heat in the resultant shock wave (34). This heating results in elevated local temperatures which can range from 1300 °K (58) to 7000 °K (42). These temperatures persist long enough for kinetic information to be obtained, although the time scale is short enough (on the order of a few milliseconds) to require extensive instrumentation to maximize data output for each run. Myerson and Watt (73) present an interesting description of the pains with which the shock tube itself is fabricated from aluminum tubing, as well as a good description of the experimental procedure. Typical monitoring instruments are: strain gauges, which are used to signal when the shock wave arrives at a given point in the tube, trigger other monitors, and determine the shock wave's velocity (73); Lyman- $\alpha$  hydrogen atom detection systems (72-3), which are used to monitor the atomic concentration continuously; and spectral line

reversal monitors, which are used to determine the gas temperature behind the shock wave (42).

Thermal dissociation of hydrogen molecules on a hot tungsten filament has been studied since at least 1912 (50). This technique consists of heating a tungsten wire to temperatures on the order of 2000 °K (38, 96) and passing a stream of hydrogen gas over it. The basis of the technique is that the hydrogen molecules which are adsorbed onto the tungsten dissociate at these high temperatures, and desorb as hydrogen atoms. Conversions of molecules to atoms are typically less than 5%, principally because the dissociation is limited by the equilibrium between molecules and atoms on the tungsten surface.

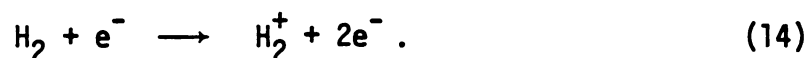
#### Direct-current Discharge

The direct-current (d.c.) discharge was the first technique developed for generating hydrogen atoms from molecules. After its initial discovery (as an atom generation technique) by Kirkby in 1906 (46), it was used extensively (2, 3, 5, 76-8, 89, 112-16) until the development of the more powerful alternating-current discharge devices in the early 1960s made it less useful.

The production of a direct-current (d.c.) discharge requires a gas container, electrodes, and a power supply. The gas may be either static or flowing, although nearly all references use a flowing system for kinetic studies. The electrodes must be immersed in the gas to be discharged, and can be constructed from nearly any suitable metal, such as tungsten. The design of the discharge tube is quite simple,

with a conceptual diagram being shown in Figure 6. The requirements on the power supply are the ability to maintain a potential of between 5000 and 7000 volts across the electrodes. The electrical currents which are used in these experiments are quite low--for example, Poole (76-78) used a maximum current of 90 milliamps in his experiments, while Amdur and Robinson (2) used only 32 milliamps. The electron acceleration which is responsible for the dissociation reactions in d.c. discharges results from the constant electric field produced across the electrodes.

The d.c. discharge is one of three hydrogen atom generation techniques which makes use of collisions between high-energy electrons and hydrogen molecules to create hydrogen atoms. The electrons found in d.c. discharges come from either of two sources. Some electrons are emitted by the anode (the negatively charged electrode). Other electrons are produced in the discharge itself, the result of ionizations which can occur when the electrons striking the molecules have sufficient energy. For example, the potential energy of the  $H_2^+$  ion (as shown in Figure 3) is approximately 16 eV above the molecular ground state. Thus, if an electron possesses more than this amount of energy, the molecule can ionize according to the reaction



The hydrogen molecules in a d.c. discharge are dissociated according to the collision mechanism discussed earlier, in which energetic particles (in this case, electrons) transfer their energy to the molecule. The energy which the electrons possess is kinetic

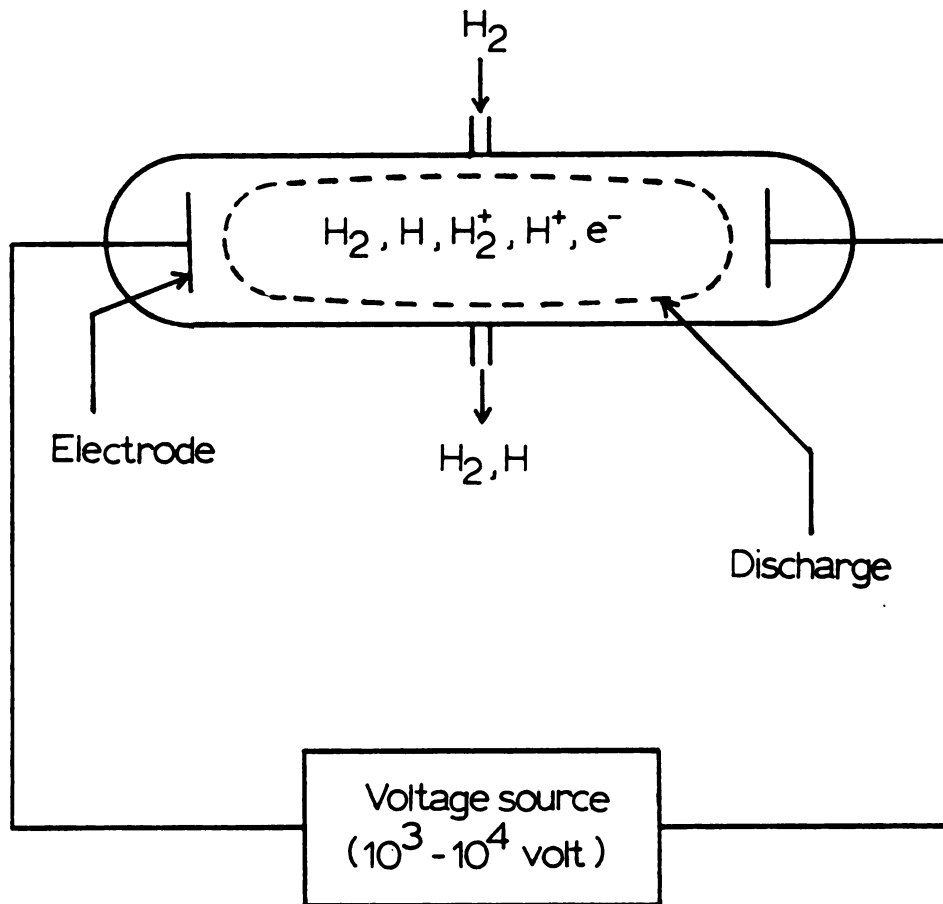


Figure 6.--Conceptual diagram of the d.c. discharge dissociation method.

energy which results from their acceleration in the electric field which exists between the two electrodes. A free electron in the discharge accelerates toward the positive electrode until it either collides with a gas molecule or one of the discharge boundaries. If the collision doesn't result in any energy transfer (i.e., if the collision is elastic), the electron simply rebounds and continues to gain energy. If the collision does result in energy transfer, the mechanism described earlier is followed.

Although d.c. discharges were used as early as 1906 (46) to generate hydrogen atoms, the lack of quantitative detection methods for hydrogen atoms kept the study of chemistry in discharges at a standstill until 1929, when Smallwood (87) used a catalytic probe detector, based on observations in a d.c. discharge by Wood (116) in 1922, to determine the rate coefficient for the hydrogen atoms recombination reaction. Amdur (2, 3, 5) performed similar research during the mid-1930s, using an improved version of Smallwood's detector.

In 1937, Poole (76, 77, 78) performed a series of experiments whose purpose was to measure the efficiency with which a d.c. discharge could produce hydrogen atoms. Observing that most of the electron acceleration takes place in the positive column of the discharge, Poole compared the power consumed in that part of the discharge to the quantity of hydrogen atoms produced in the discharge, which he measured using a catalytic probe detector. Although the experiment was too simplistic to be considered a true energy-balance measurement (such obvious energy-loss mechanisms as light emission and heat loss from the walls were neglected), this still represents the sole

experiment where an atom generator's efficiency of production was measured. An analysis of two data points taken from Poole's paper is shown in the last two columns of Table 1. Although the power absorbed was less than for the two microwave discharge experiments which are also included in Table 1 ( $\sim 50$  watts as opposed to 85-100 watts), the yield which Poole achieved ( $3.22 \text{ atoms kWh}^{-1}$ ) is nearly as high.

The most recent use of a d.c. discharge apparatus has been in experiments to measure wall recombination coefficients on various surfaces (89,112-3). This parameter, equal to the fraction of atoms striking a surface that recombine there, must be kept to a minimum in any experimental apparatus in which hydrogen atoms are to be studied. In these experiments, hydrogen atoms produced in a d.c. discharge are allowed to diffuse down sidearms. The end of one sidearm consists of a platinum plate, which has a recombination coefficient equal to one. The other sidearm's endplate is made of the material being studied. After the discharge is turned on, the recombination coefficient can be determined from the difference in temperature of the two endplates.

#### Alternating-current Discharges

The alternating-current (a.c.) discharge is the most commonly used method for generating hydrogen atoms. Although the technique was first used as early as 1922 (41), it wasn't until the 1950s that its use became significant (63,83,84). The use of a.c. discharges to create hydrogen atoms increased greatly through the

Table 1.--Results of hydrogen radical generation experiments.

	Mearns & Ekinci (65)	Shaw (84)	Poole (78)
<b>Experimental Conditions</b>			
Pressure (torr)	1	0.5	0.75
Neutral gas temp. ( $^{\circ}$ K)	420 (assumed)	...	0.42
Gas flow rate (g mole/sec)	$1.4 \times 10^{-4}$	$1 \times 10^{-5}$	$9.8 \times 10^{-5}$
Power absorbed (watts)	85	100	47.5
<b>Dimensions</b>			
Inside diameter (mm)	11	8	25
Length (cm)	12	70	54
Plasma volume ( $\text{cm}^3$ )	11.4	$\sim 2.5$	264
Area/volume ( $\text{cm}^{-1}$ )	3.6	5.0	1.6
Coating	$\text{H}_3\text{PO}_4$ on quartz	Dri-film	$\text{H}_3\text{PO}_4$
<b>Discharge Characteristics</b>			
Frequency (MHz)	2450	3000	DC
Power density (watts/ $\text{cm}^3$ )	7.5	40	0.18
Electron density (electrons/ $\text{cm}^3$ )	$7 \times 10^{11}$	...	...
Electron temperature ( $^{\circ}$ K)	50,000	...	...
P A (torr cm)	0.16	0.083	0.39
E/P (volt/cm torr)	37	17	25
Plasma space time (sec)	$3.1 \times 10^{-3}$	...	...
Conversion (%)	38	90	7.7
Yield (atoms/kwh) <sup>a</sup>	4.5	2.4	0.86

<sup>a</sup>Thermodynamic upper limit of the yield is 16.6 atoms/kwh based on dissociation energy of 104.2 k cal/g mole.

1960s, and now virtually all experiments in which flowing hydrogen is dissociated make use of this generation method.

The term "a.c. discharge" encompasses two distinct types of device, both of which use the time-varying electric field associated with electromagnetic radiation to dissociate the hydrogen molecules. The main components of these two methods are shown in Figure 7. In both cases, the electromagnetic radiation from the a.c. source creates an electromagnetic field in a structure (coils or cavity) which is outside the discharge container. This field creates another field within the container by induction, and it is the induced field which creates the discharge. However, while these devices are similar in principle, the equipment used to generate the radiation and create the discharge are quite different.

The energy for a radio-frequency (rf) discharge is generated in a high-power radio transmitter. An example of this is the apparatus used by Clyne and Thrush (21), in which a 350 watt, 17 MHz transmitter was used. In a more recent experiment (20), a 2500 watt, 20 MHz transmitter was used. The energy from the source is conducted via coaxial cable to the coils which surround the discharge tube. The coils have generally been constructed from metal-foil rings (21-24,53,54).

The sources used to create microwave radiation can be divided into three separate groups. The devices used in the first experiments (prior to 1962) were modified from radar equipment (63) or from other sources identified only by their frequency (2450-3191 MHz) and, sometimes, by their power output (44,80,84). These early

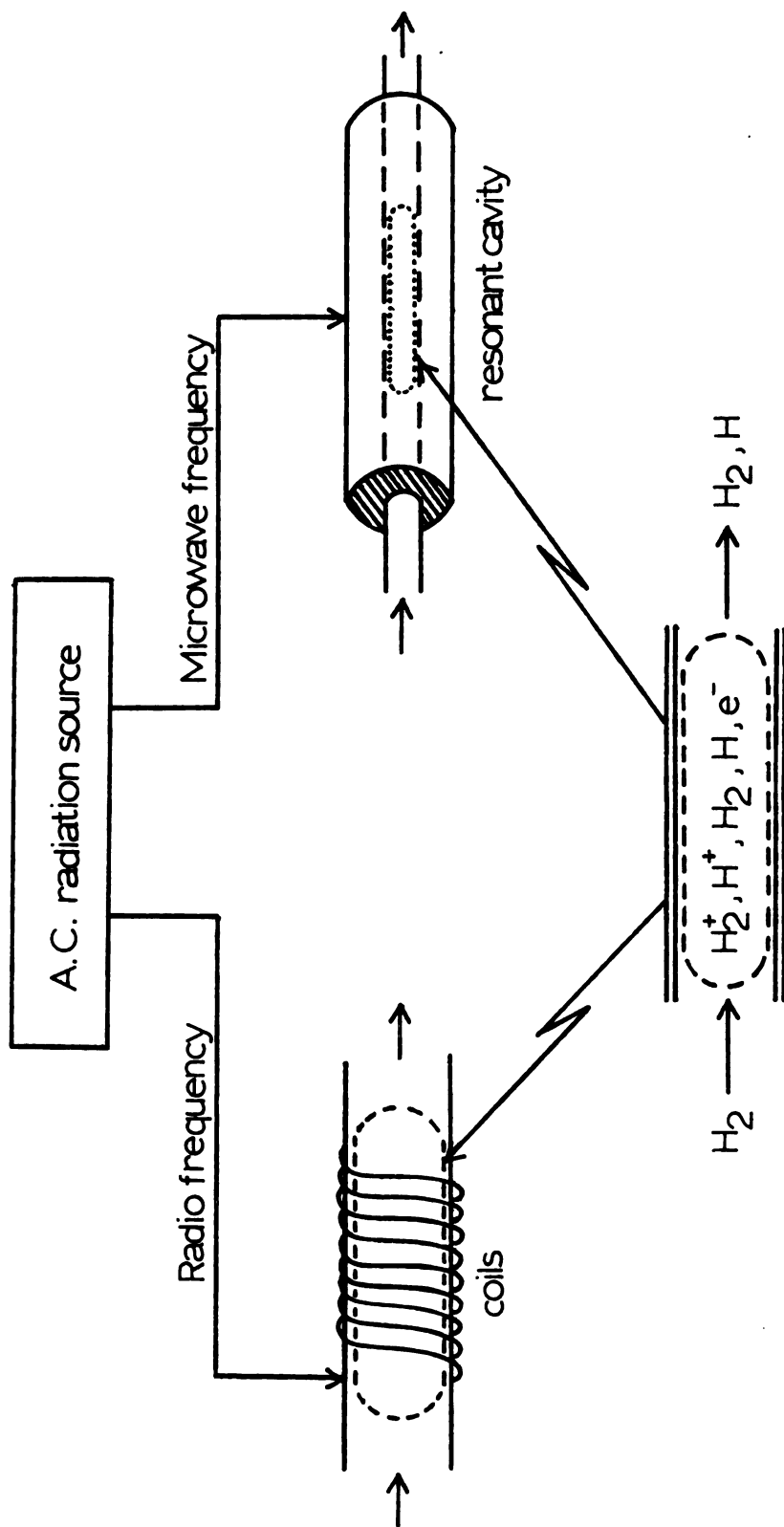


Figure 7.--Conceptual diagram of the a.c. discharge dissociation methods.

devices were superceded by two commercially-available 2450 MHz radiation sources: (1) diathermy units (8-10,13,27,65,69,79,102-9), designed for medical use in deep-heat therapy and limited in power to approximately 100 watts; and (2) modified microwave ovens (67, 68), which are capable of producing as much as 1500 watts of output power. The microwave energy from these sources is transferred through cables or waveguides to the cavity.

The purpose of the cavities used in producing microwave discharges is to confine the electromagnetic radiation in such a way as to create standing waves, called "modes," within the cavity. Since these modes can only exist under certain combinations of radiation frequency and power, cavity geometry, and cavity contents, the cavity is usually referred to as being "tuned" to a particular set of conditions, and any change in them (for example, an increase in power input to the cavity) must be accompanied by a readjustment of the cavity.

Although both a.c. and d.c. discharges dissociate hydrogen through collisions with accelerated electrons, the mechanisms by which the electrons are accelerated differ. In a d.c. discharge, it is the force applied to the electron by the constant electric field which causes the acceleration. In an a.c. discharge, on the other hand, the electric field is constantly reversing direction, meaning that the force field felt by the electrons changes direction every  $10^{-6}$  (rf) or  $10^{-9}$  (microwave) seconds. Because this means that any velocity gained during one half-cycle would be lost on the next half-cycle, a mechanism must exist for retaining some

of the gained velocity. This mechanism is a collision with some other component of the discharge. Upon collision, some of the velocity which has been gained from the electric field will be transferred into velocity components perpendicular to the field's direction. Since the electric field can't affect these components, the transferred velocity will be retained by the electrons, and succeeding collisions will add further to the electron's total energy.

Apart from an early study in 1922 (41), the rf discharge technique saw its major use during the 1960s. After an apparatus was developed by Clyne and Thrush (21,22) for use in studies of the kinetics of the reactions between hydrogen atoms and NO, NO<sub>2</sub>, and HNO, similar apparatuses were used to study the kinetics of the reactions between hydrogen atoms and HCl (24), NOCl (24), and O<sub>2</sub> (23), and to develop gas-phase titration techniques for measuring hydrogen atom concentrations using NO, NOCl, and NO<sub>2</sub> (24). Since then, no further use of the rf discharge has been reported, probably due to the greater capabilities of microwave discharge devices.

The uses to which microwave discharges have been put fall into two categories. The majority of experiments have used the discharge simply to produce a known hydrogen atom concentration for use in kinetics investigations (19, 102-9). This is generally done by passing a dilute mixture (typically 2-3%) of hydrogen in an inert gas (argon or helium) through the discharge. Dissociation is presumed to be virtually 100% at such low concentrations.

The other type of experiment where microwave discharges have seen use has been in studies of complex reaction systems. In these experiments, a mixture of the gases to be studied is passed through the discharge and the products analyzed to determine the processes occurring within the discharge. These experiments are useful as a test of the applicability of microwave discharges to large-scale chemical processing, but more investigation into efficiencies of production are necessary.

The limited data concerning the energy efficiency of hydrogen atom generation in microwave discharges indicates that this method is at least as efficient, if not more so, than d.c. discharges. This is supported by the data in Table 1, which is taken from the two microwave discharge experiments giving enough information to calculate the efficiency. The highest yield (atoms  $\text{kwh}^{-1}$ ) is 27% of the theoretical maximum of 16.6 atoms  $\text{kwh}^{-1}$ , which is obtained from the dissociation energy of hydrogen.

#### Summary--Generation

The purpose for doing this literature review was to determine the best technique, within certain qualifications, for producing hydrogen atoms for use in the proposed energy-balance experiment. The most important qualification was that the technique had to be capable of achieving high conversions (>50%) at pressures as high as 20-30 torr in a flowing system. This qualification stems from the potential application of the technique to spacecraft propulsion. Additional qualifications were introduced to make possible the use

of the apparatus in kinetics experiments.

Some of the generation methods reviewed here are clearly unsuitable for use in any experiment where a high conversion is required. Such techniques as direct photolysis, mercury photosensitization, and electron pulse radiolysis have such a low intrinsic conversion (usually <5%) that they would certainly be inadequate for any spacecraft propulsion application. Furthermore, mercury photosensitization and pulse radiolysis are more suited for experiments in static gas mixtures; mercury photosensitization because of its use of toxic mercury, and pulse radiolysis because of the pulsed nature of the dissociation.

The unsuitability of thermal dissociation is based less on infeasibility than on impracticability. It is feasible to dissociate hydrogen thermally with high conversion if some method can be found to heat the gas to the high temperatures (>5000 °K, see Figure 2) which are required. The difficulty lies in the design and use of a furnace capable of maintaining a 5000 °K tube-wall temperature over a length of 3-4 feet. Since most materials presently used in building hydrogen atom apparatuses can't be used at such high temperatures, a completely new wall material would have to be used, with the necessary research into wall recombination on the material playing a significant role. The size of the apparatus itself would present a problem, as a furnace capable of heating a 4 foot section of tubing to 5000 °K would certainly be quite large.

The high-conversion qualification is met by all three of the

electrical discharge techniques. However, d.c. discharges only achieve significant conversions when the hydrogen used in the discharge contains 2-3%  $H_2O$  or  $O_2$ . Although this might not be important when performing the energy balance experiment for which this apparatus is principally intended, impurities would certainly make its use in other experiments more difficult than would be the case when pure hydrogen is used.

The final choice of a generation technique must therefore be between an rf discharge and a microwave discharge. There isn't an obvious criterion for selecting one of these techniques over the others, but the lack of any significant work in rf discharges--beyond the work of Thrush, Brown, and their co-workers during the early 1960s--seems to indicate a preference among most workers towards the microwave discharge. (Even Brown and Thrush used a microwave discharge in their later work [18; 1967].) Potential reasons for this might include the low cost and ready availability of a high-power microwave radiation source or, perhaps, difficulties stemming from the need to attach the rf discharge electrodes directly to the reactor.

The selection of a microwave discharge as the atom generation method for the proposed apparatus is therefore based on three criteria. The primary criterion, high conversion (>50%) at relatively high pressures ( $\sim 20$  torr), eliminates all the generation techniques save the electrical discharges. The two secondary criteria, feed consisting of pure hydrogen and the demonstrated

preference of previous authors, are responsible for the selection of the microwave discharge over both the d.c. and rf discharge.

## METHODS OF HYDROGEN ATOM DETECTION

Early research into hydrogen atom chemistry (1910-1929) was hampered by a lack of a quantitative technique for measuring the atom concentration. Although it was possible to detect the presence of an active reducing agent in the effluent of a discharge (in one method, the effluent was passed over a bed of sulfur, and the  $H_2S$  formed was detected by the darkening of a piece of paper soaked in a lead acetate solution [98-100]), many researchers (6, 7, 50, 98-101) were uncertain as to the identity of the agent, simply calling it "active hydrogen." However, Langmuir was referring to the agent as atomic hydrogen as early as 1912 (49, 51-2), and by 1925 that identification appears to have been well established.

The first two quantitative methods for detecting hydrogen atom concentrations were developed in 1928-29, and were both based on Wood's observation in 1922 that metals, especially platinum, had a great ability to catalyze the recombination of hydrogen atoms (116). The Wrede-Harteck gauge (39, 118) uses platinum to recombine hydrogen atoms in a small side chamber, measuring the atom concentration from the resulting pressure drop. Catalytic probe detectors, one of which was first used in 1929 by Smallwood (87), measure the amount of heat that the recombining atoms transfer to the metal to determine the atom concentration. Although the Wrede-Harteck gauge is no longer

in common use, a catalytic probe was developed and used by Trainor et al. in 1973 (96).

The next detection method to be developed was the electron spin resonance spectrometer. The first appearance of this detector in the literature was in an article by Shaw (84) published in 1959. The complete development of this method came between 1964 and 1968, when Westenberg and de Haas (102-109) published a series of papers detailing the theory and application of the method to several free radicals. In particular, Westenberg and de Haas developed the technique of calibrating the esr spectrometer with molecular oxygen, as opposed to using known concentrations of free radicals for the same purpose.

The technique of gas-phase titration as a means of determining atomic hydrogen concentrations was also developed during the early 1960s. Developed primarily by Clyne, Thrush, and their co-workers (17, 18, 21-24, 27, 96), the technique was based on the light-emitting reaction between hydrogen atoms and nitrogen oxide gas (NO). This method of detecting hydrogen atoms, although it is a destructive analytical tool, has the advantage of being an absolute method which is species-specific. Although Wrede-Harteck gauges and catalytic probes also make absolute measurements of the atom concentration, the presence of any other free radicals causes them to lose accuracy. Since the reaction of H and NO is specific to hydrogen atoms, any other free radicals in the gas mixture won't interfere with the measurement.

The most recently developed method for measuring hydrogen atom concentrations is Lyman- $\alpha$  photometry. This technique uses the absorption of ultraviolet radiation by hydrogen atoms to measure the relative atom concentration in the gas mixture. The method was developed for the most part by J. V. Michael and his co-workers (1, 8-10, 14, 27, 66, 69-70) during the mid-1960s.

The main purpose of the following section is to determine which of the detection methods would be most suitable for the energy-balance experiment which is planned. The criteria which will be used to select the method are species-specificity and ease of calibration. Species-specificity refers to the ability of some detection methods to determine hydrogen atom concentrations without interference from other free radicals in the mixture. Although not as important for the energy-balance experiment, any future studies of hydrogen atom chemistry will rely on the ability of the system to discriminate between hydrogen atoms and other free radicals. The ease with which the instrument can be calibrated is especially important, since the atoms recombine too easily to be used to calibrate the detection system with a known atom concentration.

### Molecular Diffusion

The Wrede-Hartek molecular diffusion gauge was first developed in the late 1920s (39, 118). It takes advantage of the high efficiency with which most metals can recombine atomic hydrogen. The gauge consists of a very small diameter orifice between the flow tube and a chamber. Inside this chamber, a piece of metal catalyzes the

recombination of the hydrogen atoms. Since the hydrogen atoms which diffuse into the chamber diffuse out as molecules, there is a net molar flow rate between the tube and the chamber. This net flow rate results in a measurable difference in pressure between the tube and chamber.

There are two conceivable drawbacks to the use of Wrede-Harteck gauges. The first is the lack of specificity of the gauge. As metals can catalyze the recombination of other radicals in addition to hydrogen, the use of Wrede-Harteck gauges is limited to gas mixtures in which only one atomic species appears in significant quantity. This could be difficult in studies where, for example, the hydrogen contained water when discharged, or if there were hydrocarbon radicals in the stream due to some reaction.

The second possible problem was discussed by Poole (76) and relates to the design of the orifices in the gauge. The design of these is critical to the proper operation of the gauge. A criterion for the proper design of a gauge, ascribed by Poole to Knudson, is that the diameter of the orifice must be less than one-tenth of the mean free path of the gas. Poole lists a few papers in which this condition isn't met.

Poole also comments on the sensitivity of the concentration measurement to errors in the pressure measurement. The equation relating the percentage error in concentration,  $y$ , to the percentage error in the pressure measurement,  $x$ , is given by Poole as

$$y/x = 2(341 - A)/A \quad (15)$$

where  $A$  is the percentage of atomic hydrogen in the gas mixture. The disadvantage of a Wrede-Harteck at low concentrations is obvious, as a 1% error in the pressure measurement coupled with an atomic hydrogen percentage of 7% will result in an error in measured concentration of 95%.

### Catalytic Probe

Catalytic probe methods are similar to molecular diffusion methods in that they make use of the high efficiency which metals have for the recombination of hydrogen atoms. Whereas the Wrede-Harteck gauge relates a pressure measurement to the hydrogen atom concentration, however, the catalytic probe methods use a temperature measurement. The probe consists of a piece of metal, usually platinum or a platinum alloy, which is suspended in the flow stream. When atomic hydrogen collides with the probe and recombines with the hydrogen atoms adsorbed on the probe surface, the heat of reaction is retained in the probe, which over a period of time is equivalent to a power input to the probe. The various catalytic probe techniques in the literature differ primarily in the method for measuring this power input. Some of them measured a quantity other than the temperature of the probe itself. Smallwood (87) used an external calorimeter around the tube containing the probe to make the measurement. This design had a great potential for heat leaks, was slow to respond, and wasn't very versatile, since the calorimeter had to be built around the flow tube. Much better was the calorimeter which was used by Poole. In this design, the platinum used to recombine the atoms was plated onto

a section of copper tubing through which water flowed. A pair of thermocouples measured the increase in water temperature as it passed the section of platinum-plated copper, from which could be calculated the rate of atomic recombination on the tube. An additional advantage this design had was that the measurement range of the instrument could be altered by changing the water flow rate.

Although Poole's results show that calorimetry based on measurements of the temperature rise of water in a calorimeter can be used with success, the methods found more acceptable since then involve direct measurements of the probe's temperature. Amdur (5) measured the power input to the probe by turning the discharge off and using a heating element installed in the probe to match the electrical heating rate of the probe to the recombination heating rate. This technique, although it is fairly simple, requires two separate runs in each experiment, which complicates the use of the equipment. The last design for a catalytic probe to be described here is that used by Trainor, Ham, and Kaufman (38, 96). This probe is operated a bit differently than the rest, as it is kept at a constant temperature. This means that the probe has a certain resistance, which is related to that temperature. The probe is kept at this temperature by connecting it to one arm of a self-balancing Kelvin bridge. This circuit causes a change in the current flowing through the probe if its resistance differs from that of a standard resistor. The current causes the temperature of the probe wire to change until the resistance again matches. In actual operation, the temperature of the probe is

kept constant, and the changes in current required to maintain that temperature are monitored by recording the voltage across the probe.

When using a catalytic probe to measure hydrogen atom concentrations, several considerations have to be made to ensure that accurate measurements are being taken. The efficiency of the probe both in collecting the atoms and their heat of recombination can only be estimated by comparison with other techniques for concentration measurement, such as titration. Perturbations by the probe to the atom flow rates can be estimated using the expression

$$\ln [1 - (c'/c)] = -(\bar{v}^2 + 4k^I D)^{\frac{1}{2}} (x/D) \quad (16)$$

in which  $D$  is the diffusion coefficient,  $\bar{v}$  is the average flow velocity,  $c'$  is the actual concentration at a distance  $x$  upstream from the probe,  $c$  is the hypothetical concentration (assuming no perturbation) at that position, and  $k^I = 2k_M[H][M]$  is an effective first-order rate constant for the homogeneous recombination (96).

### Mass Spectrometry

Although the use of mass spectrometers for hydrogen atom concentration measurements is not common, it is a very powerful tool for sorting out complex reaction mixtures, such as are encountered in  $H_2/O_2$  flames and in the hydrogenation reactions of hydrocarbons. Its only drawback for quantitative work is the difficulty which its calibration poses. Since the sensitivity of a mass spectrometer detector is entirely dependent on the species, calibration requires known concentrations for each species whose concentration is of interest.

This is obviously a serious drawback when complex mixtures of unstable intermediates are involved.

There are different approaches to the use of a mass spectrometer for radical detection. One approach uses the mass spectrometer to accurately determine the product distribution from the reaction (28, 43, 117). Because these species are (presumably) sufficiently stable to allow calibration of the spectrometer, the concentrations can be measured quite accurately. However, a gas chromatograph can also be used quite effectively for the same purpose, and it is a good deal easier to use, so the advantages of a mass spectrometer aren't really used to their full advantage in this approach.

The second approach to using a mass spectrometer is to use it in conjunction with another technique. Koda et al. (47) did this when they used a mass spectrometer to determine the product distribution during an ethylene titration of hydrogen atoms. Another example of this approach is the use of a titrant (such as NO) to determine the hydrogen atom concentration (19). Because hydrogen atoms are usually present in concentrations smaller than that of the hydrogen molecules from which they are formed, the nearby molecular hydrogen peak decreases the sensitivity of the mass spectrometer to atomic hydrogen. If NO is added to the stream in small quantities, the titration endpoint can be determined as the NO flow rate where the peak at  $m/e = 30$  disappears.

In both of the examples above, the mass spectrometer is used in a special configuration known as a time-of-flight mass spectrometer. In this configuration, the distance between the reactant injection

point and the entrance of the spectrometer's detection chamber is variable. The time required for the gas to flow from the injection point to the detector, called the dwell time, is equal to the distance divided by the linear flow velocity. Examining the reaction system at various dwell times provides the equivalent kinetic information as would be found by analyzing samples from a closed reaction system as a function of times equal to the dwell times.

### Lyman- $\alpha$ Photometry

Lyman- $\alpha$  photometry is the most recent method for the detection of hydrogen atoms. First used in 1965 to detect hydrogen atoms formed in shock waves (72), it was developed primarily by J. V. Michael and various co-authors (1, 8-10, 27, 69-70). These experiments found that the apparatus could detect atomic concentrations as low as  $10^{10}$  atoms/cm<sup>3</sup>, and that the absorption followed Beer's Law (intensity linearly proportional to concentration) between 80% and 100% transmission. This range could be extended by calibrating the detector with some other detection method (69).

The hydrogen atom's emission/absorption lines can be predicted with the classical Rydberg formula,

$$\nu \text{ (cm}^{-1}\text{)} = R \left( \frac{1}{n_1^2} - \frac{1}{n_2^2} \right) \quad (17)$$

where  $\nu$  is the wavenumber corresponding to the line and  $R$  is the Rydberg constant,  $109,737.3 \text{ cm}^{-1}$ . The series of lines which occurs in the visible spectrum, the Balmer series, corresponds to transitions between the second and higher quantum numbers. The series of

ultraviolet lines which result from transitions to and from the first quantum level was discovered by Lyman and is called the Lyman series. The first line in this series, corresponding to the transition from  $n = 1$  to  $n = 2$ , is called Lyman- $\alpha$ . Its wavelength can be calculated using the Rydberg formula to be 121.5 nm.

A Lyman- $\alpha$  detector has three basic parts to be considered: the lamp used to produce the light, a filter required to limit detection to a narrow band around 121.5 nm, and a detector capable of measuring this ultraviolet light. Each of these parts has an effect on the way that the apparatus is operated, and on how sensitive the instrument will ultimately be. One of the overriding advantages of Lyman- $\alpha$  photometry is the simplicity of the equipment requirements, and this is reflected in nearly all of the systems found. The lamps are designed to produce Lyman- $\alpha$  radiation with as narrow a bandwidth as possible. This requires that the optical path length inside the lamp be as short as is possible within the requirements for lamp intensity. Also, the concentration of hydrogen ( $H_2$ ) in the lamp must be kept to a minimum in order to eliminate absorption within the lamp. The typical gas pressures inside one of these lamps are 10-20 microns  $H_2$  and less than 10 torr of some other gas, such as He or Ne (92). In one experiment (8), the lamp was filled with hydrogen and discharged. The hydrogen was then pumped out and the lamp filled with pure neon. The hydrogen which had been previously adsorbed onto the tungsten electrodes in the lamp then desorbed, and was the only hydrogen used in the lamp.

Once the Lyman- $\alpha$  radiation has been generated, it is necessary to detect it. An important part of this is to be sure what proportion of the light detected is Lyman- $\alpha$  and what proportion is due to background radiation. There are several ways in which this can be done. It is possible to design the detector itself to respond only to light which is within a narrow band around the Lyman- $\alpha$  line (14). However, it is much simpler to use a detector with a broad range and to filter the light in such a way as to select only the 121.5 nm light associated with Lyman- $\alpha$  emission. This filtering has been done both by passing it through a monochromator or through a flowing oxygen filter. Myerson et al. (72-73) used a monochromator adjusted to 121.5 nm to filter out all but the Lyman- $\alpha$  radiation. Although this is a perfectly acceptable technique, it is a waste to use a monochromator for such a minor task when another, simpler method may be used to give exactly the same result.

The simpler way to restrict the sensitivity of the detector to the Lyman- $\alpha$  radiation is to employ a filter to block out the interfering light. The simplest filter to use is a flowing stream of oxygen gas at a pressure of one atmosphere. Oxygen absorbs strongly over most of the vacuum-ultraviolet spectrum, but there is a narrow "window" of low absorption at 121.5 nm. This window means that a filter of 2 cm of oxygen will limit the background radiation seen by the detector to less than 5%, an effect which can be accounted for easily (13). The absorption of light by oxygen as a function of wavelength in the region surrounding the Lyman- $\alpha$  line is shown in Figure 8.

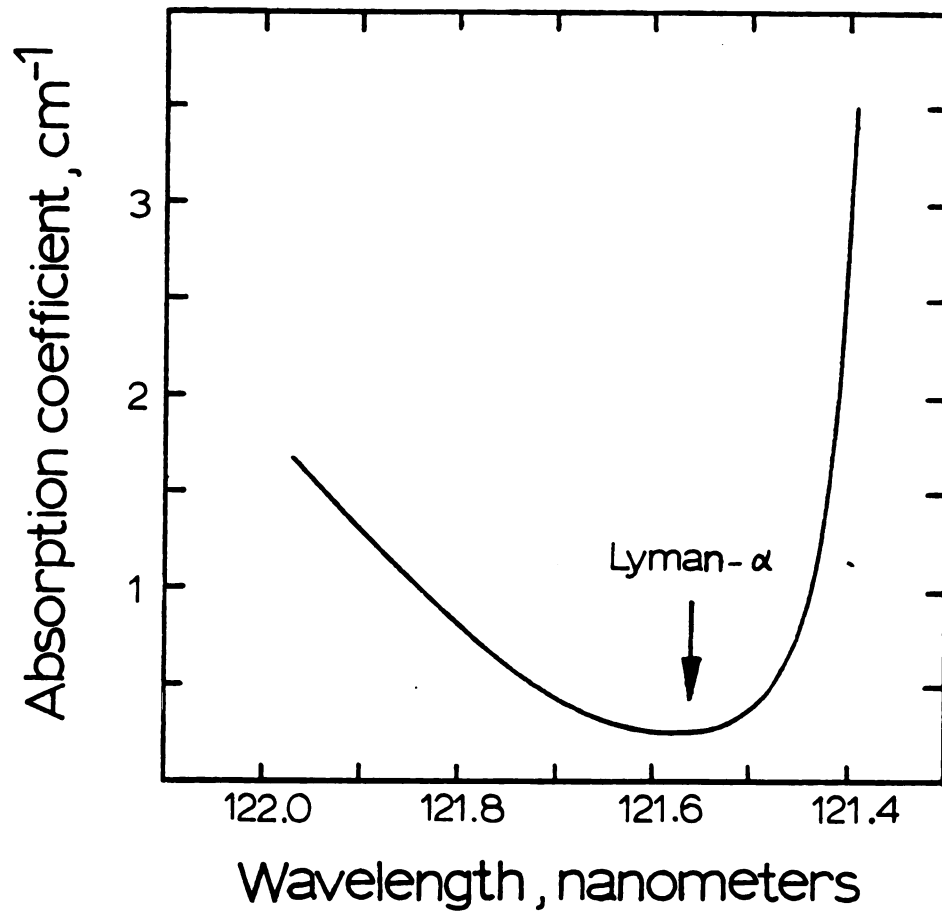


Figure 8.--Absorption of ultraviolet light by  $O_2$  in the vicinity of the  $H_2$  Lyman- $\alpha$  emission line (55).

The final component of a Lyman- $\alpha$  detection system is the detector. The nature of the detector determines the data which may be taken. These detectors are generally designed to be sensitive to a range of ultraviolet wavelengths, leaving it to the filter to limit the radiation to 121.5 nm. There are basically two types of detectors. Photon counters consist of a metal chamber containing a single electrode and filled with some easily ionizable filler gas such as iodine, carbon disulfide, or nitrogen oxide (15). When an electrical potential is placed across the gap between the wall and the electrode, an ultraviolet photon entering the detector will ionize the filler gas, allowing an electrical current to pass between the wall and electrode temporarily. These pulses of current can be counted over a certain time period, with the counting rate being proportional to the intensity of light reaching the detector. These detectors have been used in systems at steady state, as the detector measures an average photon rate, and any fluctuations in the rate of photon transmittance will be averaged out.

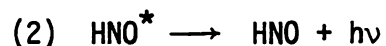
The last detector type to be considered consists of a conventional photomultiplier tube whose window is coated with a substance which fluoresces when struck by ultraviolet radiation (72-73). This method evades the necessity of detecting ultraviolet radiation by transducing it into visible radiation. The advantage of using a photomultiplier is that it allows monitoring of experiments in which the hydrogen atom concentration varies rapidly with time. The studies of Myerson et al. (72-73) were performed in a shock tube, in which the hydrogen atom concentration which was measured using this

type of detector changed from no hydrogen atoms to the maximum value within a period of a few milliseconds.

### Titration

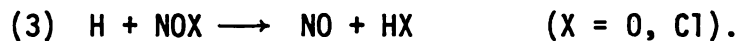
The two titration methods encountered in this survey differ in the means of analysis as well as the titrant. The ethylene titration method used by Halstead et al. (37) is a two-step measurement requiring a great deal of effort to obtain each measurement. The titrations based on observation of the red emission of HNO can be done continuously, but the toxic and corrosive properties of the various titrants make the use of the procedure difficult, as well as making accurate flow measurements difficult. The advantage which these methods have is that they are specific for hydrogen atoms and can therefore be used as standards against which other techniques may be calibrated (10).

The titration schemes based on the HNO emission all depend on the same basic reaction sequence



in which the second reaction is very fast. Since the intensity,  $I$ , is proportional to the product of  $[\text{H}]$  and  $[\text{NO}]$ , the relative hydrogen atom concentration can be found by examining the changes in  $I/[\text{NO}]$ . Therefore, titration with NO can be used to determine the relative concentration of hydrogen atoms.

The titration of hydrogen atoms with  $\text{NO}_2$  and  $\text{NOCl}$  can be used to measure the absolute concentration of hydrogen atoms. In these titrations, steps (1) and (2) are preceded by another step



The  $\text{NO}$  formed in this reaction then undergoes the subsequent reactions. If  $\text{H}$  is present in excess,  $[\text{NO}] \sim [\text{NOX}]_{\text{added}}$ , and the emission intensity

$$(4) \quad I = I_0 [\text{H}] [\text{NOX}]_{\text{added}}.$$

Recognizing that the initial hydrogen atom concentration,  $[\text{H}]_0$ , is given by the sum of  $[\text{H}]$  and  $[\text{NOX}]_{\text{added}}$ , the following equation relating the  $\text{NOX}$  addition rate (or concentration) to the emission intensity:

$$(5) \quad \frac{I}{I_0 [\text{NOX}]_{\text{added}}} = [\text{H}] = [\text{H}]_0 - [\text{NOX}]_{\text{added}}$$

By plotting the left-hand side of Equation (5) against the  $\text{NOX}$  addition rate, the intercept on the abscissa will be equal to the original hydrogen atom concentration. Alternatively, the rate of  $\text{NOX}$  addition can be adjusted until the emission is just extinguished, and this flow rate is then equal to the initial hydrogen atom flow rate. However, because this procedure introduces the uncertainty of judging the titration end-point, in addition to the uncertainties also present in the first method, the graphical method is recommended.

The ethylene titration method suggested by Halstead et al. (37) uses the reaction between the unsaturated hydrocarbon and hydrogen

to measure hydrogen atom flow rates. When ethylene is in excess, the amount of saturated products formed (in moles/sec) is exactly equal to the hydrogen atom flow rate. As used by Halstead, this method requires that a separate gas chromatographic analysis be made of the products of the reaction, which would be fairly time-consuming. A modification by Koda et al. uses a mass spectrometer to speed up the analysis of the product distribution (47).

### Magnetic Resonance

There are two analytical methods which can be placed in the category of magnetic resonance. The first, nuclear magnetic resonance (nmr) spectroscopy, has seen only limited use in the past. This appears to be due to a lack of versatility. The second, electron spin resonance (esr) spectroscopy, is probably the most sensitive and accurate atom detection method available at the present time.

Nuclear magnetic resonance spectroscopy (which, when restricted to hydrogen, is occasionally referred to as proton magnetic spectroscopy) depends on the fact that some nuclei have a magnetic moment. This can be interpreted as though the nucleus were spinning around an axis. Under the influence of a magnetic field, the axes of the nucleus become oriented either with or against the magnetic field. They remain oriented as long as the magnetic field is applied. If the nuclei are exposed to electromagnetic radiation with a certain frequency (usually in the radio-frequency part of the spectrum), the energy of that radiation can cause the axes to reverse their orientation, or "flip." The frequency which can cause this to happen is

related to the strength of the magnetic field applied to the sample. In practice, the radio signal's frequency is held constant, while the magnetic field strength is scanned through a range containing the field strength to which that frequency corresponds. This results in a graph in which the radio frequency absorption is plotted against the magnetic field strength. The pattern and relative strength of the absorptions are characteristic of the sample.

In the hydrogen atom experiments in which this technique is used (59, 82), hydrogen gas is sealed into a flask which is then discharged with a pulse of radio-frequency radiation. At a certain time,  $t_d$ , after the dissociating pulse, the spectrometer's transmitter is pulsed, allowing a measurement of the atom concentration. As this sequence of pulsing occurs (at a frequency of 1.5 cycles/sec), the magnetic field is scanned through the proton absorption, producing a spectrum for the specific value of  $t_d$  being used. The experiment can then be repeated at different  $t_d$  to obtain a complete picture of the kinetics of the reaction.

The esr spectrometer is probably the most accurate and versatile instrument for determining the concentrations of all free radicals, including hydrogen atoms. Although the instrumentation required is quite different, the idea behind this technique is the same as for nmr spectroscopy. Unpaired electrons exhibit the same property in a magnetic field as do the nuclei for which nmr spectroscopy may be used--they can orient either with or against the magnetic field, and the input of certain quantities of energy (in this case, microwave radiation) will cause the spins to "flip." The main difference in the

way that the equipment is operated is that a sinusoidal variation in the magnetic field strength is superimposed on the increase in strength which produces the spectrum. This variation causes the spectrum produced to be the first derivative spectrum of the microwave absorption as a function of the field strength.

Perhaps the greatest advantage possessed by esr spectrometry over other methods of free radical detection is that its calibration doesn't require the measurement of any free radical concentrations. In 1964, Westenberg and de Haas published a paper in which the esr intensity relations for one line of the hydrogen absorption was derived:

$$I_H = 2 \left( \frac{2kT}{hv_0 \beta f_t} \right) \int_0^{\infty} \chi'' dH \quad (18)$$

In this equation,  $\chi''$  is the complex magnetic susceptibility of hydrogen atoms,  $\beta$  is the Bohr magneton,  $v_0$  is the resonant microwave frequency,  $f_t$  is a "cavity filling-factor," and the remaining symbols have their usual meanings. A similar expression holds true for molecular oxygen, which has an esr spectrum because of its possession of unpaired electrons. The relationship between the calibration with  $O_2$  (designated by an  $O_2$  subscript) and the values associated with a measurement on an atomic species (at) is then given by

$$\frac{\chi_{at}}{\chi_{O_2}} = Q_{at} \left( \frac{M_{O_2}}{M_{at}} \right) \left( \frac{W_{O_2}}{W_{at}} \right)^{\frac{1}{2}} \left( \frac{P_{O_2}}{P_{at}} \right) \left( \frac{I_{at}}{I_{O_2}} \right) \quad (19)$$

where  $M$  = molecular weight

$W$  = microwave power level

$p$  = pressure

$X$  = mole fraction

and  $Q_{at}$  is a tabulated factor which is species-dependent (see Table 2).

The quantity  $I$  is equal to the integral of the absorption intensity over the field strength range of the absorption, and must be determined from the esr spectrum for the atomic species and  $O_2$ . Because the output from an esr is the first-derivative of the microwave absorption intensity, the value of  $I$  is determined by integrating the absorption curve twice.

In a series of papers (102-109), Westenberg and de Haas have developed the theory and practice of esr spectrometry. In particular, they have calculated the values of  $Q_{at}$  for a number of different atomic species, and used the results in kinetic series. The values of  $Q_{at}$  for atomic oxygen, nitrogen, and hydrogen are presented in Table 2. The factors for OH, Br, Cl, I, and free electrons have also been calculated (103).

### Summary--Detection

The detection methods which have been reviewed in this report can all be useful, to some extent, in the determination of hydrogen atom concentrations. The degree to which they are useful, however, depends on the specific details of the apparatus and experiment in which they are used. For example, the Wrede-Harteck gauge is fairly simple, and reasonably adequate when only hydrogen atoms are present

Table 2.-- $Q_{at}$  values for O, N, and H for several  $O_2$  lines (102).

$O_2$ Line	$Q_O$ (six line composite) $\times 10^{-3}$	$Q_N$ (one line of triplet) $\times 10^{-3}$	$Q_H$ (one line of doublet) $\times 10^{-3}$
C	2.02	5.88	1.96
E	3.71	10.8	3.61
F	5.64	16.4	5.48
G	1.67	4.88	1.63
J	4.40	12.8	4.27
K	4.96	14.4	4.82
B	1.07	3.12	1.04

in the gas being analyzed, but it would be inappropriate to use one in an experiment in which the gas contains a complex mixture of hydrogenated hydrocarbon radicals. The summary of detection methods which will be presented here will focus on those methods which would be most useful in an apparatus to be used for very general experiments on hydrogen atoms.

The requirement for generality will, for the most part, eliminate from consideration those detection techniques which aren't species-specific. The Wrede-Harteck gauge and catalytic probes are useful, especially the latter, but are restricted so much by the need for pure sources of atoms that their use would be eliminated in the most basic experiments. An additional factor which is against their use is that they are destructive analysis tools--in order to work, all of the hydrogen atoms which are present when the measurement is made are recombined. Although this isn't important when the reaction being studied can proceed concurrently, it becomes more important when reactions between hydrogen atoms and other molecules are being studied, as the measurement of the atom concentration must then be done in two steps, and the reproducibility of the atom source becomes an important factor.

Gas-phase titration of hydrogen atoms, a destructive species-specific detection method, suffers from the same drawback that the destructive nonspecific methods suffer from--all of the hydrogen atoms measured are lost in the measurement. However, the nature of the titration method makes it useful for the calibration of other

methods, as in that case it isn't necessary to use the hydrogen atoms for any other purpose.

The most useful methods for hydrogen atom detection are the spectroscopic methods because they are both species-specific and non-destructive. The use of mass spectrometers for hydrogen atom detection is made more difficult by the proximity of the molecular peak in the mass spectrum, but it is a useful device for the analysis of complex reaction mixtures that no other general detector can be used to study. Lyman- $\alpha$  photometry has the advantage of being far less expensive than the other spectroscopic methods to use and, once calibrated using some other method, can be used to measure a wide range of concentrations. ESR spectrometry, however, is probably the most versatile method for the detection of radical species. It has the advantage of being easily calibrated, and can be used to monitor many other species besides atomic hydrogen.

## KINETIC AND DISCHARGE PARAMETERS

One of the objectives of most gas-phase kinetics experiments is to generate a model of the system. This model can then be used to calculate values of any uncertain kinetic rate coefficients, or as a benchmark against which to compare the experimenter's understanding of the reaction system. In order to complete the modeling of any discharge, it is necessary to measure or estimate the values of the various parameters which are used by the model. In the following sections, past work in the kinetics of hydrogen discharges will be discussed and evaluated to the extent necessary for the development of such a model. This information will then be used to generate a model of an a.c. discharge in hydrogen which, although simple, can be examined to determine the factors which are most important in such a model.

### Gas Phase Recombination

Determinations of the gas-phase recombination rate coefficients comprise a major part of the literature available on the subject of hydrogen atoms (along with reactions between hydrogen atoms and hydrocarbons). There are two primary reasons for this fact: (1) hydrogen atom recombination rate constants, with the sole exception of those in which another hydrogen atom is the third body, are relatively easy to measure by adjusting the reaction conditions to eliminate competing

reactions, and (2) due to the (relative) simplicity of the theories of atomic recombination when applied to hydrogen atoms, the mechanics of atomic recombination can be calculated theoretically and the results related to experiment more easily than is the case for a complex system such as oxygen, where excited molecular species exhibit stability which can complicate the analysis.

Since the colliding atoms possess, at a minimum, a total energy equal to the dissociation energy, a third body is required in the recombination reaction to absorb the excess energy. The recombination reaction for hydrogen atoms and some general third species, M, is written



The identity of M depends on the species present in the reaction system and their relative abundance. Some experimental values for  $k_M$  can be found in Table 3 for various M. Careful examination of the table indicates that the values of this coefficient reflect the fact that the species M doesn't interact chemically with the hydrogen atoms, but merely accepts excess energy from them. It should also be noted that there is no entry corresponding to  $M = \text{H}$ . This species presents special problems experimentally which will be explained in a following section.

The experimental determination of most of the kinetic rate coefficients is simple, providing that the apparatus being used to determine the atomic concentration profiles is simple. What is essentially done is to perform an experiment in which the species M

Table 3.--Hydrogen gas-phase recombination rate coefficients.  $H + H + M \rightarrow H_2$ ,  $M = H_2, Ar, He$ .

M	$k \times 10^{-15}$ , $\text{cm}^6 \text{mole}^{-2} \text{sec}^{-1}$	Temperature Range, °K	Method (gen/det)	Reference
H <sub>2</sub>	10.4	...	Thermal/catalytic probe	5
	$2.7 \pm 0.4$	...	Microwave/ESR	13
	$10(0.243-1.95 \times 10^{-4}T)$	2500-7000	Shock tube/Na line reversal	42
	$3.0 \pm 0.1$	77-900	...	38
	$8.9 \pm 0.4$	...	Microwave/molecular diffusion	48
	$6.8 \pm 1.0$	...	rf/catalytic probe	53
	$2.9 \pm 0.14$	298	Thermal/catalytic probe	96
$6.7 \pm 0.8$	77	Thermal/catalytic probe	96	
Ar	$10(0.787-2.75 \times 10^{-4}T)$	2500-7000	Shock tube/Na line reversal	42
	$4.5 \pm 0.8$	...	rf/catalytic probe	53
	$4.6 \pm 0.5$	291	rf/catalytic probe	54
	1	1300-1700	Shock tube/OH concentration	58
	$3.3 \pm 0.2$	298	Thermal/catalytic probe	96
	$9.9 \pm 1.7$	77	Thermal/catalytic probe	96
He	$2.5 \pm 0.14$	298	Thermal/catalytic probe	96
	$4.3 \pm 0.5$	77	Thermal/catalytic probe	96

plays the predominant part in the recombination of hydrogen atoms introduced into the experiment. For example, in the case where the feed composition is 98:2 Ar:H<sub>2</sub> at a low pressure, argon will be the predominant species present in the gas phase. If the assumption is made that only the recombination catalyzed by argon is important, then any unrelated terms in the rate equation can be omitted (in this case, M=Ar and M=H), and the determination of  $k_{Ar}$  is straightforward. If the wall recombination term can also be made unimportant (for instance, by use of a wall coating to reduce the catalytic efficiency of the wall), then determination of  $k_{Ar}$  is made even more simple.

If it is desired that no assumption about the relative importance of the recombination terms be made, then it is necessary to perform some regression analysis to determine the rate coefficients from the experimental data. Because the values of regression coefficients depend on the data used to determine them, and are also inter-related (unless the regression uses special functions, such as Chebychev polynomials, as a basis), this technique must be used with care, and with due regard for the sensitivity of the coefficients derived to any errors in the data or assumed coefficients.

The case when M = H is one in which the simplicity referred to above doesn't hold true. The problem here is that the concentration of hydrogen atoms in most experiments is likely to be much lower than any of the other possible M species. This effect can be seen most clearly in the form of the rate equation for gas-phase recombination

$$r_H = \{ k_M' [M'] + k_{H_2} [H_2] + k_H [H] \} [H]^2 \quad (21)$$

where M' is some inert species such as argon. It is difficult to get high conversion of hydrogen molecules to atoms without using very low concentrations of hydrogen in an inert gas such as argon. However, this merely makes the first term rather than the second term greater than the  $k_H [H]$  term. For this reason, most of the values of  $k_H$  found in the literature must be viewed with some skepticism. Some representative values for  $k_H$  are given in Table 4, which was taken from reference 95.

Table 4.--Hydrogen atom recombination coefficients: M = H, T = 290-300 °K.

$k_H$ ( $10^{15} \text{ cm}^6 \text{ mole}^{-2} \text{ sec}^{-1}$ )	Reference
400	88
0.5	90
13.0	5

The spread of three orders of magnitude is typical of this kind of data. For this reason, a theoretical estimate of  $k_H$  was used in the model developed later in this report.

Theoretical treatments of hydrogen atom recombination use statistical mechanics and Monte Carlo simulations of collisions to determine the kinetic rate coefficients. These approaches have usually been classical in nature, primarily to avoid the added complication which comes from the inclusion of quantum mechanics in

the problem. The authors usually associated with these types of calculations are Shui (85-86) and Keck (45) and their co-workers. More recently, Roberts has had some success in using a semi-classical approach (which includes a limited use of quantum mechanics) to describe the reaction (110). It is this approach which will be used as a basis for the following discussion, as it appears to be more complete and accurate than the purely classical theories.

The basic strategy for calculating the rate coefficients using Monte Carlo is straightforward. After initializing the system of interacting species with a random initial configuration, including an appropriate collision energy, the equations of motion are used to follow the path of the species as they interact. By specifying the collision energy and varying the interaction parameter  $b$  (which is equal to the distance between the species' lines of flight), over a sufficient range, a reaction cross-section  $\bar{\sigma}(E)$  can be determined for that particular energy. As the collision energy is varied, the reaction cross-section is therefore determined as a discrete function of the collision energy. This cross-section function then gives the rate constant for the reaction through the integral

$$k(T) = (kT)^{-2} \int_0^{\infty} E \bar{\sigma}(E) \exp[-E/kT] dE \quad (22)$$

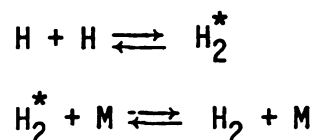
or some variation, depending on how the theory is constructed. For example, the Roberts theory uses the equation

$$k_r(T) = (kT)^{-2} \sum_i \bar{v}_r K_{eq}^i \int_0^{\infty} E \bar{\sigma}_i(E) \exp[-E/kT] dE \quad (23)$$

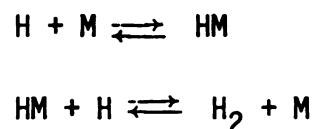
where  $\bar{v}_r = \left(\frac{8 kT}{\pi \mu}\right)^{\frac{1}{2}}$ ,  $\mu = \frac{M_{H_2} M_M}{M_{H_2} + M_M}$ ,  $K_{eq}^i$  is equal to the equilibrium coefficient for formation of the  $i^{\text{th}}$  collision complex, and the summation index,  $i$ , runs over all significant complexes.

The theoretical calculation of reaction rate coefficients is further complicated by the presence of two separate submechanisms to describe the energy transfer process. These two submechanisms are:

(a) the energy transfer mechanism



(b) the chaperone mechanism



The energy transfer mechanism accomplishes the transfer of the entire excess energy of the hydrogen atoms (measured relative to the energy of the stable hydrogen molecule they hope to form) to M in a single step. The chaperone mechanism transfers the same energy in two separate steps. The relative importance of these two mechanisms in the reaction with a particular M is determined primarily by the affinity of M for hydrogen atoms. Nonreactive species, such as the inert gases and molecular hydrogen, take part in the recombination through the energy transfer mechanism. This has been shown to be the case by Whitlock et al. (110), who calculated cross-sections for collisions between  $MH^*$  and H atoms for  $M = H_2$ . This information is reproduced in Table 5. The very large values for the dissociation

cross-section of  $MH^*$  indicates that this complex would almost certainly dissociate upon collision with another atom.

Table 5.--Cross-sections for collision of  $MH^*$  with H atoms for  $M = H_2$  (110).

State ( $v_{i,j}$ )	Energy E/k( $^{\circ}$ K)	Cross-Section $\text{Å}^2$			
		H <sub>2</sub> Formation	Stabilization to HM	Replace- ment of H	Dissocia- tion
(0, 1)	50	8.8 ± 4.3	13.3 ± 5.2	4.4 ± 8.1	>150
	300	0	2.2 ± 2.2	0	>175
(0, 0)	300	4.4 ± 2.5	...	1.5 ± 1.5	> 93

It should be noted that the submechanisms invoked in the theories of atomic recombination are not experimentally detectable, and that the distinction between hydrogen atoms used in discussing the chaperone mechanism for  $M = H$  is an artifact of the trajectory calculation. The hydrogen atoms are considered distinguishable in this kind of calculation, whether they are in fact or not.

The gas-phase recombination coefficients used in the model developed in this report were chosen primarily for the ease with which they could be used in the model. Since the coefficients for  $M = H_2$  are, for the most part, consistent with each other, no advantage was apparent in going to great lengths to achieve slightly more accurate values. The value of  $k_{H_2}$  used in the program was the function determined by Hurle, Jones, and Rosenfeld (42):

$$\log k_{H_2} = 15.243 - 1.95 \times 10^{-4} T \quad (24)$$

where  $k_{H_2}$  has units of  $\text{cm}^6 \text{mole}^{-2} \text{sec}^{-1}$ .

The lack of consistency in values for  $M = H$  argued for the use of a theoretical determination of this value. As the theoretical model developed by Whitlock et al. (110) was the most recent, and because it apparently fits the data for inert  $M$  well, the value of  $k_H$  used in the model was determined from their calculations. For ease of computation, their data (reproduced here as Figure 9) were reduced using a linear regression routine to the equation

$$k_H = 9.085 \times 10^{15} \exp [35.38/T] \quad (25)$$

where the units are again  $\text{cm}^6 \text{mole}^{-2} \text{sec}^{-1}$ .

### Wall Recombination

Wall recombination is a problem common to all experiments involving free radicals. In general, recombination of free radicals can involve virtually all species and surfaces to which the atoms are exposed. This involvement may either be helping to bring the radicals together (as in wall recombination) or by stabilizing the excited product of the collision of two radicals (as in homogeneous gas-phase recombination). The latter of these can be controlled to some extent by working at lower pressure. The wall recombination, however, is more complicated. The ability of a surface to catalyze recombination can be expressed as the fraction of atoms striking the surface which recombine there. This number, known as the wall recombination coefficient, has been measured for hydrogen on many surfaces (1, 55,

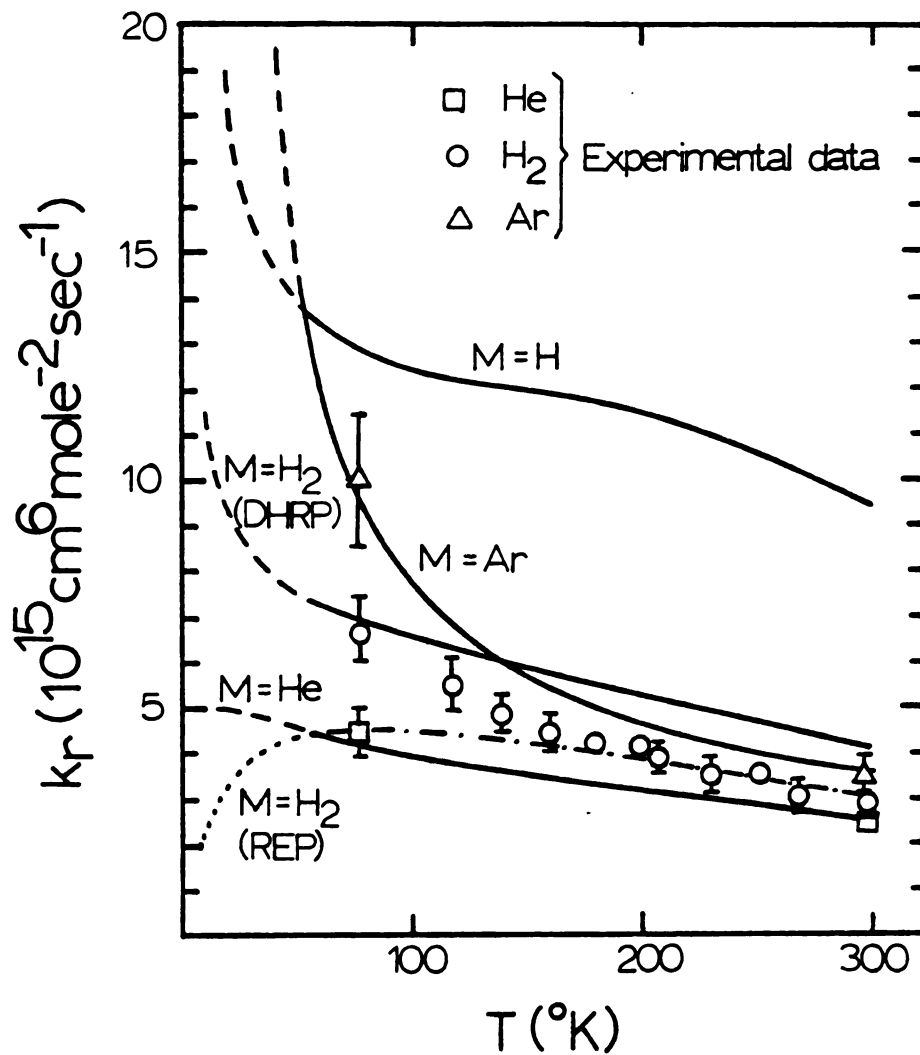


Figure 9.--Gas-phase recombination of hydrogen atoms: Theoretical rate coefficients for  $\text{H} + \text{H} + \text{M} \rightarrow \text{H}_2 + \text{M}$  for  $\text{M} = \text{H}, \text{Ar}, \text{He},$  and  $\text{H}_2$ . The REP curve for  $\text{M} = \text{H}_2$  calculated using a purely repulsive exponential potential; the DHRP curve calculated using an exp-6 potential (110).

74, 79, 98-99), and is related to the surface rate coefficient for a cylindrical surface by the equation

$$k_s = \gamma \bar{c}/4 \quad (26)$$

where  $\bar{c}$  is the average molecular speed and the recombination coefficient is  $\gamma$ .

Some values for  $\gamma$  are given in Table 6. The metals have the highest recombination coefficients, with platinum's being equal to one. Quartz has a coefficient on the order of  $10^{-3}$ , and Pyrex glass has a coefficient on the order of  $10^{-2}$ . Although the last two coefficients are quite small, they are important in many experimental plasmas. In addition, these coefficients can vary in any given experiment with the experimental history of the tube (77).

In order to control this variability and to lessen the importance of the loss mechanism, the walls of the tubing within and downstream from the discharge are almost invariably coated with a substance to reduce the wall recombination coefficient to a value on the order of  $10^{-6}$ . The substances most commonly used are phosphoric acid, Dri-Film (Silar Laboratories), and water. Phosphoric acid is applied as a syrupy coating to the walls of the tube, and has historically been the coating of choice (2). This coating has a tendency to flow, however, and the design of the apparatus must include some means of controlling this effect (30). Dri-Film has no such disadvantage, being a vapor-deposited mixture of methylchlorosilanes which polymerize on the tube (111). This coating has begun to overtake

Table 6.--Hydrogen atom wall recombination coefficients.

Material	Reference	Recombination coefficient(T, °K)
Pyrex glass	---	$4 \times 10^{-5}$ - $4 \times 10^{-2}$ (see Figure 10)
Quartz	1	.0012(298), .0018(333), .0023(369) .0032(369), .0045(470)
	89	.0007(298), .0034(798)
	113	.0028(300)
Phosphoric acid	89	.00002(288)
$Al_2O_3^\dagger$	89	0.33(288), 0.27(473), 0.22(673)
Platinum	89	1.0(288), 1.1(473, 673)
	112	$0.19 \exp[-1040/RT]$
	95	0.0089(661)
Tungsten	112	0.065(353), 0.054(578), 0.067(1088)
Aluminum <sup>†</sup>	112	0.29(328), 0.27(733)
Palladium	112	0.080(448), 0.052(673), 0.086(763)

<sup>†</sup>The entries for  $Al_2O_3$  and aluminum are so similar as to suggest that the pure aluminum surface might have become oxidized before the measurement of the recombination coefficient.

phosphoric acid as the coating of choice, due to its ease of application and the apparent permanency of the coating.

The use of water as a wall coating requires special mention, as there appears to be some question about how the coating functions. The use of water as a coating, or treatment, for the walls of a discharge tube stems from the observation made in 1922 by Wood (116) that it was difficult to find any hydrogen dissociation in discharges unless the hydrogen was saturated with water vapor. Wood apparently reasoned that the water coated the tube downstream from the plasma, while neglecting the possibility of water-catalyzed dissociation of hydrogen in the discharge. In fact, in the papers of Amdur (5), Amdur and Robinson (2), and Poole (76-8), the water saturation was used in conjunction with phosphoric acid coatings. The exact effect of the water is further confused by the papers of Kaufman and del Greco (44), who found that hydroxyl radical was continuously generated downstream from a discharge in water, and Rony and Hanson (79), who found that the addition of water to a microwave discharge in hydrogen had no effect on the yield of hydrogen atoms, while adding oxygen did have an effect. These results are contradictory at a basic level, as hydroxyl radicals generated downstream from the discharge could generate hydrogen atoms through the reaction



The effect of water on a hydrogen discharge could be deduced by modeling such a discharge, but the only model of a water-containing

discharge [Bell (12), who modeled the data of Poole (78)] completely neglected the water present in the hydrogen.

There are two types of experiment which can produce data on wall recombination. If the experimental conditions used allow it, the wall recombination coefficient can be included in a discharge model as a variable. Its value can then be determined in much the same way as any kinetic coefficient. This has been done by Mandl and Salop (59) and Amdur (5), who respectively modeled static and flowing systems. These experiments were atypical, however, since the recombination coefficient is usually minimized through use of a wall coating, and then neglected. The reason for this is that these experiments are most often concerned with determining other kinetic parameters, and the wall recombination reactions interfere with this work by limiting the hydrogen atom concentrations available.

The second type of experiment is responsible for most of the data on hydrogen atom wall recombination. The technique consists of allowing atoms from a discharge to diffuse into side-arms, one of which has a catalytic end-plate. The other sidearm contains an end-plate made from the material to be studied. The difference between temperatures of the side-arms (measured with a thermocouple) can be used to determine the value of  $\gamma$  (89, 112-113). The possibility of gas-phase recombination is minimized by operating at pressures of 60-80 microns. Similar techniques have been used to determine the recombination coefficient of oxygen atoms on several surfaces (57).

The experiments by Wood and Wise (112-113) concentrated primarily on recombination on Pyrex glass. Although five measurements were

made on quartz (primarily at room temperature), this was not emphasized. A similar lack of experimental data occurs for the "poisoned," or coated, surfaces. Although wall coatings like phosphoric acid and Dri-Film have been used to limit wall recombination in nearly all hydrogen atom experiments, any analysis of their effects appears to be limited to asserting that their use makes wall recombination negligible. It seems apparent (59, 82) that the value of  $\gamma$  for most coated surfaces is on the order of  $10^{-6}$ .

Theoretical modeling of wall recombination for hydrogen atoms has been restricted to glass surfaces. The reason for this is the previously described lack of experimental data for any other surfaces. There have been two approaches to this modeling. The first approach (112-113) was to include both Rideal ( $S-H + H \rightarrow S + H_2$ ) and Hinshelwood ( $S-H + S-H \rightarrow 2S + H_2$ ) mechanisms, where S is the surface to which the hydrogen atoms are adsorbed. Although the agreement between this model and the experimental data over the temperature range 77-250 °K is good, the agreement breaks down outside that range. This behavior has been attributed to inclusion of the Hinshelwood mechanism (35). These authors achieved far better agreement over the entire temperature range of experimental data by using only the Rideal mechanism in the analysis. Their analysis also reproduces the temperature dependence of the wall recombination reaction order which has been experimentally observed. This dependence is as follows:

	$T < 48.5 \text{ }^\circ\text{K}$	1st order
48.5 °K < T < 111 °K		2nd order
111 °K < T < 833 °K		1st order
T > 833 °K		2nd order

The basis for this behavior is the presence of two types of binding sites on the glass surface, with heats of adsorption of 42 kcal/mole and 2.1 kcal/mole. Because these energies are far apart, the adsorption of hydrogen to each kind of site is independent of the other type of site, and the overall value of  $\gamma$  is the sum of the contributions from each type of site. The results of this study, along with the experimental data which support it, are reproduced in Figure 10. It should be observed that no experimental data exist to support their results for extremely low temperatures. This, and the application of the model to other surfaces, remains to be done.

In the hydrogen discharge model presented in the following sections, the value of the recombination coefficient has been used as a variable. The primary reasons for doing this are: (1) the indeterminacy of the wall temperature in the discharge zone; (2) the use of quartz discharge tubes in the apparatus; and (3) the probable use of wall coatings in the experimental apparatus. When actual measurements of the tube temperature, quartz recombination coefficient, and coated surface recombination coefficient can be obtained, those values could be used in an enhanced model.

### Discharge Parameters

Although the recombination data previously described are necessary in almost any discharge model, the most important information which is required is that which describes the effects of the discharge on the dissociation of hydrogen. These effects are manifested in the electron density,  $n_e$ , and the dissociation rate constant,  $k_d$ , both

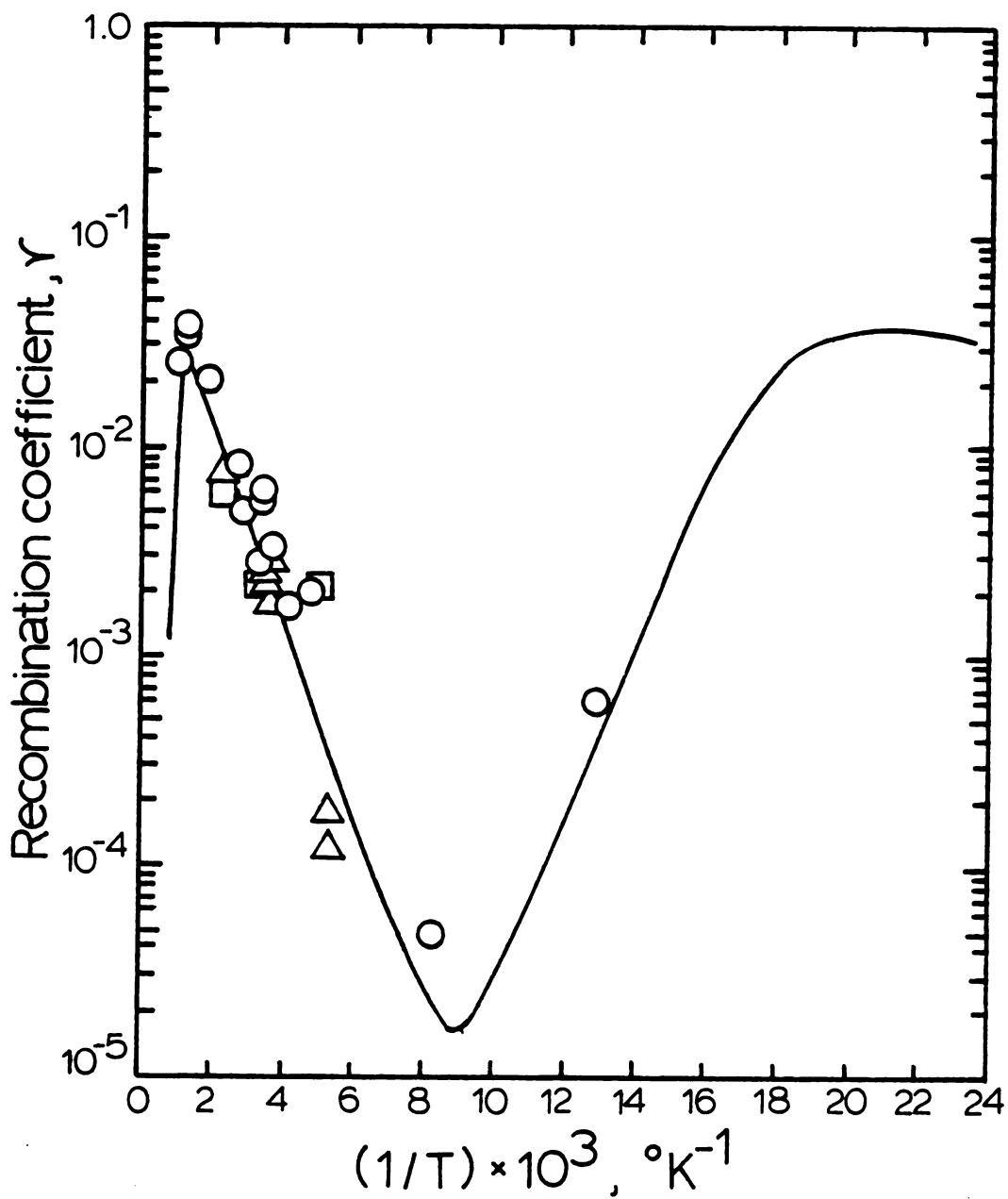


Figure 10.--Theoretical and experimental values of the wall recombination coefficient (35).

of which are dependent on discharge features which are only partially understood. The primary work on the task of coupling of these two quantities to measurable quantities for use in kinetic modeling was done by Bell (12). His theoretical developments were used in the model of hydrogen discharges which is presented here.

The determination of an electron-impact dissociation rate constant parallels closely the theoretical determination of gas-phase recombination coefficients described earlier. Cross-sections, which in this case are derived from experiment and not from theoretical Monte Carlo calculations, are integrated over the total range of electron energy to result in a rate constant which is a function of the electron temperature. Work done by Varnerin and Brown (97) allows the rate constant to be considered to be a function of the quantity  $E_e/p$ , in which  $E_e$  is an effective electric field strength and  $p$  is the gas pressure. This quantity is important because the electron density can be expressed as a function of  $E_e/p$ .

In the models to be presented in this paper, the dissociation constant determined by Bell (12) was used. In order to make the use of a computer for this discharge model easier, Bell's results, reproduced in this paper as Figure 13, were converted by a linear regression routine to the following formula:

$$k_d \text{ (cm}^3\text{/sec)} = 2.7857 \times 10^{-15} (E_e/p)^{4.0591}$$

This equation is in qualitative agreement with the expected limiting behavior of  $k_d$ . As the electron temperature (and therefore  $E_e/p$ ) approaches infinity, the dissociative rate constant would also be

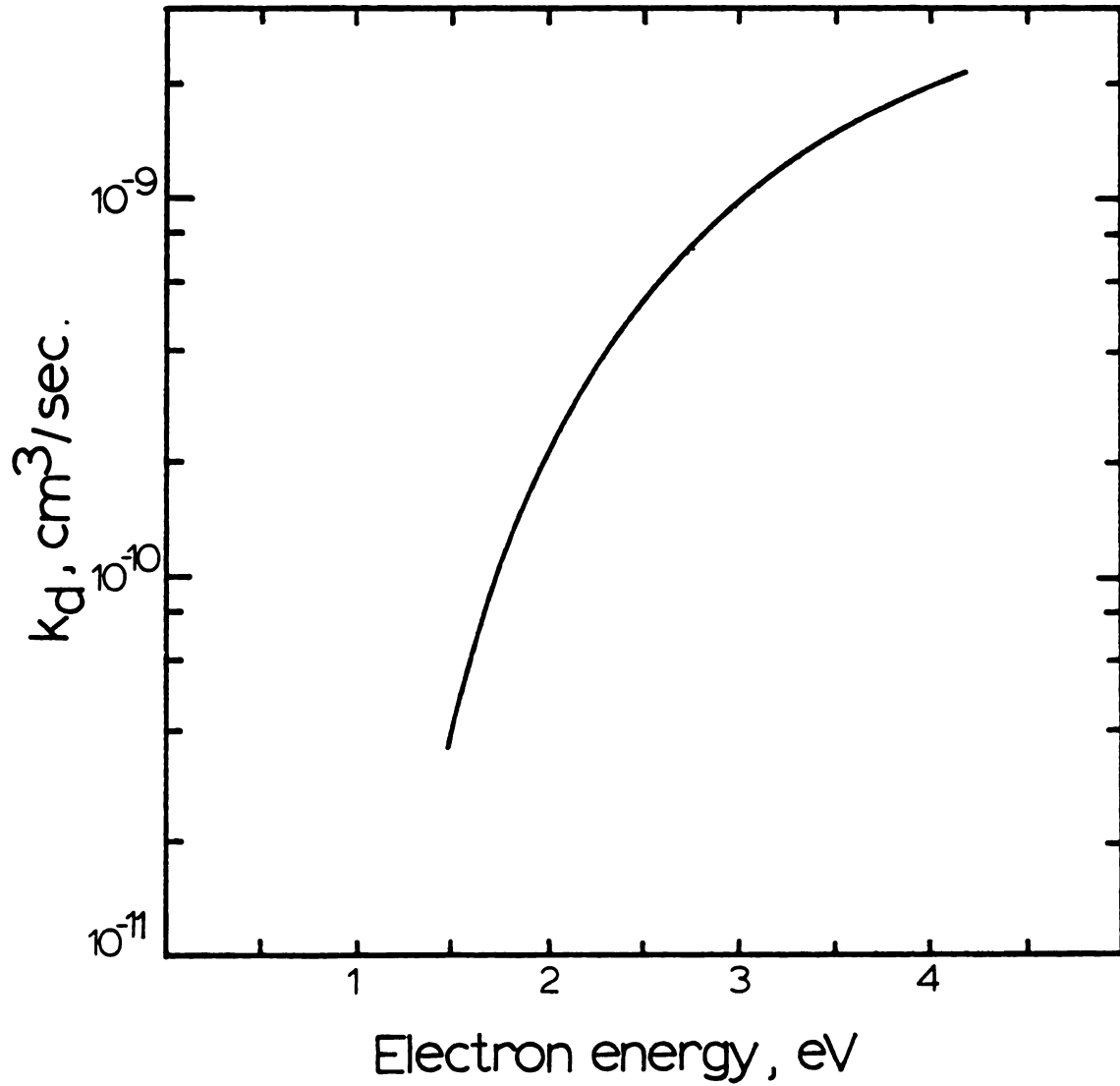


Figure 11.--Dependence of electron-impact dissociation rate constant on the electron energy (12).

expected to go to infinity, since the impact of an infinitely fast electron would certainly transfer sufficient energy to cause dissociation. As the electron temperature approaches zero, the probability of a collision causing dissociation would also be expected to approach zero, as a very slow electron would transfer a negligible amount of energy. In this case, the agreement between the expected behavior of  $k_d$  and that predicted by Equation 19 is not as good, as the equation predicts that the coefficient would decrease to a constant value of  $2.7857 \times 10^{-15} \text{ cm}^3/\text{sec}$ .

The quantity  $E_e/p$  which was just used to determine the dissociation rate constant occurs in the theoretical calculation of both that rate constant and the average electron density. It was first determined by Rose and Brown (72) as a function of the quantities  $p\Lambda$  and  $n_e^2$ . The characteristic length,  $\Lambda$ , results from the theoretical description of gaseous discharges, and is dependent on the geometry. In the case of a cylindrical discharge,  $\Lambda$  is equal to the tube radius divided by 2.405, which is the first zero of the Bessel function  $J_0$ . As before,  $p$  represents the discharge pressure. The value of  $n_e^2$  for the types of discharge being modeled is large enough that it can be considered to be infinite, allowing the determination of  $E_e/p$  solely as a function of  $p\Lambda$ . As was the case with the dissociative rate constant, a linear regression of the curve presented by Bell and reproduced as Figure 12 was used in the computer model described here. The formula which resulted was:

$$E_e/p = 15.8304 (p\Lambda)^{-0.3927} \quad (29)$$

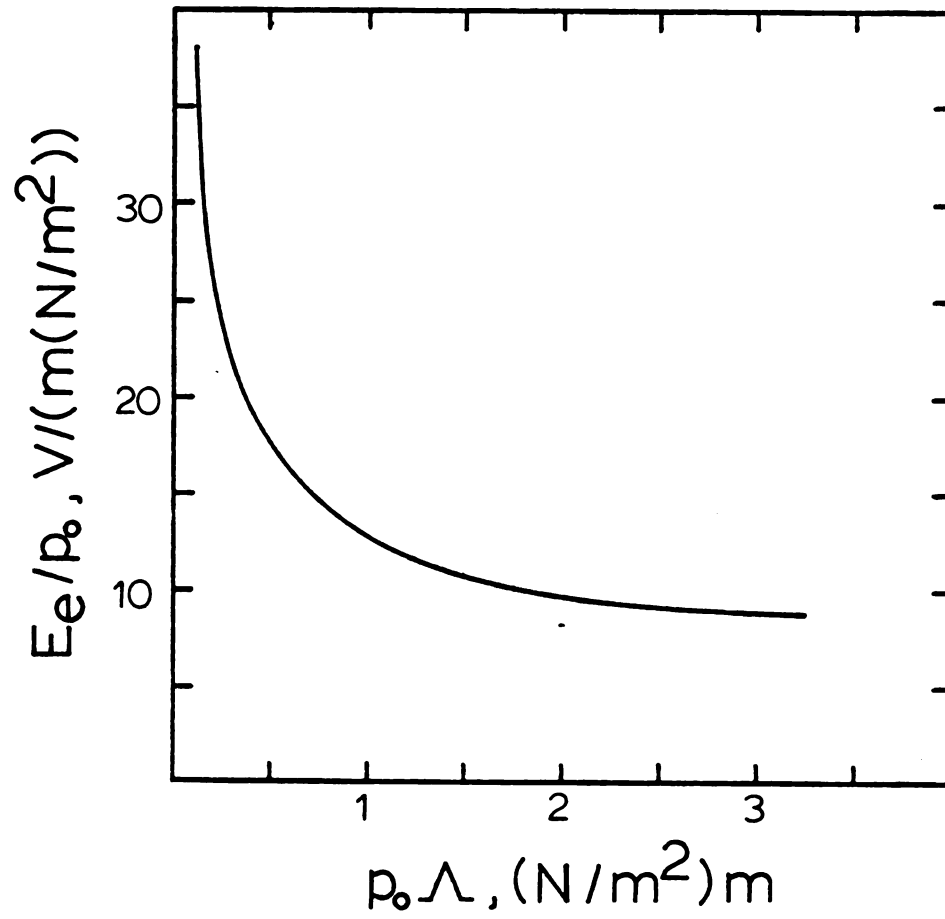


Figure 12.--Relationship between discharge parameters  $E_e/p$  and  $\rho\Lambda$  (12).

The qualitative behavior of this formula also matches that expected for  $E_e/p$  versus  $p\lambda$ .

The electron density can either be determined experimentally or by theoretical calculations. The experimental determination of electron densities in d.c. discharges and low-power a.c. discharges is well documented, and the Langmuir probes which are used can provide useful information. However, the use of a probe for the measurement of electron densities in a high-power a.c. discharge is not possible for safety reasons. Any metal object which is placed in an operating microwave discharge (as a probe must be) and projects outside the discharge zone can serve as a channel for the transmittal of microwave energy outside the discharge. This could damage the electronic apparatus connected to the probe and radiate considerable amounts of microwave radiation into the laboratory. This effect is most important for the high-power microwave discharges which are under consideration here. For these reasons, the experimental apparatus to be proposed in the final section of this report will determine electron densities from the Stark broadening of the hydrogen Balmer- $\beta$  line. This optical method, although it requires a considerable investment in apparatus, is both safe and more accurate than the probe method (36).

The alternative to experimental measurement of electron densities (and the only choice for modeling of the discharge) is the use of a theoretical analysis of the discharge to determine a function relating the electron density to measurable properties of the discharge. The most prevalent equation was developed by Bell in 1972 (12)

and later used by Mearns and Ekinici (65). The derivation of the equation is given in Bell's paper, and only involves the integration of a point power input over the discharge volume, resulting in the following equation:

$$\frac{n_e}{\bar{P}\Lambda} = \frac{4.85 \times 10^9 m_e}{e^2 p \cdot \Lambda (E_e/p)^2} \quad (30)$$

where  $\bar{P}$  = microwave power density, watts/cm<sup>3</sup>. After substituting appropriate values for the constants, and bringing the units into consistency, the equation becomes:

$$n_e = \frac{3.8398 \times 10^{13} P \Lambda}{V_D (p\Lambda) (E_e/p)^2} \quad (31)$$

where  $n_e$  has units of cm<sup>-3</sup>,  $P$  is the total power to the discharge in watts, and  $V_D$  is the discharge volume in cm<sup>3</sup>. This is the equation used by Bell.

Although Equation 31 was used by Mearns and Ekinici (65), they also used a Langmuir probe to determine the electron densities experimentally (this was made possible by the low microwave power levels used in their experiment). Figure 13, which is reproduced from their paper, shows that the agreement between their data and theoretical prediction is not very good, and gets worse as the power increases. Since it is high power levels that are of the most experimental interest, this discrepancy is significant. The solution which has been arrived at for the model to be described in this paper is to treat the electron density as a variable. Although this means that

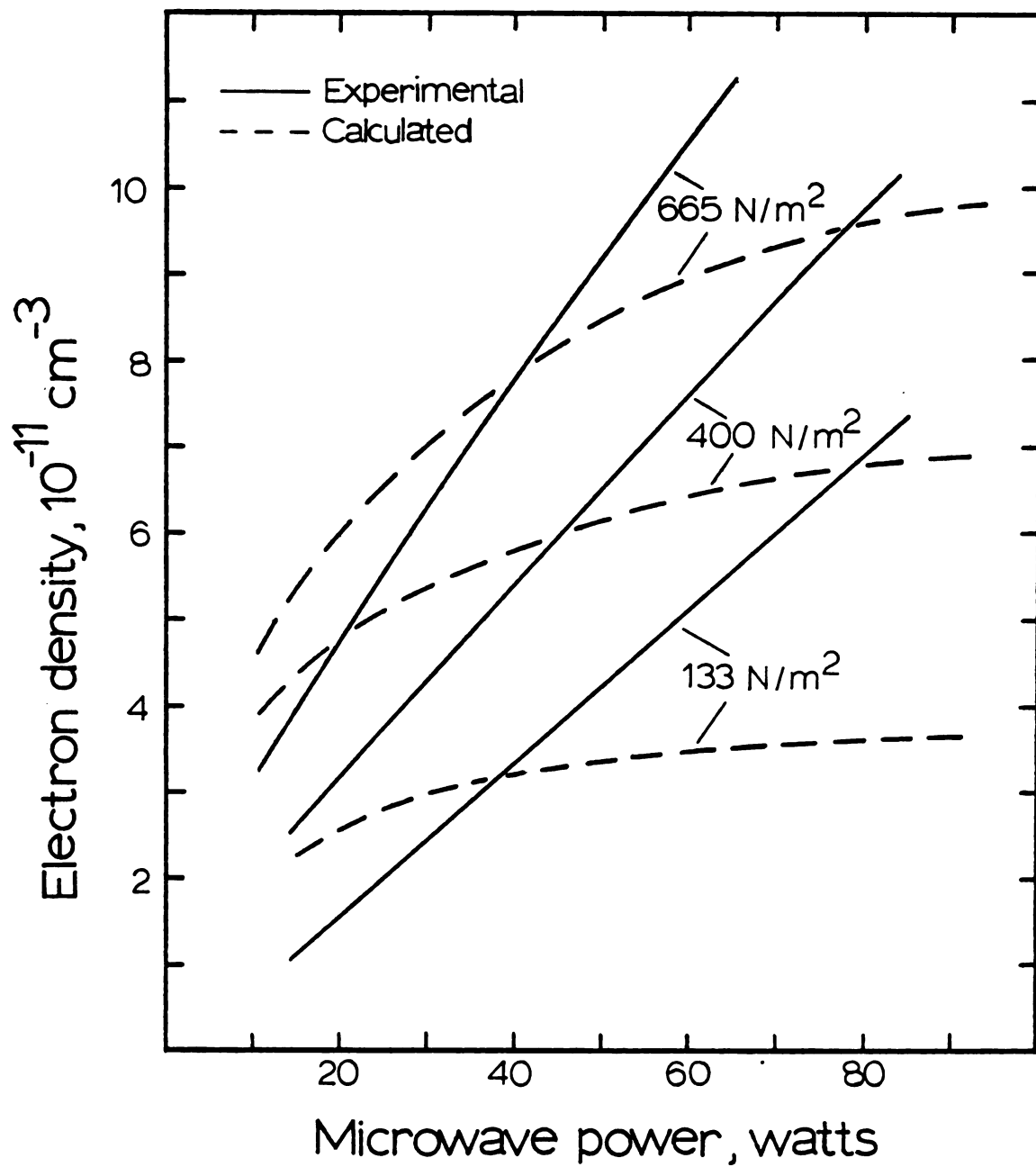


Figure 13.--Comparison of theoretical and experimental electron density as a function of microwave power input (65).

little information can be obtained to relate conversions to the power inputs, it does allow for more flexibility in the model itself. For the sake of comparison, a series of calculations were also made in which Bell's model was used to calculate the electron density.

## MODELING THE MICROWAVE DISCHARGE

Having determined the generation and detection methods to be used in the apparatus, as well as some of the kinetic parameters within the discharge, the discharge can now be mathematically modeled. The goal of this modeling is to develop preliminary, qualitative generalizations about the behavior of the discharge under different experimental conditions. This information can be used as a temporary substitute for laboratory experience (to be used during the design of the apparatus) and also for determining the experimental variables, if any, towards which the model displays any sensitivity and which, therefore, must be measured more accurately in any experiment to be modeled.

### Rationale

The development of the discharge model has been based on several assumptions. Since this was intended to be a preliminary effort, no attempt was made to include all factors which might have some effect on the conversion within the discharge. In some cases, the theories presently available for estimating the values of kinetic parameters aren't sufficiently well-developed to be useful, and assumptions were used to make the modeling possible. More often, however, an assumption was used to make the calculations of discharge conversion more simple, so that a larger range of experimental conditions could be examined.

In this discussion, the assumptions which were used in the model will be outlined, and the reasons for their use given.

The greatest barrier to the development of a discharge model capable of accurately predicting outlet conversions for any arbitrary set of reaction conditions is the lack of an adequate discharge theory relating the electron properties (density and energy distribution) to the experimental parameters which determine them (reactor geometry, power input, and pressure). A commonly used discharge theory was developed by Bell in 1972 (12), and was based on an assumption that the dependence of the electron density on the microwave power density is uniform throughout the volume of the discharge. However, this theory has been shown to underpredict the electron density at power levels as low as 40 watts, with the error becoming greater as the power level increases (65; see Figure 13). That trend in the error increase is especially important because the microwave source to be used in the proposed apparatus (a modified microwave oven [67,68]) is at least an order of magnitude more powerful than the source used by Mearns and Ekinici (65).

The electron density is one of the quantities appearing in the discharge model whose inclusion in the model is made more difficult by the lack of an adequate discharge theory. The electron density in a microwave discharge is partially determined by the type of gas being discharged, its density, and the tube diameter (12). It also depends on the electron energies (through the ionization reactions which occur in the discharge), the frequency of the microwave

radiation, and the power input to the discharge (12,80). Finally, since the electric field strength can vary with position in the discharge (the resonance modes in the cavity have structure), a spatial variation of the electron density might be expected within the discharge.

By virtue of their dependence on the hydrogen atom concentration, the gas and wall temperatures are indirectly dependent on the electron density and, therefore, on any theory for predicting the electron density. Any increase in the rate of the exothermic recombination reactions will have the effect of raising the local temperature. This increase in the recombination rate could be brought about by an increase in the hydrogen atom concentration, which would be the effect of a higher electron density. The local temperature increase would be experienced more severely by the wall of the discharge tube than by the gas, since the gas is in contact with the discharge for a fraction of a second, while the tube is in contact with the discharge continuously.

The difficulties in modeling the electron density in a microwave discharge can be surmounted in either of two ways. The theory developed by Bell (12) can be used, despite the shortcomings it has as shown in Figure 13, with the understanding that the predicted electron densities are much too small. The alternative approach is to use the electron density as a variable in the calculation and vary it through a range great enough to include the probable value in the discharge. Although the second approach was the one used most often in the model

discussed here, Bell's theory was used in a few calculations in order to compare the two approaches.

Because the methods for modeling the electron density in this model are so crude, and since the model was only intended to be a preliminary attempt, the gas and wall temperatures weren't calculated from a complete energy balance within the discharge. Two different operating variables resulted from this simplification: the gas temperature and the wall recombination coefficient. The gas temperature, once fixed, was sufficient information to determine the gas-phase recombination rate coefficients used in the model, since the relationship between these coefficients and the gas temperature is well defined. On the other hand, the relationship between wall temperature and wall recombination coefficients isn't very well defined on glass, and even less well defined for other wall materials. Therefore, the wall recombination coefficient, and not the wall temperature, was chosen as the other modeling variable.

It was assumed for computational simplicity that the microwave discharge could be modeled as a continuously-stirred tank reactor (CSTR). In this ideal reactor model, the species concentrations and the temperature are assumed to be uniform throughout the discharge volume, with the result that the outlet concentration of hydrogen atoms is given by the solution of a fourth-degree polynomial. In contrast, the use of a plug-flow or laminar-flow reactor model (both of which are differential models) would require an integration over the length of the reactor to determine the outlet concentration. Due

to the wide range of experimental conditions to be examined, and the large number of separate calculations to be made during that examination, the faster algebraic solution of the CSTR model was preferred over the integrated solution of the other two models.

The CSTR model for the discharge, although convenient when calculating the conversion, presumes the existence of mixing within the discharge. Although this mixing is usually the result of turbulence in the fluid, the flow within a low-pressure discharge can be shown to be nonturbulent. At the pressures typically found in gas discharges ( $\sim 0.5$ - $20.0$  torr), the maximum capacity of most rotary vacuum pumps limits the flow rate through the discharge to  $F_0 = 0.06$  moles  $\text{sec}^{-1}$ . This value can be used to calculate the Reynolds number,  $N_{Re}$ , for the discharge. The Reynolds number is a dimensionless number which indicates the presence of turbulent flow within a tube when greater than 2200:

$$N_{Re} = \frac{D_t u \rho}{\mu(T)} = \frac{4F_0 M_w}{\pi \mu(T) D_t} \quad (32)$$

where  $\mu(T)$  is viscosity,  $M_w$  is the molecular weight,  $\rho$  is the gas density,  $D_t$  is the diameter of the tube, and  $u$  is the velocity through the tube. When the Reynolds number is calculated using  $F_0 = 0.06$  moles  $\text{sec}^{-1}$ ,  $D_t = 2.50$  cm, and a kinetic theory approximation for the hydrogen viscosity (64), it is found to be equal to 250. Since this represents an upper limit on  $N_{Re}$  (most flow rates are much lower than  $0.06$  moles  $\text{sec}^{-1}$ ), it is an indication that the flow through the discharge is nonturbulent.

Despite the lack of turbulence in the discharge, it may still be possible to treat the discharge as a CSTR, since other effects like thermal mixing, uniform electron densities, or electromagnetic effects could cause either mixing or uniformity of atom concentration within the discharge. The presence of thermal gradients in the discharge, for example, could give rise to mixing as a result of differences in gas density. The hydrogen atom concentration might also be made essentially uniform if the electrons' ability to move freely in the discharge is great enough to cause the hydrogen dissociation rate to be much larger than the recombination rate. In either case, the effect will be to make the discharge behave like a CSTR to some extent.

#### Development of the Discharge Model Equation

The final step in the development of this hydrogen discharge model is the development of the mathematical relationship between the experimental parameters (pressure, temperature, etc.) and the conversion of molecular hydrogen to atoms within the discharge. This relationship, or modeling equation, is developed from a balance of mass around the discharge and takes advantage of the characteristics of the CSTR model. In particular, the fact that the concentration of hydrogen atoms in the discharge outlet stream is identical to the concentration within the discharge itself is used to simplify the model equation to a fourth-degree polynomial in the conversion.

The analysis of the discharge model is done by calculating the outlet conversion for a range of experimental parameters broad enough

to include any conceivable experiment. Comparison is made easier by assigning to four of the experimental parameters a "standard value" selected from the literature as being typical for microwave discharges. The calculation of outlet conversion is done while varying one parameter through its range, with the remaining variables being kept at their standard values.

The development of the model equation begins with the derivation of the rate expression which describes hydrogen atom production in the discharge. This expression, which has the units of  $\text{mole cm}^{-3} \text{sec}^{-1}$ , is a linear combination of rate expressions for each of the elementary reactions which occur inside the discharge. These reactions, their rate expressions, and the rate expression for the discharge are shown in Table 7. Because wall recombination is expressed as a surface rate ( $\text{moles cm}^{-2} \text{sec}^{-1}$ ), the corresponding term in the rate equation must be multiplied by the reactor's surface-to-volume ratio,  $R$ , to bring the units into agreement. For the cylindrical reactor considered here, the surface-to-volume ratio is  $4/D_t$ .

The model equation itself is developed from the steady-state mass balance around the discharge. Expressed in terms of the hydrogen atoms themselves, this balance equation is

$$\begin{aligned} \text{moles H at reactor outlet/sec} = \\ \text{moles H produced in the discharge/sec} \\ + \text{moles H at reactor inlet/sec} \end{aligned} \quad (33)$$

This can be further simplified, since the rate of atom production in the discharge is given by  $r_H V$  (where  $V$  is the volume of the discharge),

Table 7.--Reactions and rate expressions to be used in the discharge model.

Reaction	Contribution to H atom production
$e^- + H_2 \xrightarrow{k_d} 2H + e^-$	$r_1 = 2k_d n_e [H_2]$
$H + H + H_2 \xrightarrow{k_{H_2}} H_2 + H_2$	$r_2 = -2k_{H_2} [H_2][H]^2$
$H + H + H \xrightarrow{k_H} H_2 + H$	$r_3 = -2k_H [H]^3$
$H \xrightarrow{\text{wall}} \frac{1}{2}H_2$	$r_4 = \frac{\gamma \bar{C}}{4} [H]$
Overall rate expression	
$r_H = 2k_d n_e [H_2] - 2k_{H_2} [H_2][H]^2 - 2k_H [H]^3 - \frac{\gamma \bar{C}}{4} [H]$	

and also because there is no atomic hydrogen coming into the reactor at the inlet:

$$\text{moles H at reactor outlet/sec} = r_H V \quad (34)$$

This equation is the basis for the model equation.

Although the model equation could be solved in its present form, any analysis of the modeling results will be easier if the concentration terms are re-expressed in terms of the H<sub>2</sub> conversion, X. The advantage of this substitution is that, unlike concentration, conversion separates the extent of reaction from the gas density. The model equation's terms, expressed as conversion, are

$$\text{moles H at outlet/sec} = F_0 (2X) \quad (35)$$

$$[H] = \frac{2X}{(1+X)} \beta \quad (36)$$

$$[H_2] = \frac{(1-X)}{(1+X)} \beta \quad (37)$$

where  $\beta$  is the gas density,  $p/RT$ , and  $F_0$  is the hydrogen flow rate into the discharge. After making the substitutions, clearing fractions, and rearranging, the modeling equation becomes a fourth-degree polynomial in X:

$$AX^4 + BX^3 + CX^2 + DX + E = 0 \quad (38)$$

where  $A = 2F_0$

$$B = 6F_0 + \frac{1}{2}\pi D_t^2 L k_d n_e \beta + 4\pi D_t^2 L k_H \beta^3 - 2\pi D_t^2 L k_{H_2} \beta^3 + \frac{1}{2}\gamma \bar{c} \pi \beta D_t L,$$

$$C = 6F_0 + \frac{1}{2}\pi D_t^2 L k_d n_e \beta + 2\pi D_t^2 L k_{H_2} \beta^3 + \gamma \bar{c} \pi \beta D_t L,$$

$$D = 2F_0 - \frac{1}{2}\pi D_t^2 L k_d n_e \beta,$$

$$E = \frac{1}{2}\gamma \bar{c} \beta \pi D_t L,$$

and where  $\bar{c}$  is the mean molecular speed ( $= \sqrt{8kT/\pi m}$ ),  $D_t$  is the tube diameter, and  $L$  is the discharge length (both with units of cm).

This is the equation used to model the hydrogen discharge.

The strategy for analyzing the discharge model was simply to calculate the outlet conversion at as many different combinations of the experimental variables as possible. The analysis was divided into three sets of calculations. First, the outlet conversion was calculated over the entire range of flow rates, under all possible combinations of the pressure, recombination coefficient, gas temperature, and tube diameter, and with the electron density held constant at its "standard value" of  $10^{12} \text{ cm}^{-3}$ . The electron density was then varied over its entire range, with the flow rate, gas temperature, and tube diameter held at their respective standard values. This calculation was repeated for all of the pressures and recombination coefficients used in the first calculation. Finally, Bell's discharge theory (12) was used to calculate the electron density from the microwave power input, with the resulting conversion being plotted versus flow rate for pressures between 0.5 and 10.0 torr. The experimental parameters, their standard values, ranges, and the references from which the standard values were drawn, have been summarized in Table 8.

Equation 38 was solved by using a Newton-Raphson iteration technique. After establishing the value of all experimental parameters, the coefficients A-E were calculated, and an initial value

Table 8.--Experimental parameters used in the discharge model.

Variable	Range	Standard value	(ref)
Flow rate, $F_0$ , $\mu\text{moles sec}^{-1}$	50-10,000	500	(65)
Electron density, $n_e$ , $\text{cm}^{-3}$	$10^{10}$ - $10^{20}$	$10^{12}$	(67,68)
Gas temperature, $T$ , $^{\circ}\text{K}$	300-1000	400	(65)
Tube diameter, $D_t$ , cm	1.25-5.0	2.50	(67,68)
Pressure, $p$ , torr	0.5-760.0	---	
Recombination coefficient, $\gamma$	$10^{-6}$ - $10^{-1}$	---	
Power input, $P$ , watts	100-3000	---	
Discharge length, $L$ , cm	---	30.0	(65)

of  $X = 0.5$  stored. The iteration continued until the relative difference between successive iterations fell below  $10^{-5}$ , at which point the solution was stored in a result matrix. A listing of the Fortran program, which was run on a CDC Cyber 175-750 computer at Michigan State University, is located in Appendix A.

### Results of the Discharge Modeling

The objectives of the modeling done in this research were twofold. The primary objective was to develop a general understanding about the behavior of the discharge under different experimental conditions for use in designing the hydrogen discharge apparatus. The information gained in this manner could be used as a way of becoming familiar with the discharge's characteristics before any experimentation was begun. Another use for the information could be to determine the conditions under which the conversion of hydrogen molecules to atoms could be maximized.

The secondary objective of the modeling was to determine whether the model is particularly sensitive to variations in any of the experimental parameters. Any such sensitivity would become especially important if an attempt was made to model the actual conversion data from the experimental apparatus. A knowledge of the parameters which affect the model most significantly would make it possible to stress their accurate measurement, either eliminating or reducing a potentially severe source of error in the calculations.

Both of these objectives were met in this research by plotting curves in which the changes in conversion which occur upon the vari-

ation of specific experimental parameters can be clearly seen. The numerical output from the computer program was plotted in either of two forms for analysis. In most cases, the outlet conversion (y-axis) was plotted versus the flow rate entering the discharge (x-axis). In cases where the electron density was the parameter of interest (or where the behavior of the discharge could be shown more clearly), a semi-logarithmic plot of conversion (y-axis) versus  $\log_{10}$  [electron density] (x-axis) was used.

The quantitative behavior of the model is presented in five series of related figures. Within each series, in addition to the conversion and the x-axis variable, two other experimental variables are used as parameters in creating the graphs. One of these parameters is varied through a range of values within each figure, creating a family of curves. The remaining parameter is kept constant within each figure, but is changed from figure to figure within the series. The advantage of using two parameters to produce figures is the large amount of data which can be presented in concise form.

The effects of pressure on conversion are shown in Figures 14-16, where the conversion is plotted versus flow rate for several pressures, and at three different wall recombination coefficients. As expected, conversion is high for the low pressures and flow rates. The dependence on flow rate can be attributed to the increased residence time which results from low flow rates. The decrease in conversion which accompanies a pressure increase is a result of the third-order density dependence of the gas-phase recombination rates.

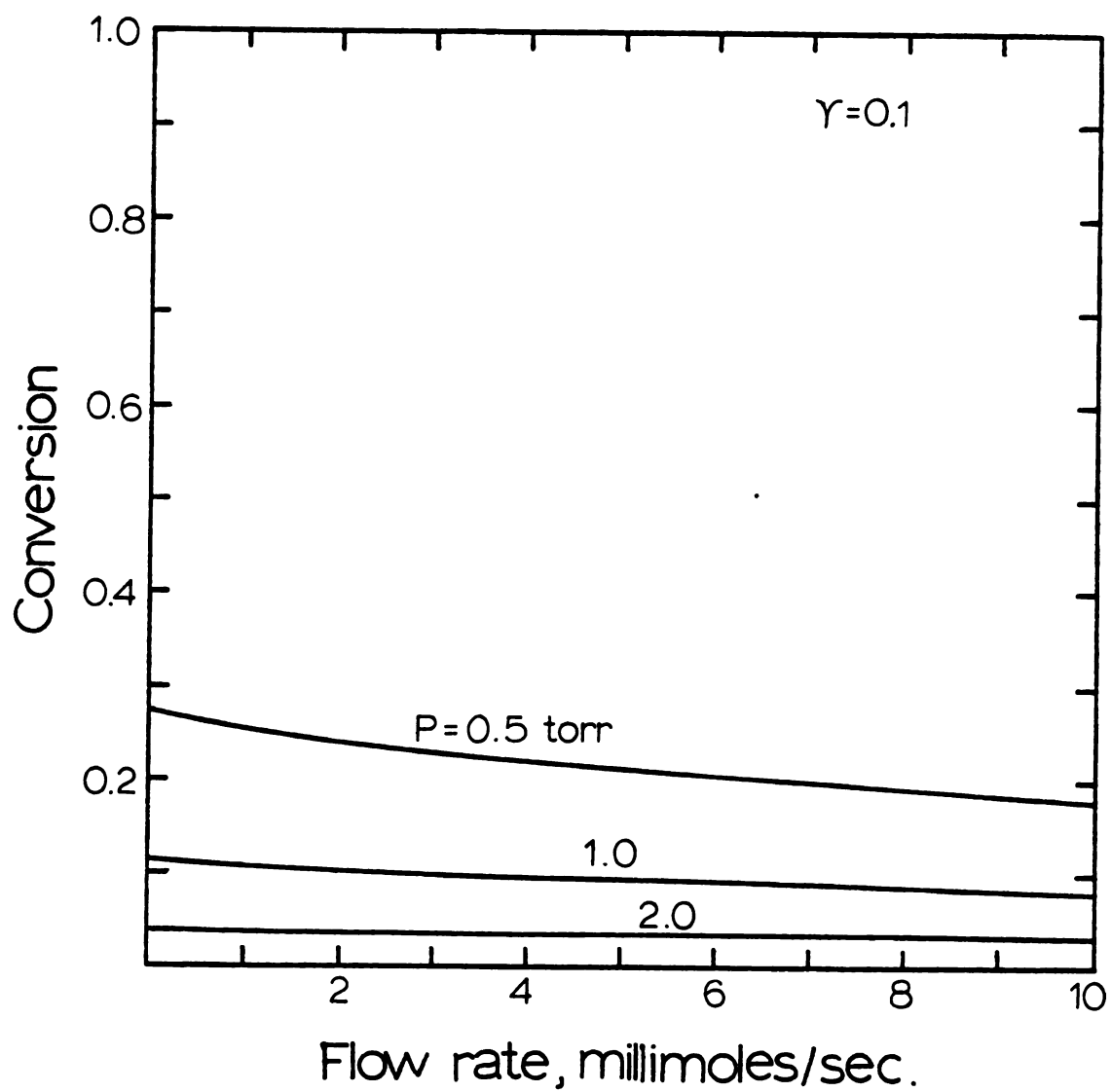


Figure 14.--Pressure and flow rate dependence of discharge conversion for  $\gamma = 0.1$ .

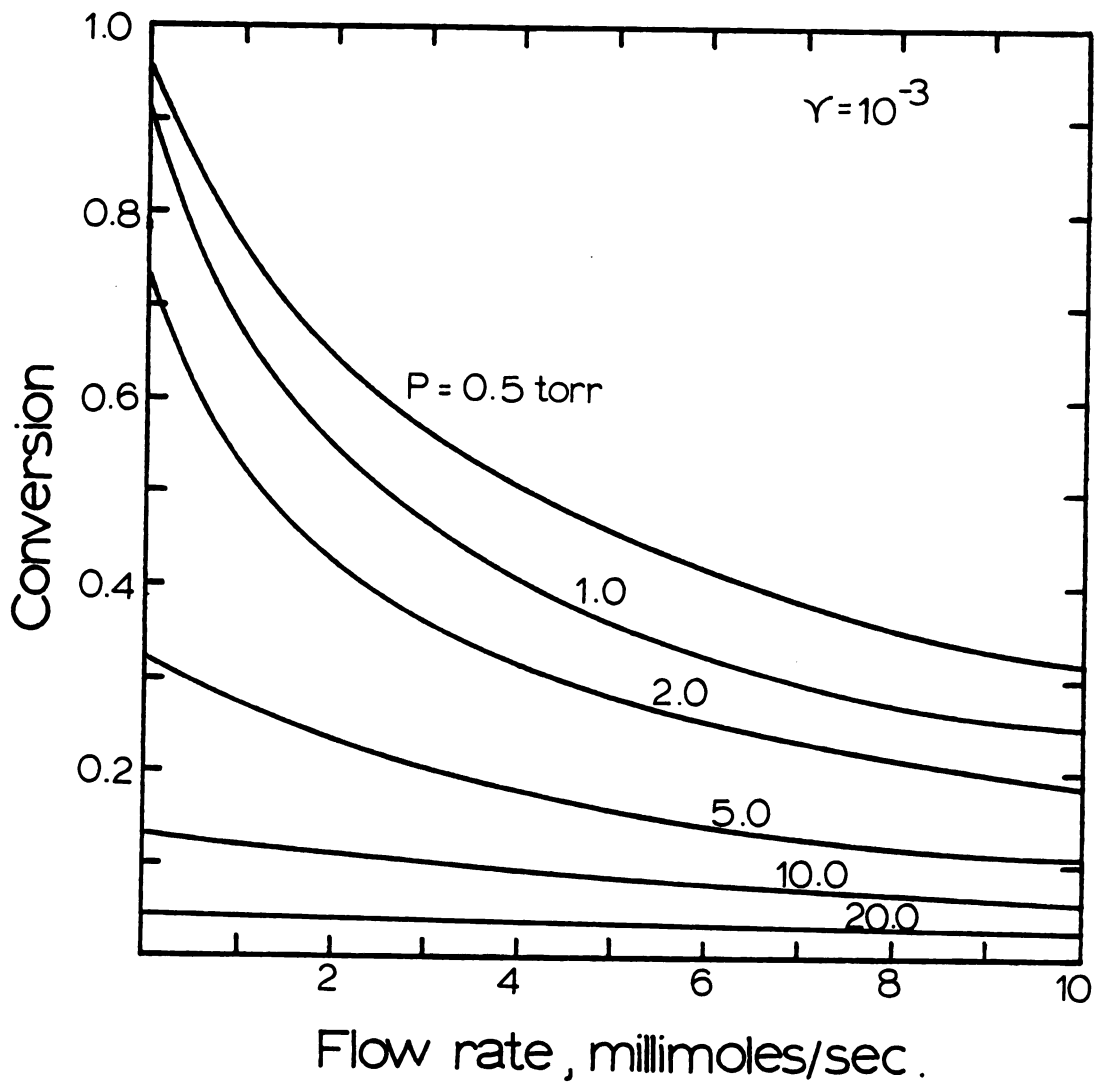


Figure 15.--Pressure and flow rate dependence of discharge conversion for  $\gamma = 10^{-3}$ .

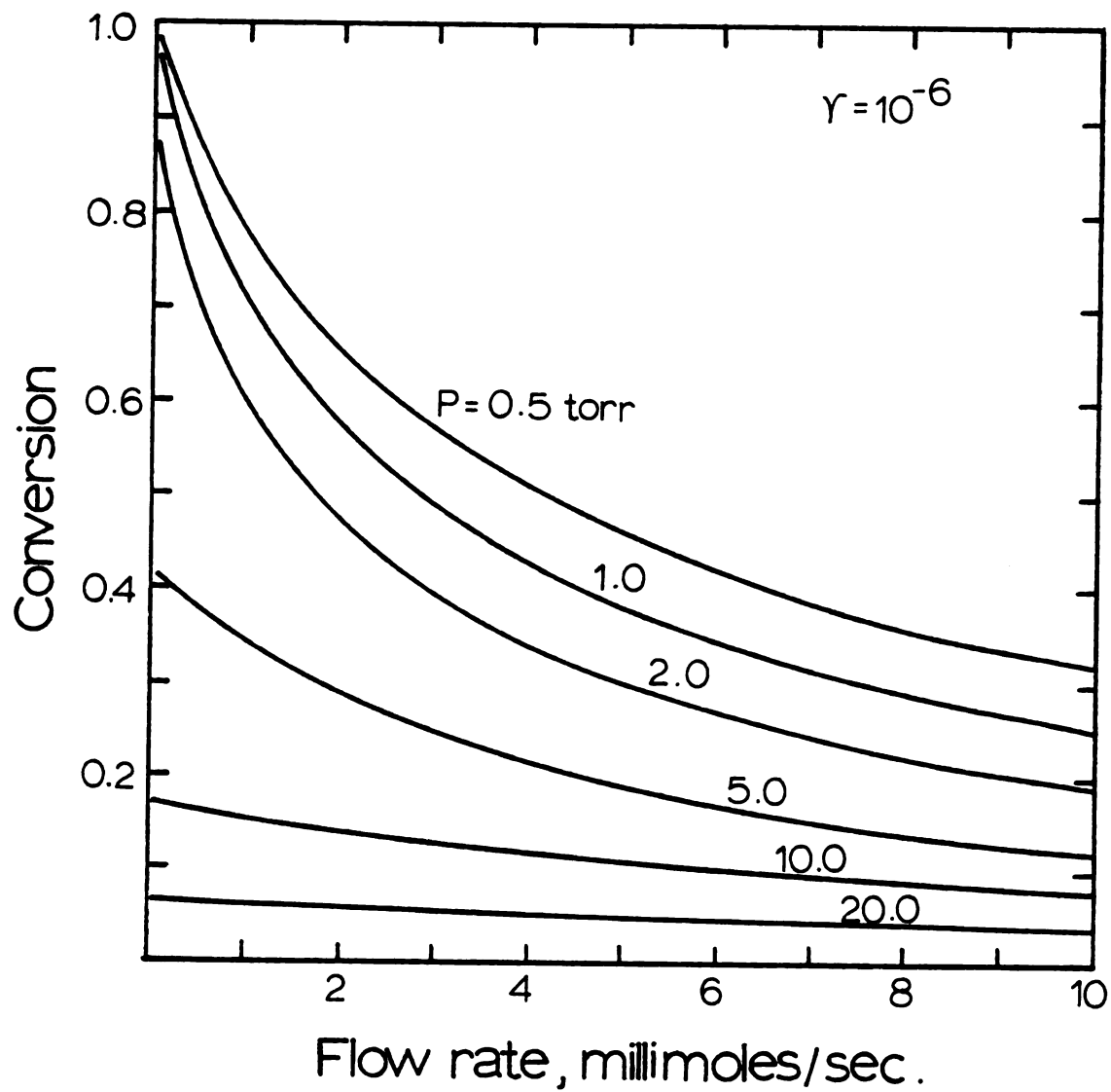


Figure 16.--Pressure and flow rate dependence of discharge conversion for  $\gamma = 10^{-6}$ .

These figures also help to illustrate the important role of the wall recombination coefficient,  $\gamma$ , which is capable of decreasing the maximum conversion from virtually 100% at  $\gamma = 10^{-6}$  and low flow rates to below 30% when  $\gamma = 10^{-1}$  for the same flow rates.

The effects of gas temperature on conversion are shown in Figures 17-18, where conversion is plotted versus flow rate at three temperatures and two pressures. The gas temperature can contribute to the rate equation (Table 7) in three different ways, considered in terms of their individual effects on conversion:

- (1) The recombination rate coefficients,  $k_H$ , and  $k_{H_2}$ , are exponentially decreasing functions of temperature; an increase in temperature will result in an increase in discharge conversion (see Figure 9).
- (2) The gas density,  $\beta$ , is inversely proportional to the temperature; an increase in temperature would have its greatest effect in decreasing the gas-phase recombination rate, and would result in an increase in conversion.
- (3) The mean molecular speed,  $\bar{c}$ , is proportional to the square root of the temperature, and occurs only in the wall recombination term of the rate equation; an increase in temperature will cause a small decrease in conversion.

One additional effect of increasing the gas temperature, an increase in conversion due to chemical equilibrium between atoms and molecules, would be negligible at the temperatures (300-1000 °K) and pressures considered here (as shown in Figure 2). The curves clearly show that an increase in conversion with increased temperature does occur and, therefore, that the first two temperature effects in the model predominate over the third effect.

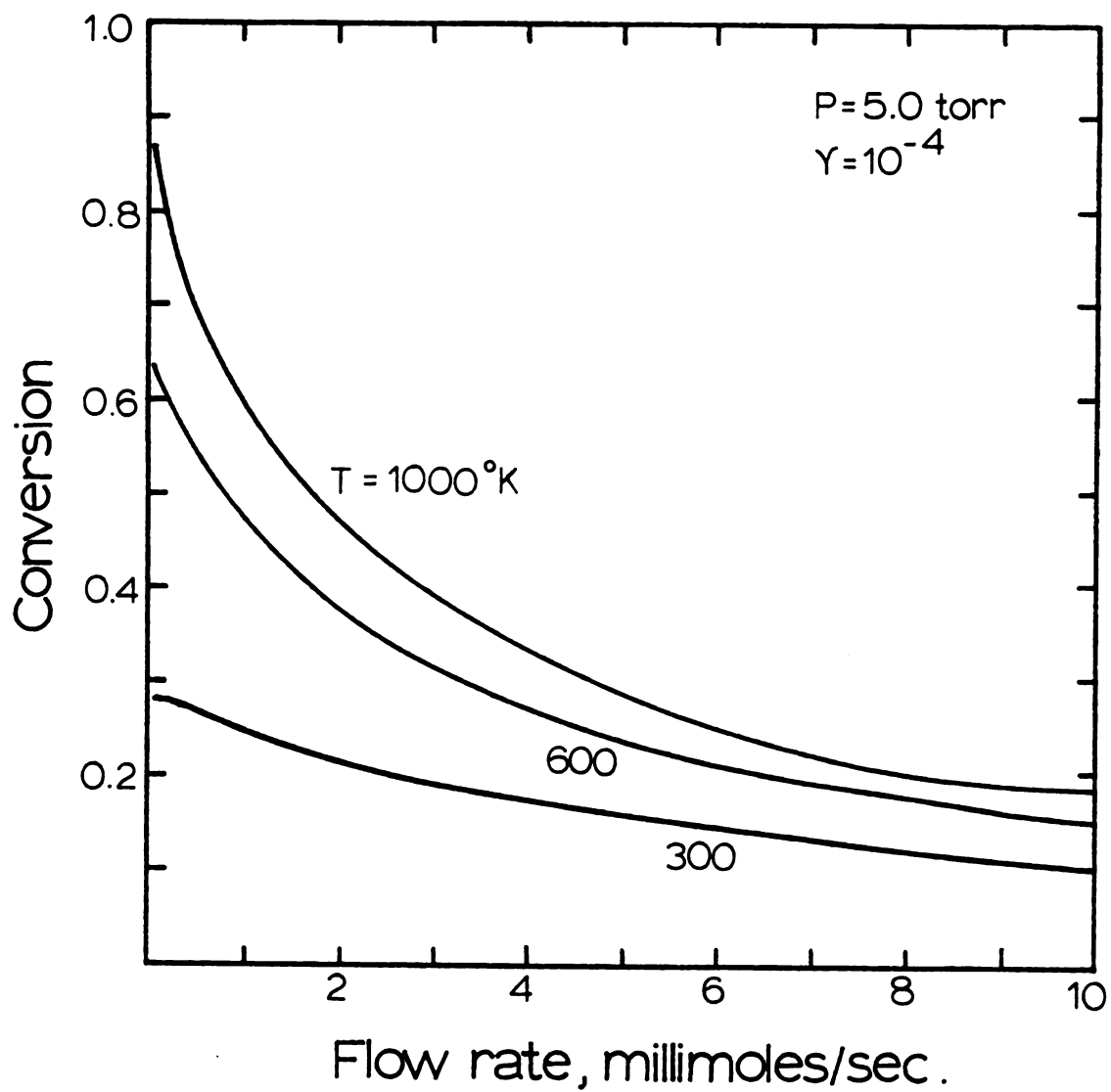


Figure 17.--Dependence of conversion on discharge temperature for a pressure of 5.0 torr.

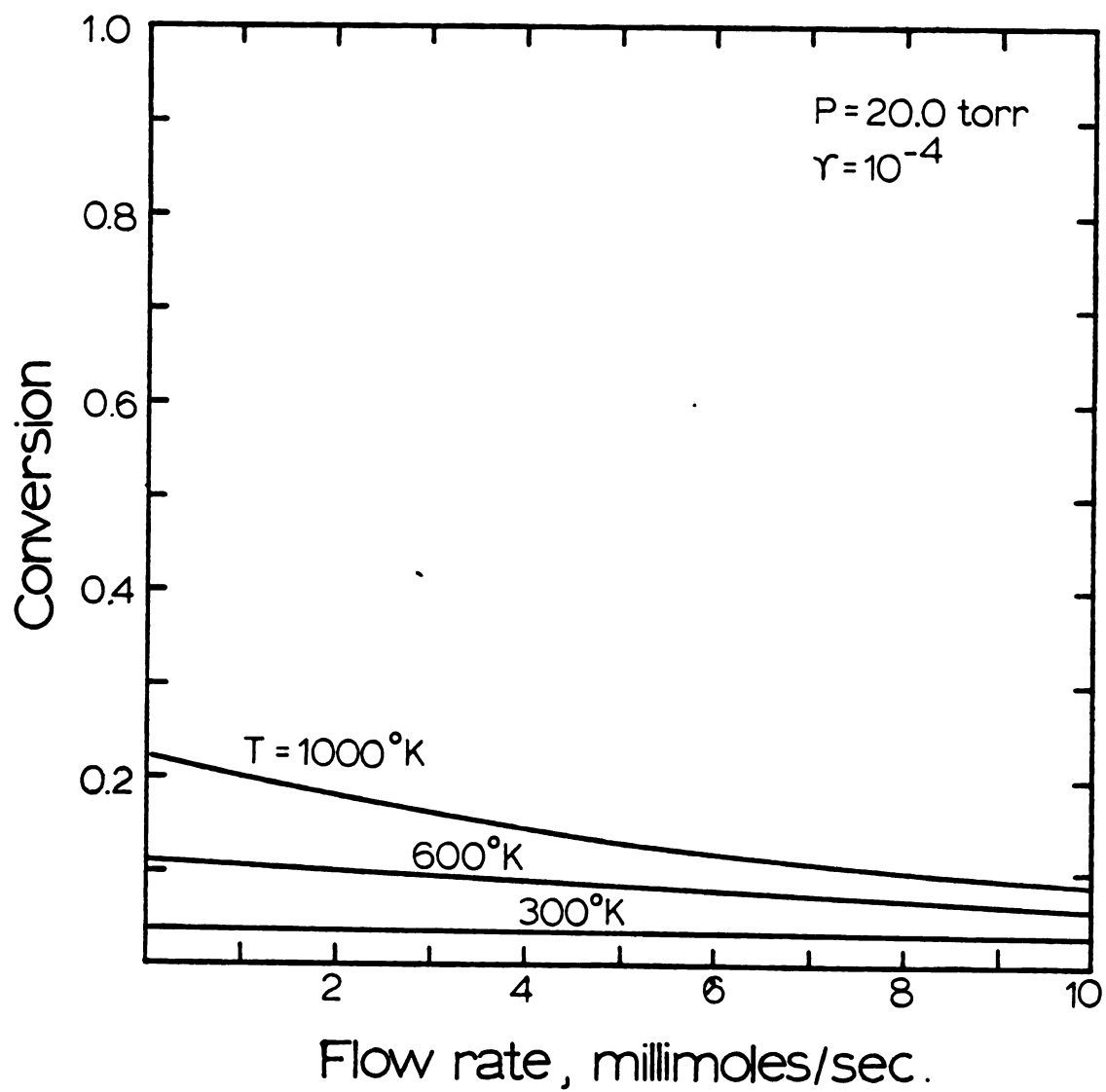


Figure 18.--Dependence of conversion on discharge temperature for a pressure of 20.0 torr.

The third series of figures shows the importance of the wall recombination coefficient,  $\gamma$ , in determining the discharge conversion. In Figures 19-21, where conversion is plotted versus electron density using semi-logarithmic axes, the wall recombination coefficient has been varied from  $10^{-6}$  to  $10^{-1}$ , while the pressure has been increased from 1.0 torr (Figure 19) to 20.0 torr (Figure 21). The results show that, at the low pressures where gas-phase recombination is a minor effect, wall recombination predominates as the atom-loss mechanism. As the pressure is increased, however, recombination on the wall is superseded by gas-phase recombination, to the point where the effects of wall recombination at 20.0 torr are almost completely negligible. Figures 19 and 20 also show that there is very little increase in conversion in going from  $\gamma = 10^{-3}$  to  $\gamma = 10^{-6}$ , which indicates that the need for a wall coating in experiments using quartz ( $\gamma = 10^{-3}$ ) reactor walls is less than when glass ( $\gamma = 10^{-2}$ ) walls are used, and that the effort which is required to decrease the wall recombination coefficient below  $10^{-3}$  may not result in significant improvements in conversion.

The effects of tube diameter on discharge conversion are shown in Figures 22-24. In these figures, the conversion is plotted versus flow rate for three diameters, and at three different pressures. At very low pressures (0.5 torr), where gas-phase recombination is less important than wall recombination, conversion is greatest when the distance between the reactor walls ( $D_t$ ) is large. As the pressure is increased, the conversion in smaller tubes begins to become greater

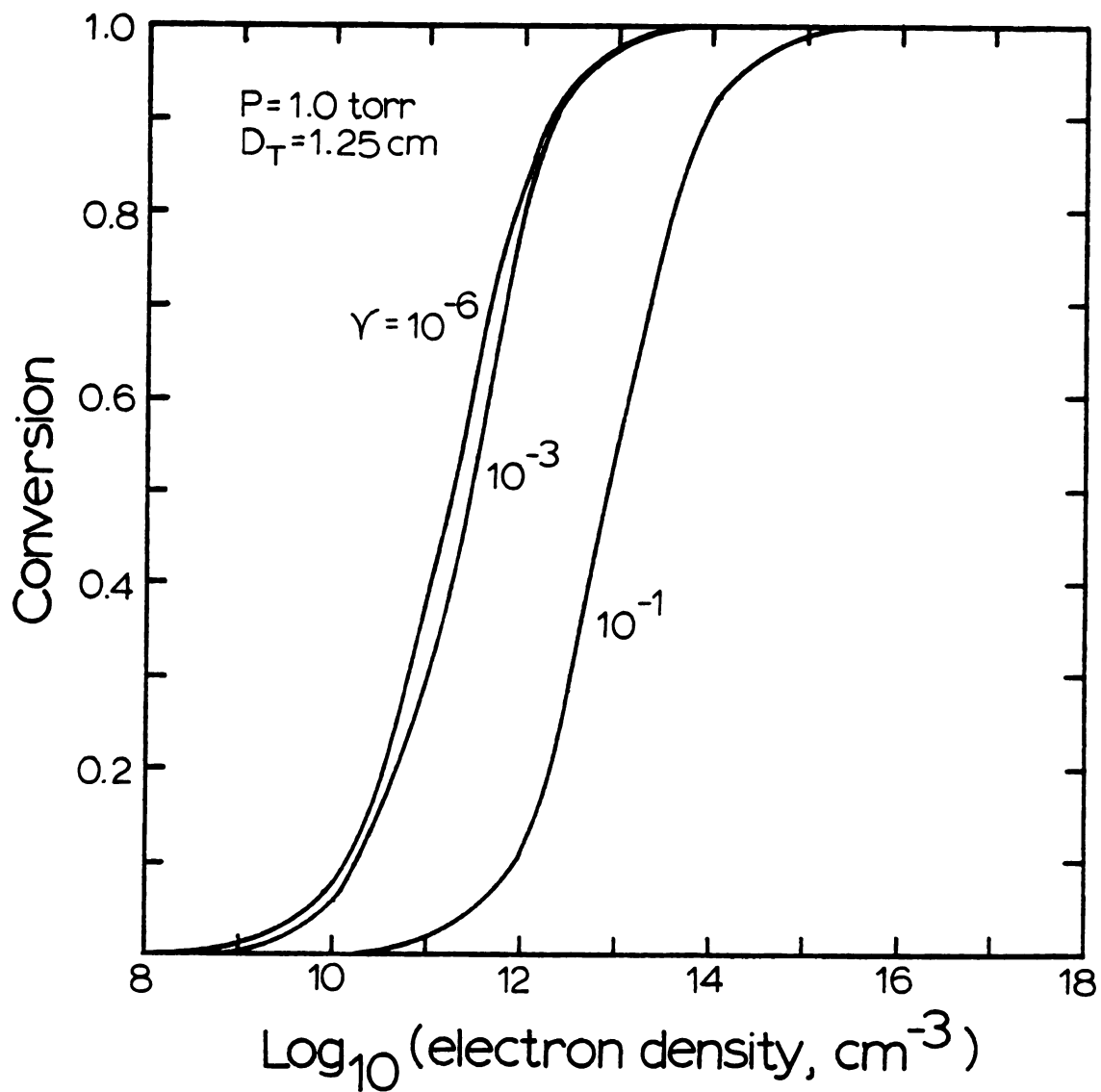


Figure 19.--Discharge conversion dependence on the wall recombination coefficient at 1.0 torr.

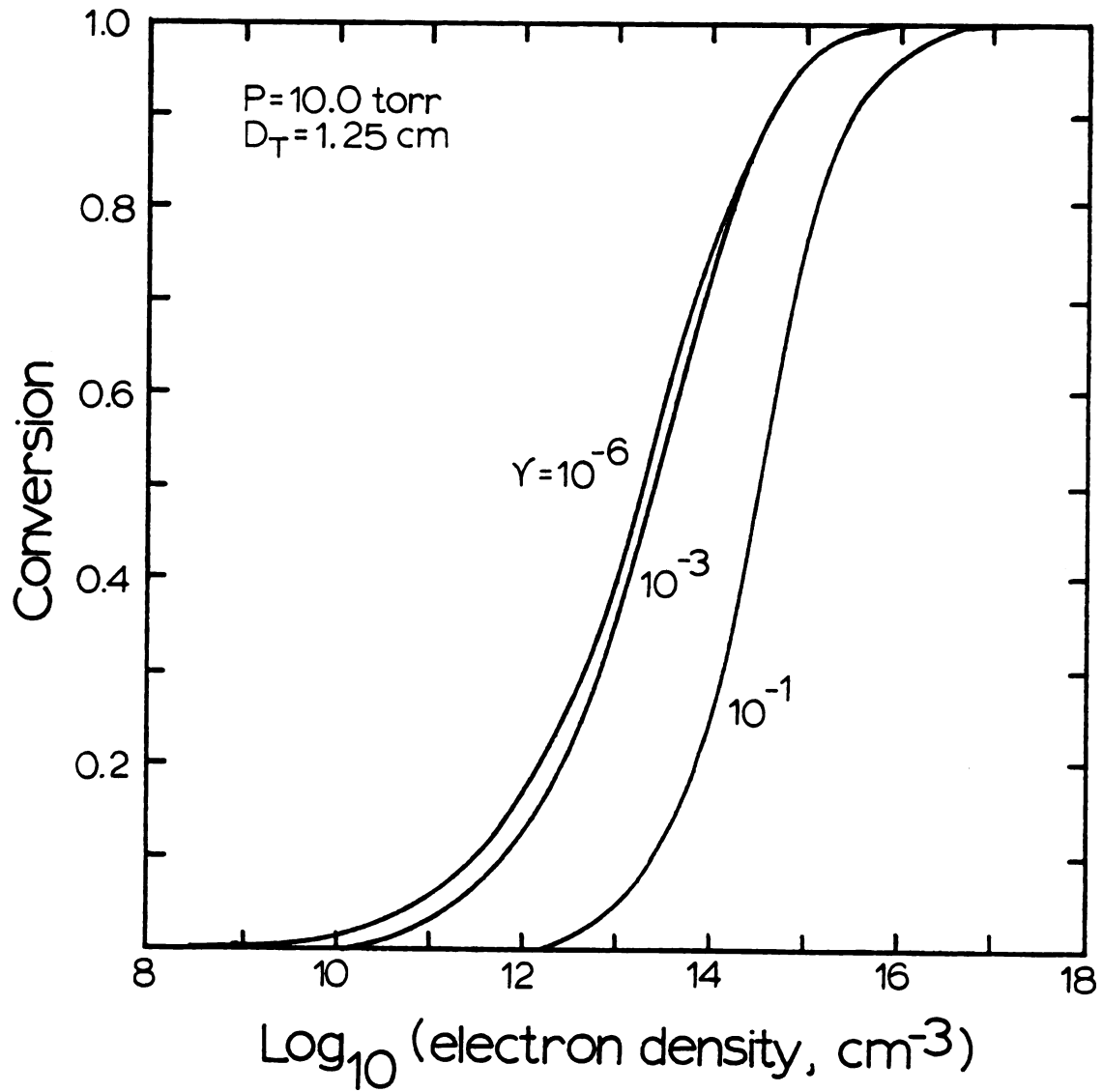


Figure 20.--Discharge conversion dependence on the wall recombination coefficient at 10.0 torr.

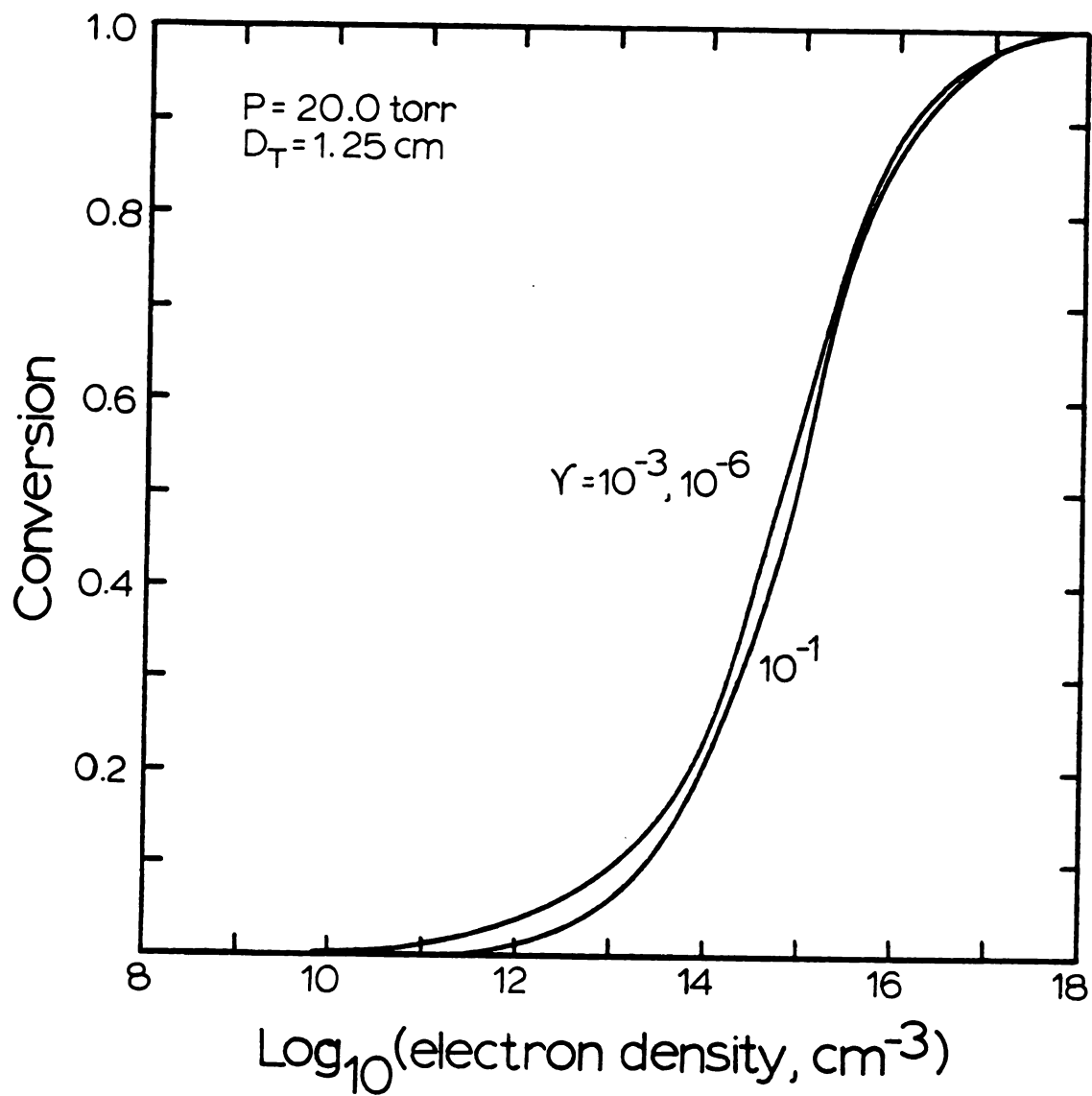


Figure 21.--Discharge conversion dependence on the wall recombination coefficient at 20.0 torr.

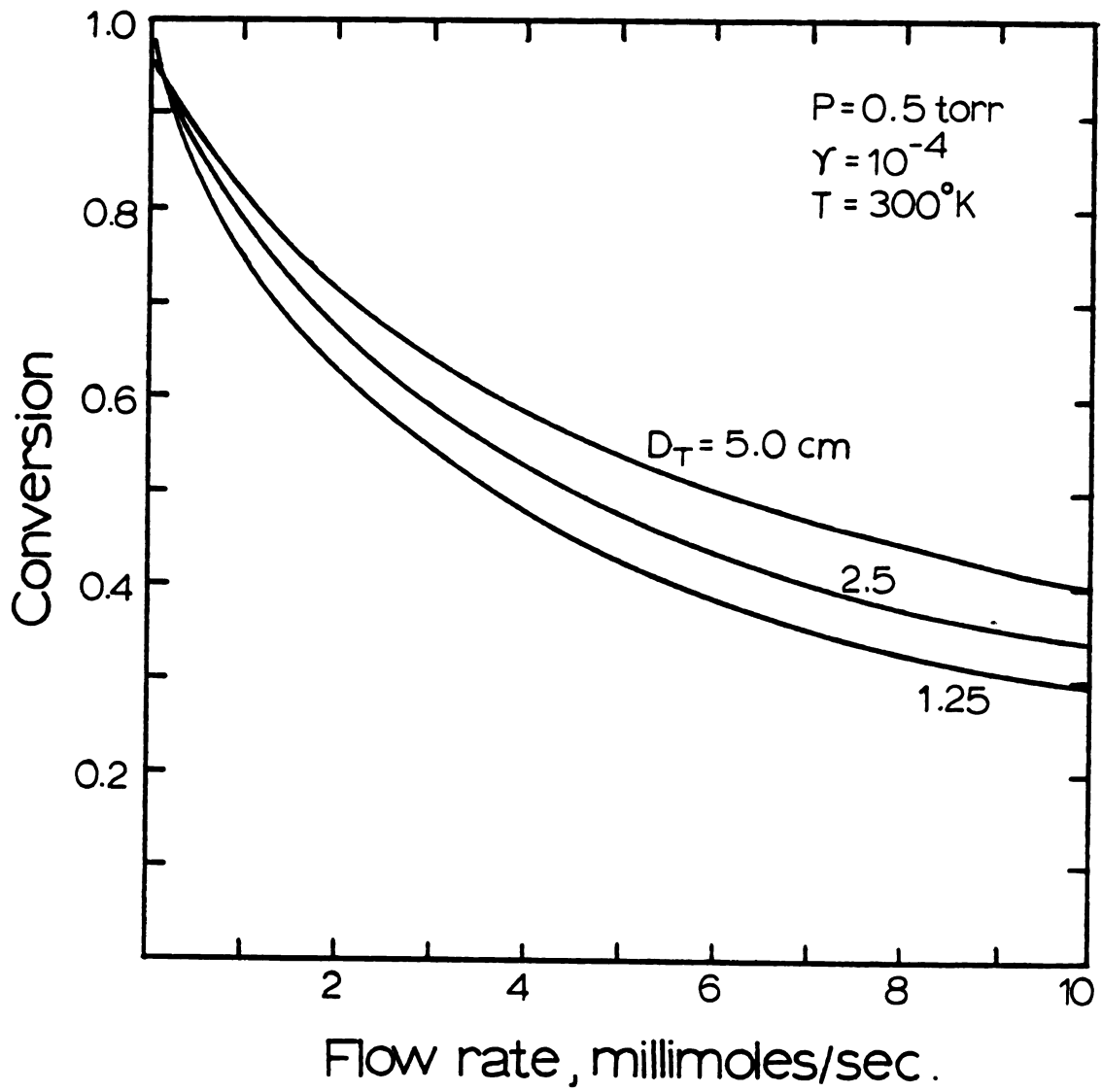


Figure 22.--Effects of increasing discharge tube diameter on discharge conversion at 0.5 torr.

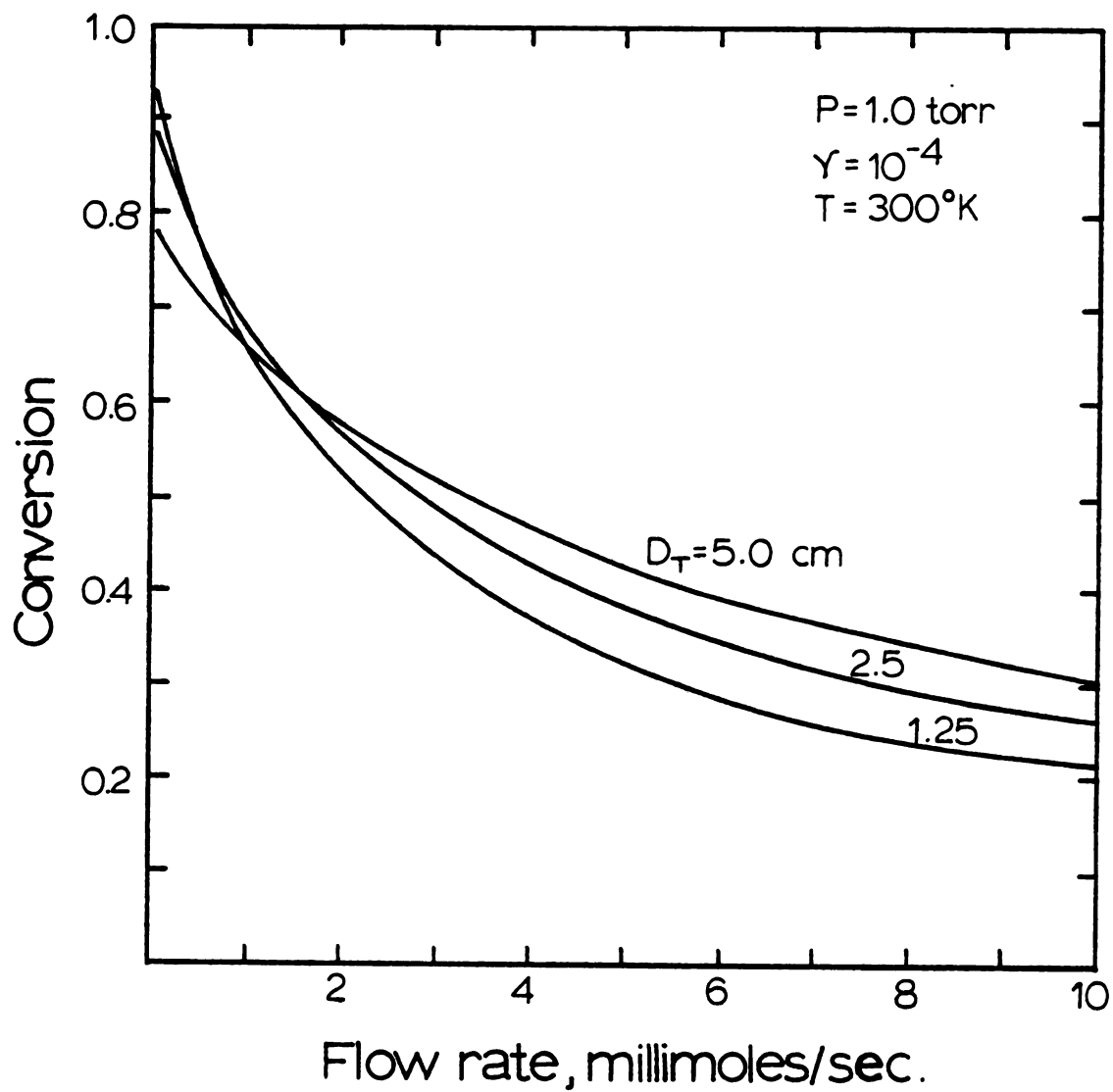


Figure 23.--Effects of increasing discharge tube diameter on discharge conversion at 1.0 torr.

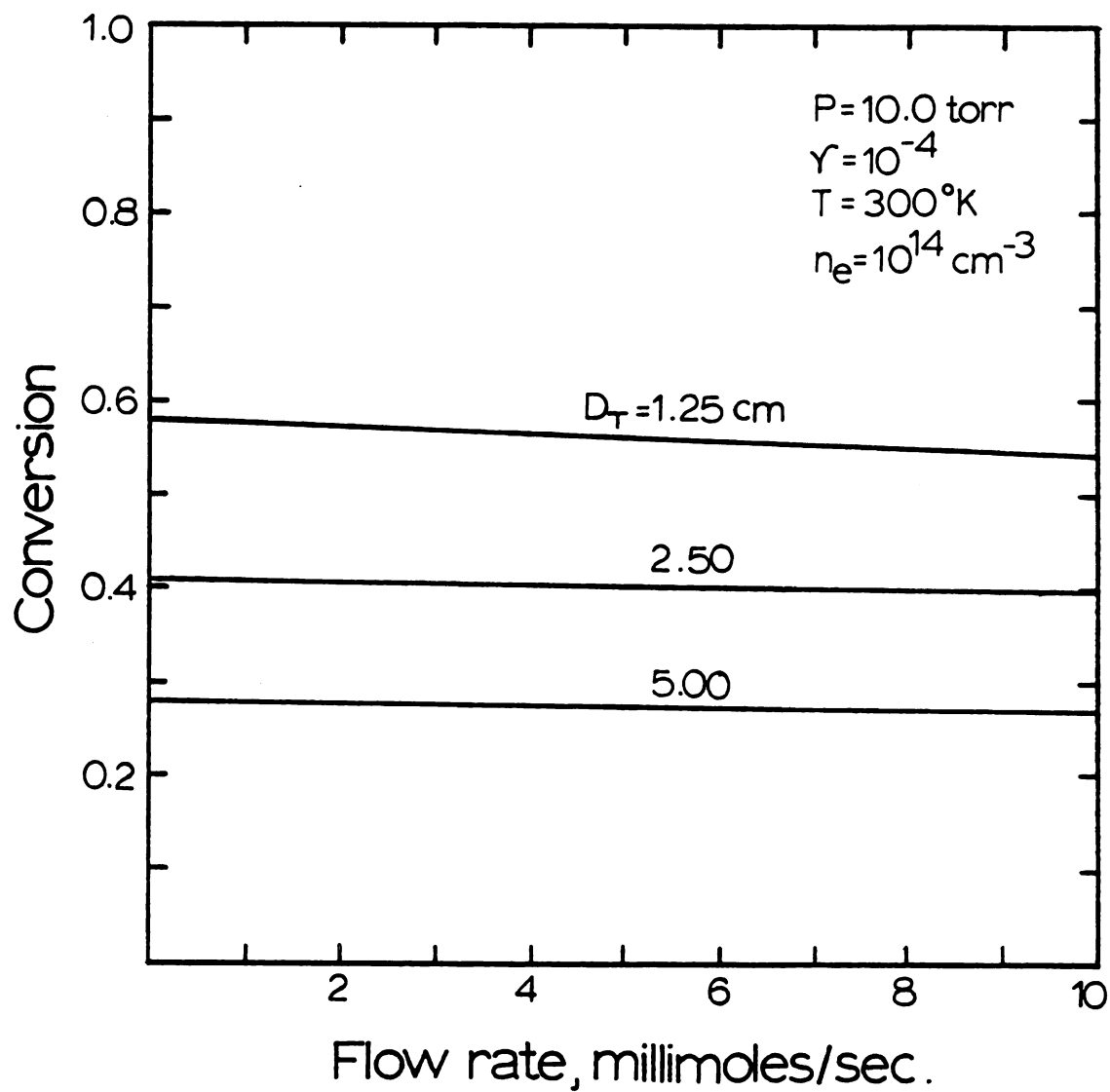


Figure 24.--Effects of increasing discharge tube diameter on discharge conversion at 10.0 torr.

as the effects of gas-phase recombination become more important. Finally, when the pressure reaches 10.0 torr, the original order of conversion's dependence on tube diameter ( $D_t = 5.0 \text{ cm} > 2.50 \text{ cm} > 1.25 \text{ cm}$ ) is reversed, and conversion is greatest when the volume available for gas-phase recombination reactions is minimized.

As discussed in the rationale, the electron density was included in these calculations in two completely separate manners. In the first set of calculations, the discharge theory developed by Bell (12) was used to calculate the electron density from the tube diameter, pressure, and the microwave power input. The results of those calculations are presented in Figures 25-27, in which conversion is plotted versus flow rate for a range of power inputs between 100 and 3000 watts, using gas pressures of 0.5, 1.0, and 10.0 torr. Although the conversion at the two lower pressures (Figures 25 and 26) is quite high ( $> 50\%$ ), the conversion at 10.0 torr (Figure 27) has dropped below 20% for even the smallest flow rates. This result appears to be supported by the work of Mearns and Ekinici (65), in which conversions of 10% were reported at  $p = 3 \text{ torr}$  and  $P = 100 \text{ watts}$ . This implies that there is a limit on the pressures at which a hydrogen discharge will produce a significant number of atoms, and that this limit is below 20 torr. However, the under-estimation of the electron density by Bell's theory could explain the low conversions, and actual conversions in high power discharges (greater than 100 watts) might be higher.

The second method which was used to include the electron density

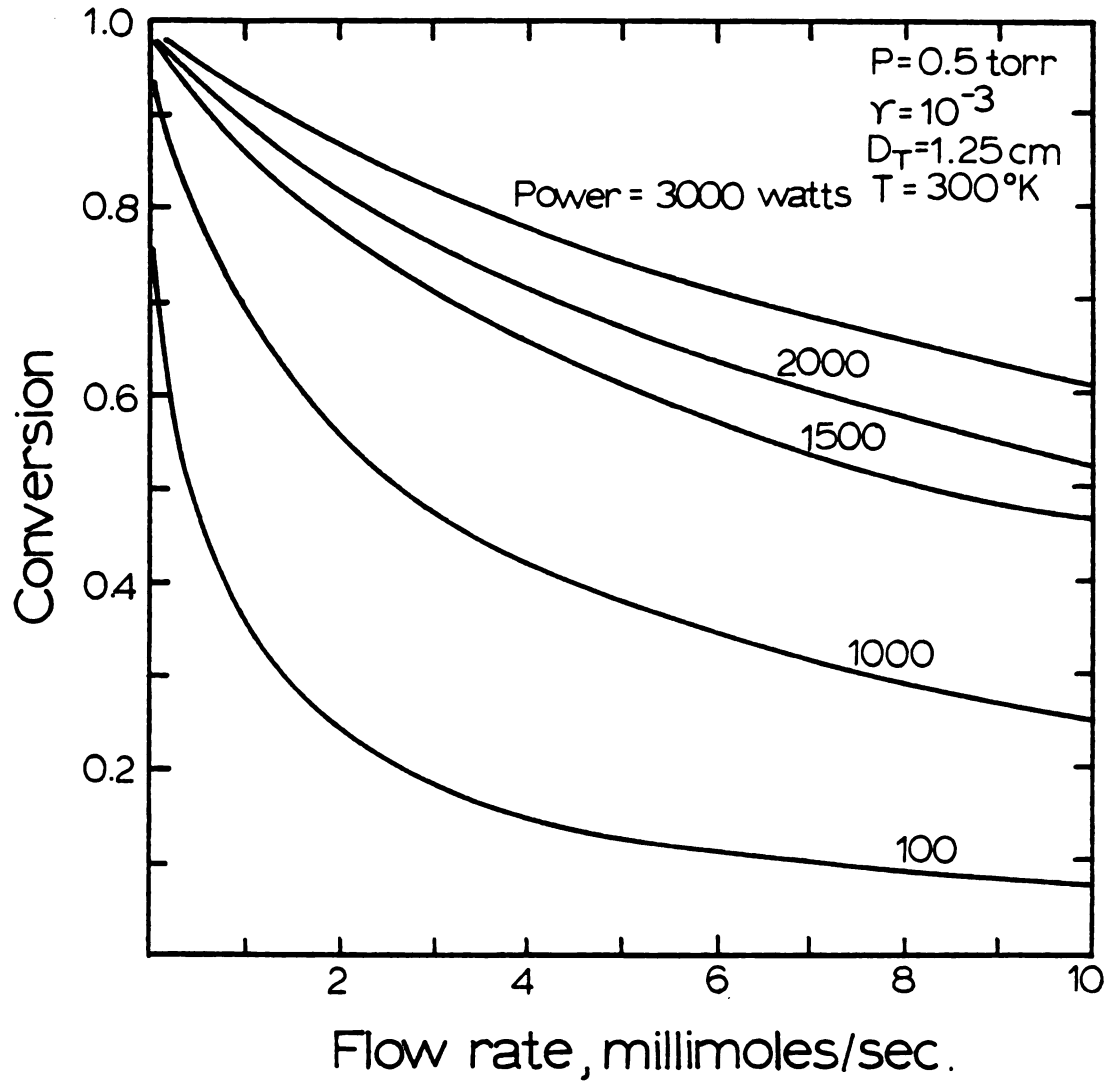


Figure 25.--Dependence of discharge conversion on microwave power input using theoretical relations of Bell (12) at 0.5 torr.

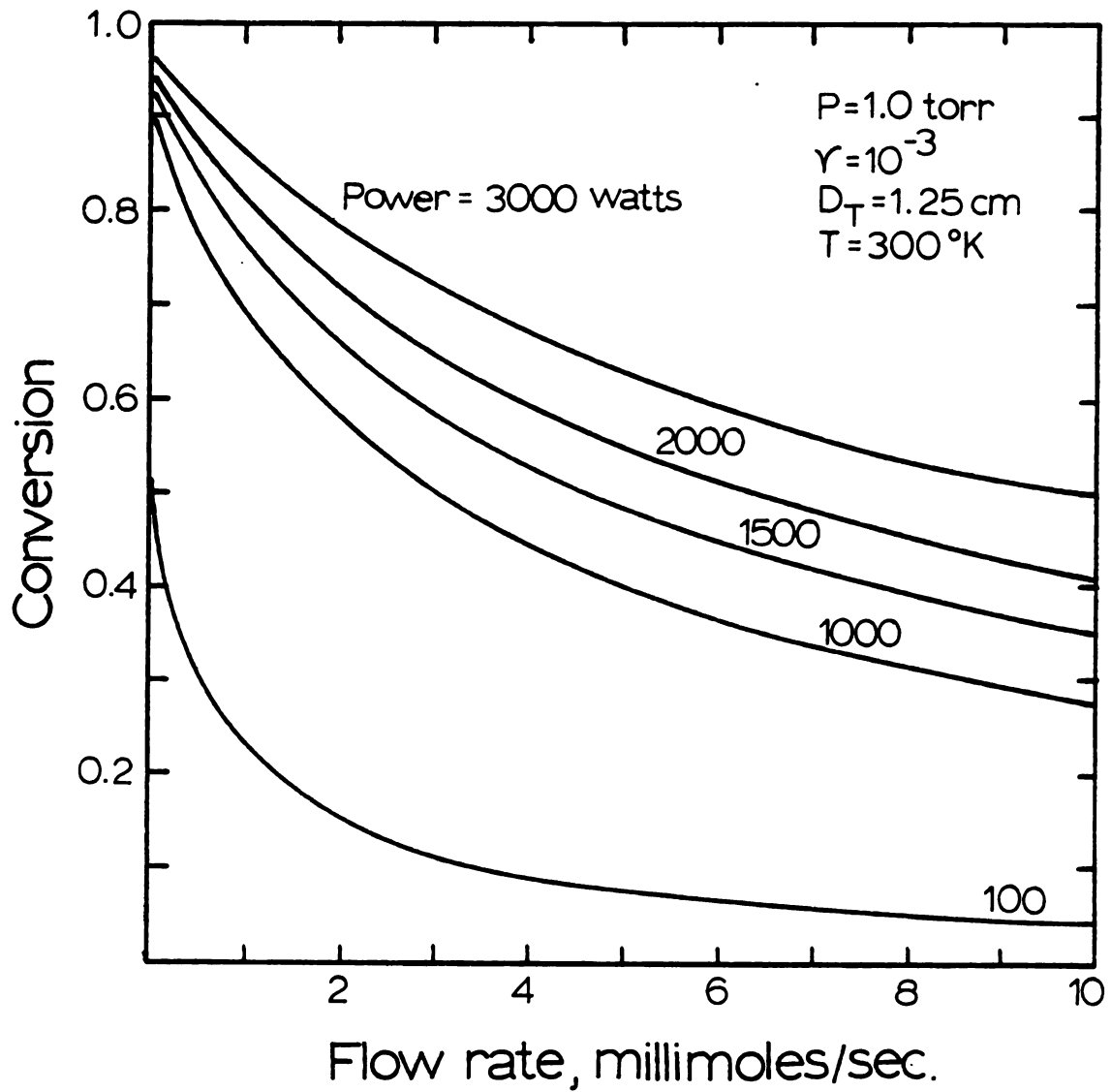


Figure 26.--Dependence of discharge conversion on microwave power input using theoretical relations of Bell (12) at 1.0 torr.

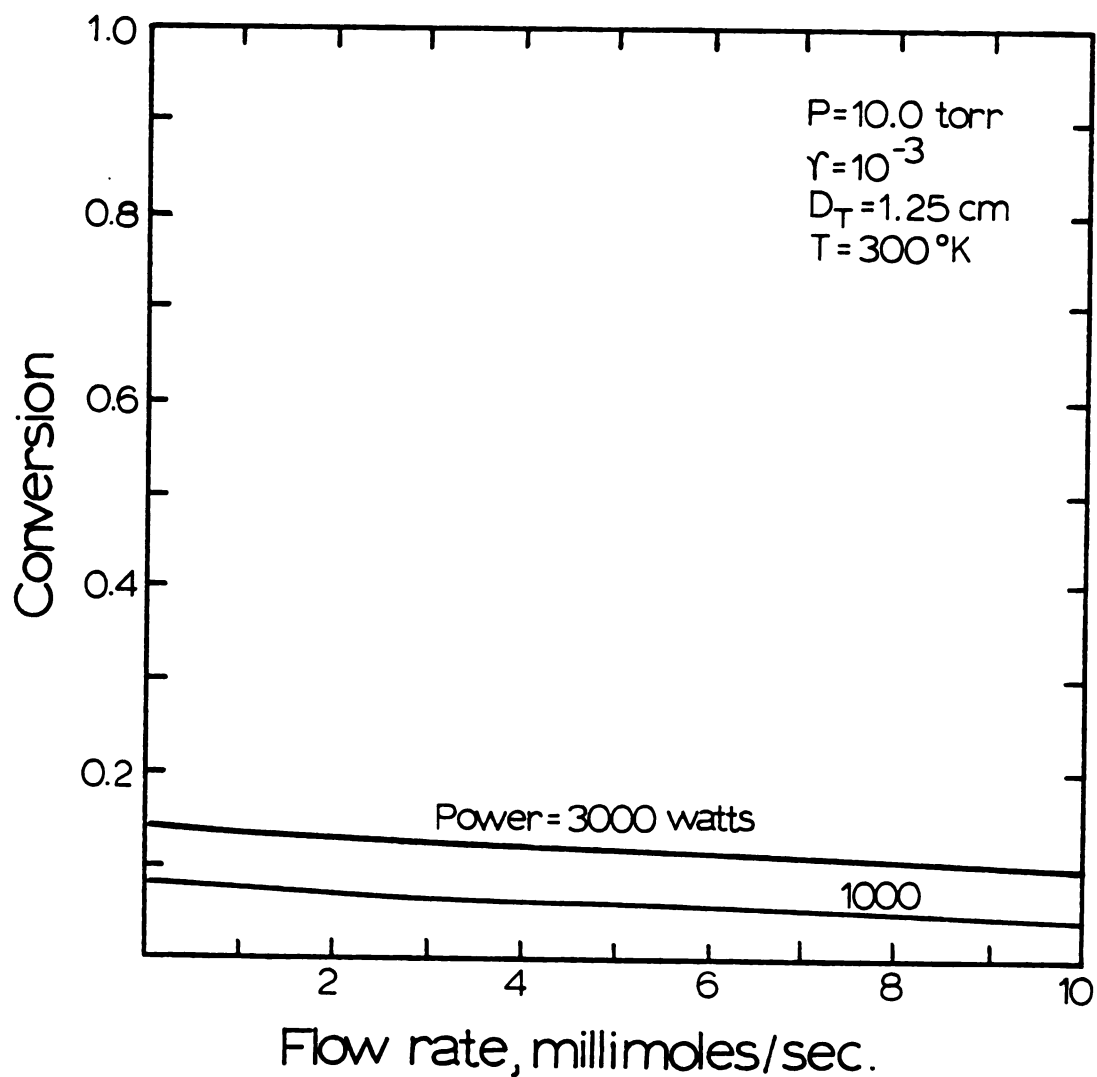


Figure 27.--Dependence of discharge conversion on microwave power input using theoretical relations of Bell (12) at 10.0 torr.

in the discharge model was to treat it simply as another experimental parameter, like pressure or temperature. The results of that calculation are presented in Figure 28, in which conversion is plotted versus  $\log_{10}$  (electron density) for pressures between 1.0 torr and 760.0 torr. It is evident that there is a pressure-dependent "threshold" electron density, below which the conversion is negligible. This threshold might explain the low conversions found in Figure 27, since the electron density predicted by Bell's theory for the conditions in Figure 27 is only  $2.6 \times 10^{12} \text{ cm}^{-3}$ , which is quite close to the threshold value for a pressure of 10.0 torr. The existence of the threshold also indicates the necessity for accurate electron density measurements when modeling the hydrogen discharge using experimental data.

Several conclusions can be drawn from the simple discharge model presented here. These conclusions will be used both in the design and the operation of the microwave discharge hydrogen atom generation apparatus. The conclusions can be summarized as follows:

- (1) High conversions can only be attained at pressures less than 10-20 torr, and then only for low flow rates.
- (2) The effects of high gas temperature are greatest at low flow rates, and appear to exert their influence through the gas density and recombination rate constants.
- (3) Reduction of the wall recombination coefficient below  $10^{-3}$  results in little gain in conversion, especially at higher pressures where gas-phase recombination predominates.

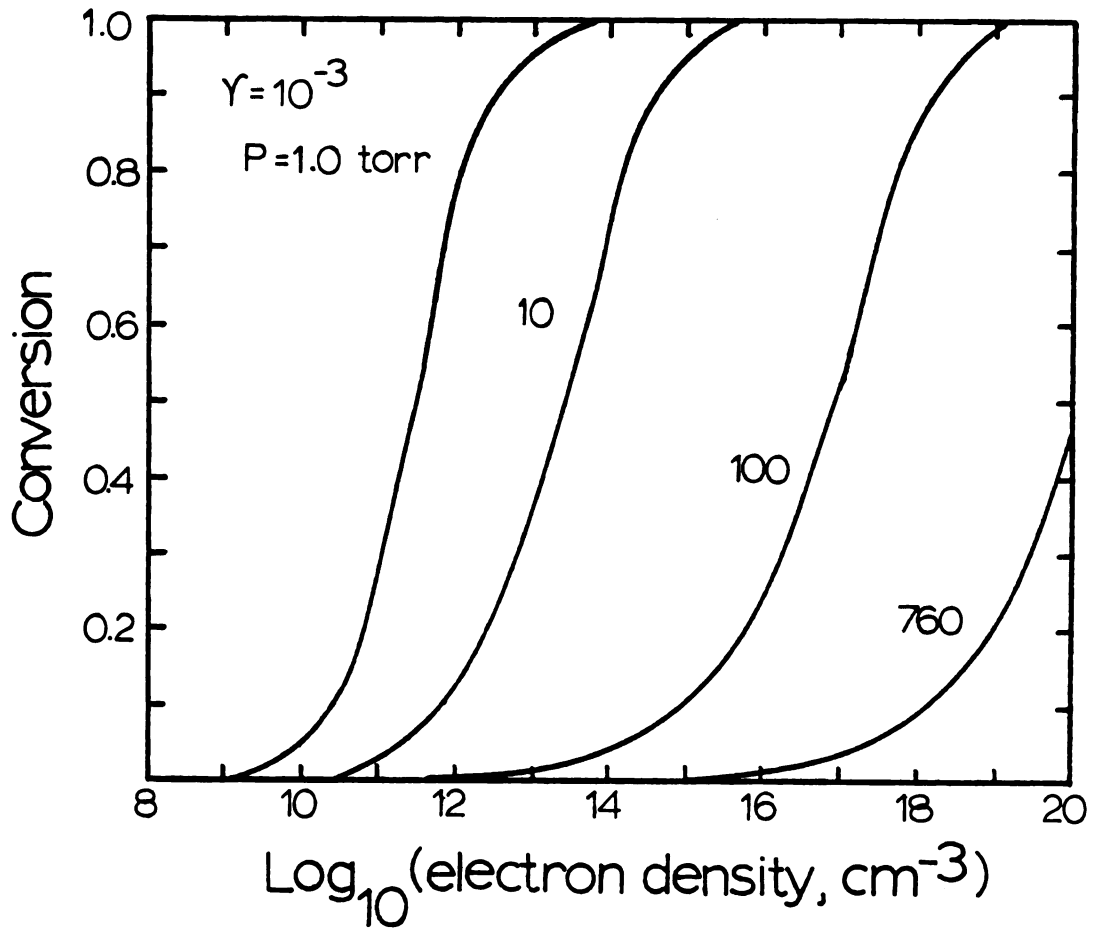


Figure 28.--Dependence of the discharge conversion on electron density.

- (4) The effects of tube diameter are dependent on the gas pressure. At pressures sufficiently low that gas-phase recombination is less important ( $<5$  torr), conversion increases with increasing tube diameter. As the pressure increases, this relationship reverses itself.
- (5) The discharge model exhibits a pressure-dependent electron density threshold below which conversion of molecules to atoms is negligible.
- (6) Since variations in electron density of only an order of magnitude can cause a precipitous drop in conversion, accurate measurements of the electron density will be required to accurately model hydrogen discharges.

## MODELING THE DOWNSTREAM REGION

Although the discharge model is more important from the standpoint of producing hydrogen atoms in an electrical discharge, the importance of experiments intended to measure hydrogen atom reaction kinetics, both in the gas phase and on walls, entails that a model of the region downstream from the discharge be developed. This is a much simpler task than modeling the discharge, in particular because there aren't any free electrons present in the reaction system to add complexity to the kinetics or flow. Therefore, a simple plug-flow reactor (PFR) model was used to determine the experimental conditions which will allow hydrogen atoms generated in the discharge to travel downstream for the greatest distance.

### Rationale and Model Development

The downstream region of the apparatus is defined as the complete length of tubing from the discharge at one end to the vacuum pump at the other. Any use of this region for hydrogen atom kinetics experiments requires that some of the atoms created in the discharge be able to travel down the tube to the experimental site. The quantity used to characterize that ability was the quenching distance, which was defined as the distance from the discharge where the atom concentration falls below a pre-determined threshold value of  $10^8$  atoms  $\text{cm}^{-3}$ . Although this value is much lower than the  $10^{14}$ - $10^{15}$  atoms  $\text{cm}^{-3}$  which

could be found in the downstream region of a low-pressure, high power microwave discharge, it was convenient when plotting the results of the model. The purpose of the downstream region model was to determine whether large quenching distances ( $\sim 1-2$  meters) were feasible and, if so, the experimental conditions needed to achieve those large quenching distances.

As was the case with the discharge model, certain simplifications had to be made in the downstream region model to make the calculations more tractable. One simplification was made possible by the relatively constant separation between concentration profiles (concentration vs. downstream distance) for initial conversions between 10% and 90%, as seen in preliminary calculations. Since the profiles were so similar, a single calculation, using an initial conversion of 50%, was made in all subsequent calculations of the quenching distance.

An isothermal, plug-flow reactor model was used to represent the downstream region. Of the three types of ideal reactor (plug-flow, laminar-flow, and continuously-stirred tank), the continuously-stirred tank reactor is clearly inappropriate for use as the downstream model, since it considers all concentrations to be uniform throughout the reactor, and not decreasing with downstream distance as would be expected in the downstream region. A laminar-flow reactor model, although probably a more accurate description of the flow in the nonturbulent downstream region, is complicated by the requirement of including a parabolic velocity profile and the effects of radial diffusion in the calculations. Therefore, a plug-flow reactor (PFR)

model was chosen to represent the flow in the downstream region.

The development of the modeling equation begins with the reaction rate equation. This equation is identical to the equation used in the discharge (Table 7), with one important exception. Since the electrons which cause the dissociation of hydrogen in the discharge don't exist in the downstream region, the original rate equation's atom generation term,  $2k_d n_e [H_2]$ , can be omitted in that region. This leaves the following as the downstream region reaction rate equation:

$$r_H' = -2k_{H_2} [H_2][H]^2 - 2k_H [H]^3 - \frac{\gamma \bar{C}}{D_t} [H] \quad (39)$$

The model equation for a PFR can be derived from a steady-state balance of mass around a differential element of volume. In a cylindrical reactor, that element is given by  $V = \frac{\pi}{4} D_t^2 \Delta z$ , where  $\Delta z$  is a small distance down the axis of the reactor. Using the relationship given by Equation 33 between input, output, and production within the volume element,

$$2F_0 X \Big|_{z+\Delta z} - 2F_0 X \Big|_z = \left( \frac{\pi}{4} D_t^2 \Delta z \right) r_H' \quad (40)$$

where conversion has been substituted for concentration using Equations 35-37. After dividint through by  $2F_0 \Delta z$  and taking the limit of both sides as  $\Delta z \rightarrow 0$ , Equation 40 is transformed into the differential equation

$$\frac{dX}{dz} = \frac{\pi D_t^2}{8F_0} r_H' \quad (41)$$

Each individual solution of Equation 41 was obtained by using the Euler technique, with a user-adjusted stepsize. Once a convergent stepsize was reached, halving the stepsize again only changed the quenching distance by less than 1%.

Although the numerical techniques used to solve the discharge and downstream models were different, the approach to the analysis of the models was the same. After making a series of calculations of the quenching distance,  $Q_D$ , using several values of the experimental parameters, the results were plotted on graphs of quenching distance (y-axis) versus flow rate (x-axis). Within each graph, only the parameters of interest were varied, with all remaining parameters held at standard values selected on the basis of literature references. The experimental parameters, their ranges, standard values, and the references used are summarized in Table 9.

The calculations were performed, using the Fortran program STREAM2 listed in Appendix B, on the Michigan State University CDC Cyber 175-750 computer. The program is designed to be operated from a terminal. After prompting the user for initial values of the experimental parameters, the quenching distance is calculated in a step-wise fashion for six flow rates between 50 and 2000  $\mu\text{moles sec}^{-1}$ . If the calculated conversion falls outside the range  $[0,1]$ , then the program prompts for a new stepsize, and restarts the calculations from the beginning.

Table 9.--Experimental parameters used in the downstream region model.

Variable	Range	Standard value	(ref)
Threshold concentration, $N_H, \text{cm}^{-3}$	$10^8$ - $5 \times 10^{15}$	$10^8$	a
Gas temperature, T, °K	420,800	420	(65)
Pressure, p, torr	0.5-20.0	0.5	(84)
Tube Diameter, $D_t$ , cm	1.25,5.0	1.25	(65)
Recombination coefficient, $\gamma$	$10^{-1}$ - $10^{-4}$	$10^{-3}$	(35)
Flow rate, $F_0, \mu\text{moles sec}^{-1}$	50-2000	---	---

<sup>a</sup>The standard value of the threshold concentration was chosen arbitrarily to produce the clearest figures.

### Results of the Downstream Region Modeling

The objective of the downstream modeling was to examine the effects of varying the experimental conditions on the quenching distance. More specifically, it was necessary to find the experimental conditions under which the quenching distance was large enough to ensure the success of experiments to be carried out downstream from the discharge. It was also important to find out, through an examination of their effects on the quenching distance, whether the model possessed any special sensitivities towards variations in the experimental parameters. These results can all be used in designing the experimental apparatus.

The results of the downstream region model are presented in the form of graphs in which the quenching distance,  $Q_D$  (meters), is plotted versus the hydrogen flow rate at the discharge inlet,  $F_0$  ( $\mu\text{moles sec}^{-1}$ ). Each of the experimental parameters is individually varied through a range of values sufficient to demonstrate its effect on  $Q_D$ . Unless otherwise indicated on the graph, when a particular parameter is being examined, all other parameters are held constant at standard values derived from the literature.

The first results are shown in Figure 29, where the quenching distance is plotted versus flow rate using the concentration threshold as the parameter. These calculations were originally done to make certain that the standard threshold value,  $10^8 \text{ cm}^{-3}$ , was a reasonable choice, but the Figure also shows, by the change in  $Q_D$  with  $N_H$  at a fixed flow rate, that the atom concentrations decrease quite rapidly

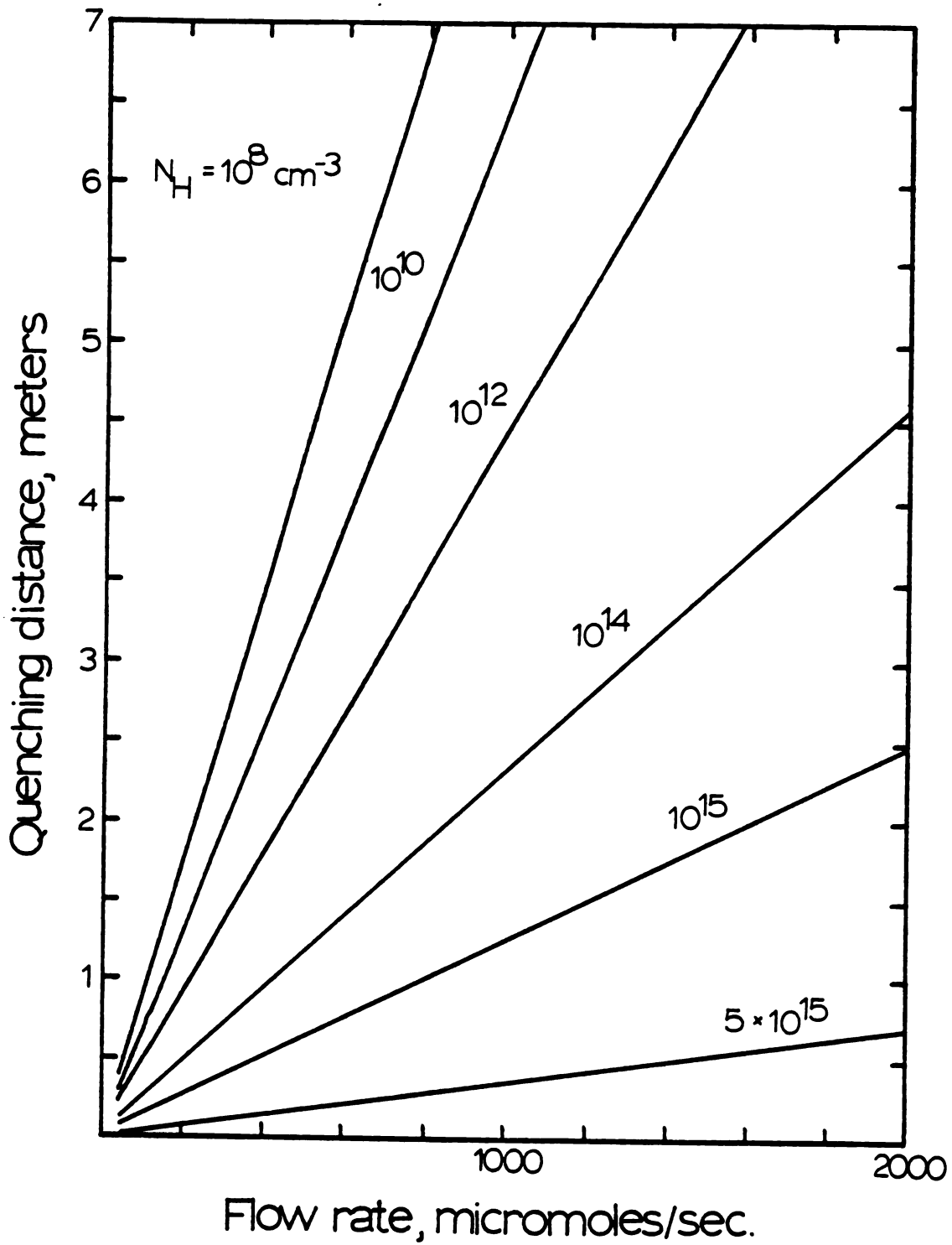


Figure 29.--Effects on the downstream quenching distance of changing the threshold concentration.

in the initial part of the downstream region. This could have a bearing on the detection system used in the apparatus, since most detectors possess a minimum concentration which they are able to detect accurately.

The effects of increasing the gas temperature from the standard value of 420 °K to 800 °K at pressures of 1.0 and 20.0 torr are shown in Figure 30. The increase in quenching which results is almost negligible, an indication that temperature effects of this magnitude in the downstream region are virtually unimportant.

Figure 31 shows the effects of pressure on the quenching distance for five pressures in the range between 0.5 and 20.0 torr. As expected, the quenching distance is high at the low pressures, a result of the control which the gas-phase recombination terms have over the model. The large decrease in  $Q_D$  between 1.0 and 5.0 torr indicates that most experiments in the downstream region will have to be performed within that pressure range.

The importance of the tube diameter in determining the quenching distance is shown in Figure 32, where quenching distance has been plotted versus flow rate for tube diameters of 1.25 and 5.0 cm, at pressures of 0.5 and 5.0 torr. The most probable reason for the increase in  $Q_D$  is difference in velocity in the different tubes--the velocity through a 1.25 cm tube is sixteen times that through the 5.0 cm tube, under the same conditions. The large increase in  $Q_D$  indicates that, whenever possible, a small tube should be used to transport the hydrogen atoms from the discharge to the experimental site. It might

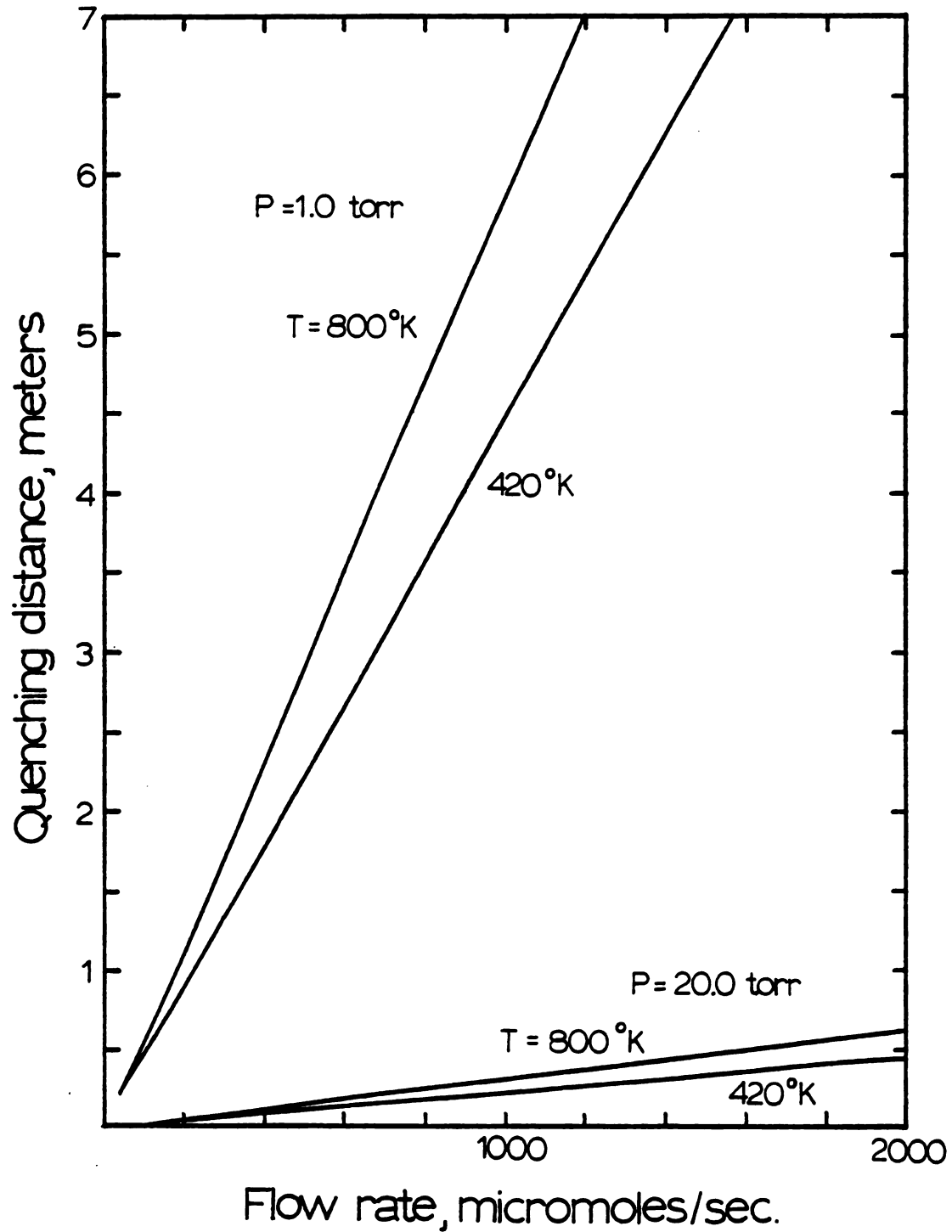


Figure 30.--Temperature dependence of the downstream quenching distance at two pressures.

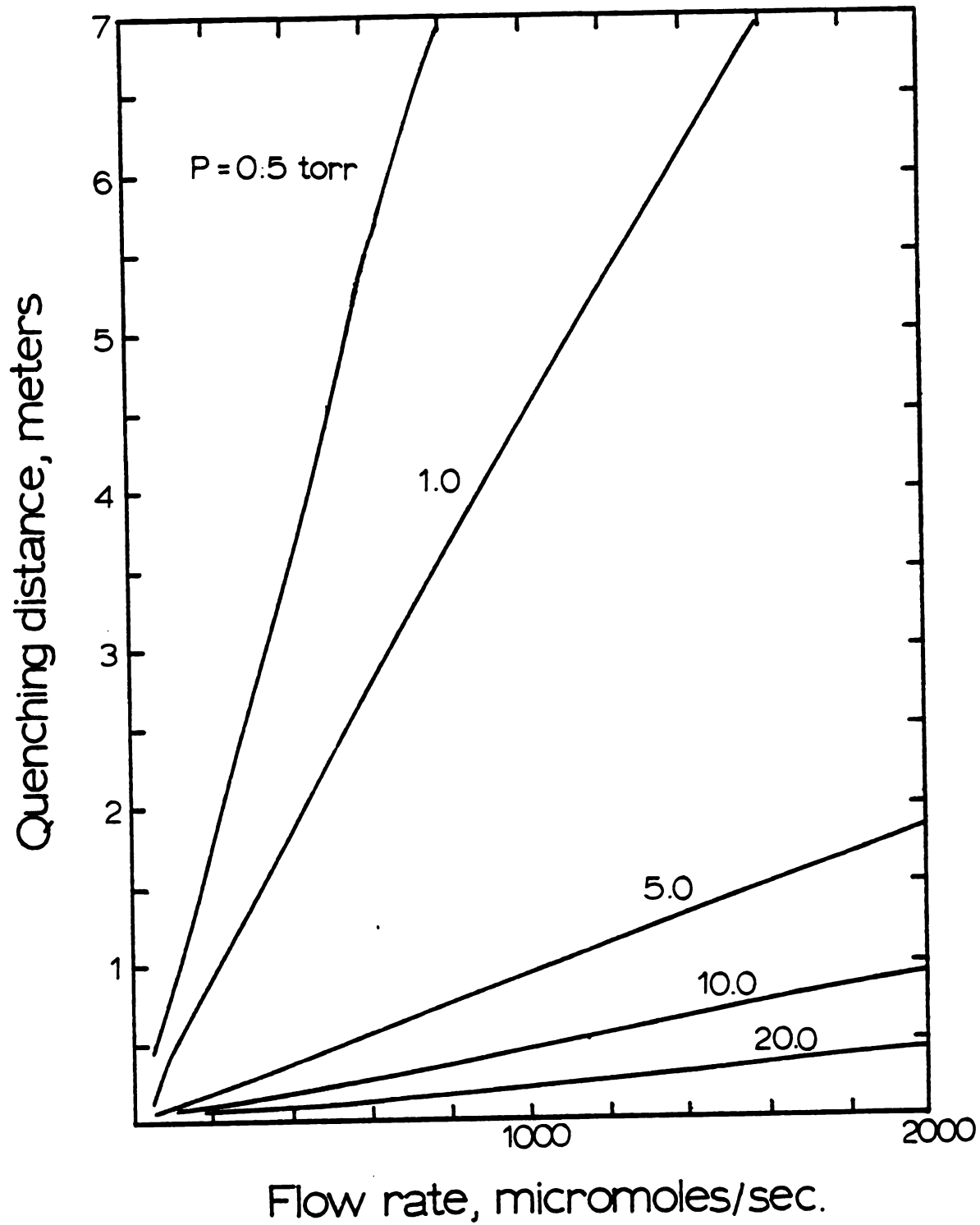


Figure 31.--Pressure dependence of the downstream quenching distance.

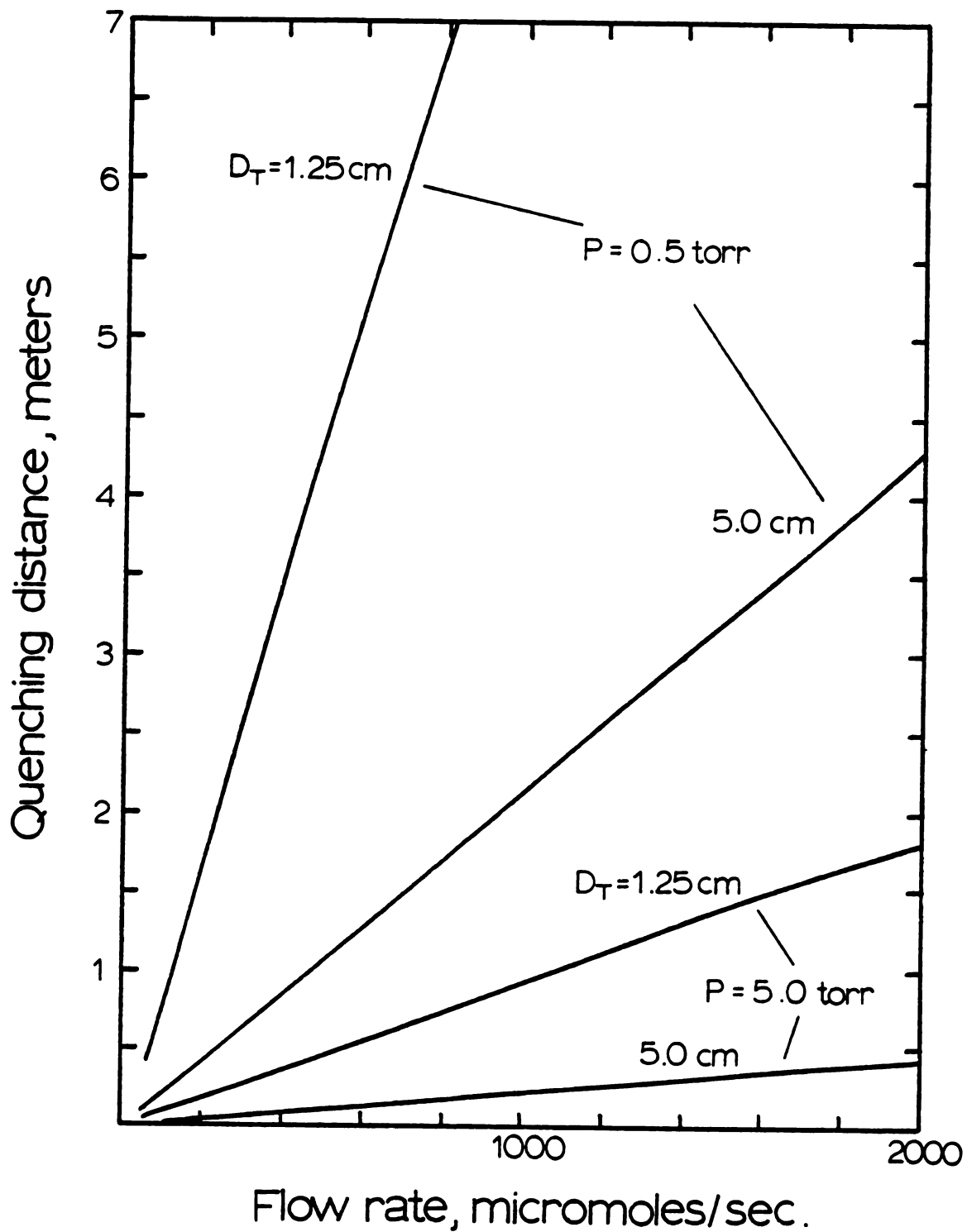


Figure 32.--Effects of varying tube diameter on quenching distance at pressures of 0.5 and 5.0 torr.

even prove useful to place a constriction in the tube between the discharge and experimental site, merely to maintain a high atom concentration.

The greatest change in the quenching distance is found when the wall recombination coefficient is varied. This is demonstrated in Figure 33, where the quenching distance is plotted versus flow rate for four values of the recombination coefficient between  $10^{-4}$  and  $10^{-1}$ . Although not included in the figure, calculations using  $\gamma = 10^{-6}$  resulted in quenching distances of between 100 ( $F_0 = 50 \mu\text{moles sec}^{-1}$ ) and 5000 meters ( $F_0 = 2000 \mu\text{moles sec}^{-1}$ ). These results show that the walls of the downstream region should always be coated with Dri-Film or its equivalent.

The results of the downstream region modeling provide information which will make it possible to design an apparatus in which hydrogen atom kinetics experiments, as well as the energy balance experiment, can be carried out. The conclusions can be summarized as follows:

- (1) Quenching distances using different threshold concentrations show that the decrease in atom concentration is fastest in the first few meters of the downstream region, with small concentrations persisting for much larger distances.
- (2) The effects of variations in gas temperature are virtually negligible.
- (3) Pressure affects the quenching distance in the expected way, with a large decrease in  $Q_D$  between 1.0 and 5.0 torr.
- (4) The quenching distance is appreciably longer for small tubes, probably due to an increase in velocity. This indicates that downstream tubing should be as small as possible.

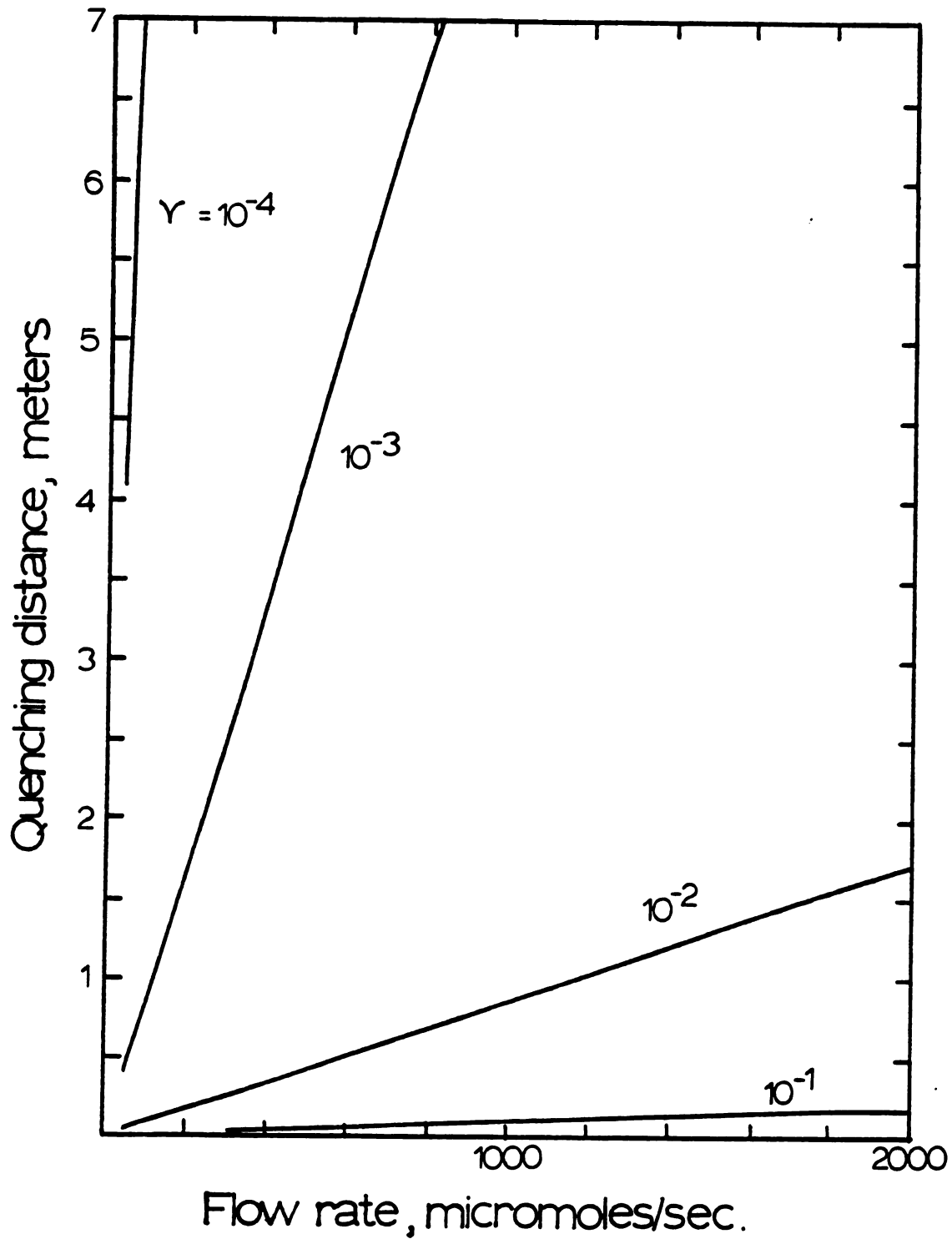


Figure 33.--Dependence of the quenching distance on the wall recombination coefficient,  $\gamma$ .

- (5) The large effect which the wall recombination coefficient has on the quenching distance shows that the use of a wall coating, such as Dri-Film, in the downstream region will greatly enhance the system's ability to transport hydrogen atoms over long distances.

## APPARATUS DESIGN

The objective of this research was to design an experimental apparatus in which the energy balance around a hydrogen atom generator could be measured. The design was based on an extensive review of the literature concerning atomic hydrogen, after which a microwave discharge atom generator and esr spectrometer/gas-phase titration detection systems were selected as the best methods for this type of research. Two models were then developed to provide more support for the proposed design. The CSTR discharge model was used to determine the experimental conditions conducive to large conversions, and to determine the sensitivity of the system to variations in the experimental conditions. A PFR model of the downstream region was used to make certain that measureable concentrations of hydrogen atoms could exist, under appropriate experimental conditions, for long distances downstream from the discharge outlet.

In the following section, incorporation of these results into the experimental apparatus will be discussed for two experiments, the energy balance experiment itself and an additional experiment for measuring wall recombination coefficients. A schematic diagram of the entire proposed apparatus is shown in Figure 34. This diagram includes components for both the energy balance and wall recombination experiments.



### Energy Balance Experiment

As well as being the primary experimental objective, the construction of an apparatus in which an accurate energy balance can be made is perhaps the most difficult. The development of a detailed energy balance on a discharge reactor system has not yet been attempted, and can be expected to present some special experimental problems. The energy balance around the discharge can be divided into three parts, two of which (referred to here as the energy inputs and outputs) can be well defined. The third part, which will be called "energy losses," can be expected to cause the major problem in the experiment.

The energy inputs to the plasma consist simply of the microwave power input to the plasma and the energy brought in with the inlet gas as sensible heat. The measurement of the microwave power input to the plasma (calculated as the difference between the incident and reflected power readings measured by thermocouple power meters located on the waveguide) is well established (67,68), and any losses which might occur in the connections to the microwave cavity can be accounted for in the thermal balance around the cavity. An assumption which has been made here is that there is a minimal amount of microwave radiation leakage from the waveguide system, which is equivalent to assuming that the difference in power readings is equal to the energy absorbed in the cavity.

Both the input and output of sensible heat in the gas stream can be measured using thermocouples of standard design. It will be neces-

sary to enclose the junctions, however, as any recombination of radicals on the bare metal surfaces of the thermocouple would result in an excessively high temperature reading in the outlet sensor. One suitable coating would be Teflon, which has been found to have wall recombination characteristics similar to an  $H_3BO_3$  coating on quartz (106). Finally, the coatings on both thermocouples should be uniform, in order to minimize the effects of heat transfer through the coating material. Differential operation of the thermocouples should also help to minimize this effect.

The final energy output to be considered is the chemical energy possessed by the hydrogen atoms exiting from the discharge. The analysis of this contribution to the energy balance is complicated by the difficulty of measuring the atomic concentrations directly at the outlet of the discharge. This restriction stems primarily from the physical size of the esr spectrometer, but an additional factor is the electrical noise produced by the discharge, which makes the operation of electrical devices in the near vicinity of the discharge impossible. Also, since the esr spectrometer uses microwave frequencies as an excitation source, there exists a possibility that the discharge would interfere with the instrument. In any event, the inclusion of a section of the downstream flow system in the thermal balance on the discharge would allow the use of atomic concentration measurements from the downstream region of the system.

It is the energy losses in the cavity region which will cause the most difficulty in the analysis of the energy balance. There are

three potential contributions to the thermal output of the discharge which must be considered separately: (1) transfer of heat produced in the discharge to the cavity and environment surrounding the discharge, (2) leakage of microwave radiation from the cavity and discharge tube, and (3) emission of light from the discharge. The strategy for taking all of this energy into account will be to convert each to thermal energy within an insulated "container" to be placed around the cavity and a portion of the flow system downstream from the discharge. When this is done properly, the discharge/cavity system will become a calorimeter, allowing accurate measurements to be made of the remaining energy loss.

The conversion of any microwave leakage to heat must be done by enclosing the cavity in a layer of metal screen. The screen must be in good electrical contact with the cavity, and will have to be heaviest in the section around the downstream end of the discharge tube, as this is the position which emits the greatest amount of microwave radiation when the discharge is operating. It is probable that the requirements for including this energy loss mechanism in the energy balance can most easily be met by including the screen as an inner layer on the insulation which will surround the cavity.

An energy loss mechanism which can be expected to be much more important than leakage of microwave radiation is emission of light by the discharge. This light can be very intense at high power levels, and is also a function of the pressure maintained within the discharge. The trapping of light within the calorimeter can be done in either of

two ways: reflectively or absorptively. The absorptive technique would put a light-absorbing coating (flat black paint, for example) on the inner surface of the container to force all of the light emitted by the discharge to be converted to heat on the surface of the insulation. The reflective technique places a reflective coating on the insulation surface in order to keep the insulation surface cool. In order for this technique to be effective, it is necessary to have some absorbing surface within the calorimeter. The cavity, since it absorbs some heat from the discharge already, would seem to be the most convenient surface to use. Although it isn't entirely clear which of the two techniques would actually be better, it does make sense to keep the cavity insulation as cool as possible to minimize heat transfer through it to the outside environment. This being the case, the recommended technique here is that the reflective coating, coupled with an absorptive coating on the cavity, be used to convert the discharge emission to heat.

One additional loss mechanism which must be included in the calorimeter is the emission of light down the axis of the flow tube. Even if the tube leaving the reactor is bent at a  $90^\circ$  angle (as is planned in the reactor design, due to space limitations), some light would be reflected at the corner, and would be lost down the tube. One technique which has been used previously to limit light loss from a discharge is the inclusion of a light trap at the point where the tube is angled. The purpose of the light traps in previous discharge experiments (19) has been to eliminate interference with

optical detection systems, but it should serve as well to confine discharge light to the volume enclosed by the calorimeter insulation. The type of trap which has been included in this design is a Wood's horn. This trap functions by reflecting any incident light from surface to surface farther down the "horn" of the trap until all of the incident light is transmitted through the glass in the walls of the tube.

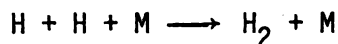
Once the energy losses have been converted to heat, it is necessary to measure that heat. That measurement will be made in the present apparatus in two ways. First of all, the temperature rise of the cooling water which is presently used to prevent the cavity from over-heating can be measured by the inclusion of a thermocouple in the lines. This measurement, and the inclusion of a flowmeter in the line, will allow the measurement of the heat which is carried from the calorimeter by the cooling water. Additional heat produced within the cavity can be accounted for by measuring the temperature rise in cooling air to be blown through the calorimeter. Additional thermocoupling in the calorimeter could be used to determine the amount of heat which is lost through thermal conduction through the insulation. The temperature measurements to be made are shown in Figure 34, which shows the entire proposed reactor system for the energy balance experiment, as well as additional facilities for the energy balance experiment to be discussed below. With the inclusion of the large number of thermocouples on which measurements must be made (in addition to such measurements as air, water, and hydrogen

flow rates, pressure, incident and reflected power, etc.), it seems likely that some sort of automatic data-logging technique would be very useful.

### Wall Recombination Experiment

As was indicated in the description of previous wall recombination coefficient measurements, there is still a great need for accurate measurements of this quantity for surfaces other than Pyrex. The discharge apparatus which will be used for energy balance experiments would also serve as a source of hydrogen atoms for a wall recombination experiment. As the requirements for additional equipment are small, this experiment is quite feasible.

Wall recombination reactions, especially on coated surfaces, can best be studied in reaction systems designed to minimize gas phase recombination. This conclusion stems from the necessity for using regression analysis of the concentration data to determine the wall recombination coefficients. The interdependency of regression coefficients demands that the number of adjustable constants be kept to a minimum. Since the kinetic rate constant for hydrogen atom recombination with  $M=H$  or  $H_2$  aren't especially well defined, these constants would have to be allowed to "float." This necessity could be eliminated, however, by using low pressures, and an inert gas diluent. The effect of the first would be to lower species concentrations in the gas phase. The effect of the second would be to effectively limit gas phase recombination reactions to



where M is the inert gas. Since the rate coefficients for inert gas stabilized recombination are much more readily available, this quantity could be fixed, leaving  $\gamma$  as the only adjustable parameter.

The concentration of hydrogen atoms should be measured at both ends of the test section. A suitable detection system at the upstream end would be a gas-phase titration system. Since one of these would have to be installed for the energy balance experiment in any event, this entails no major new equipment. The measurement of the downstream end of the discharge tube could either be made using another titration detector or with an esr spectrometer. The advantage of using the latter is that its high sensitivity would allow accurate measurements even if the recombination caused the atom concentration to drop sharply in the test section.

The section of tubing over which the measurements would be made has been termed the test section. It would be a removable, jacketed tube made of whatever material was desired to be studied. The removability would allow different tubes with different surfaces to be installed with a minimum of disruption to the rest of the system. The length of the tube itself could be varied to permit the best measurement. The jacket to be used should be capable of operating over a wide range of temperatures. A suitable heat exchange fluid could be circulated through the jacket to maintain the wall temperature at a constant value over the time of the experiment. The range of temperature needed to fully evaluate Gelb and Kim's model (35), for example, would be from 50 °K to 1000 °K.

As was shown in a previous section, the proper selection of experimental conditions can lessen the decay of atom concentration downstream from the reactor considerably. For example, Figure 33 indicates that, even at very low flow rates (<100 micromoles/sec), reducing the wall recombination coefficient below  $10^{-4}$  increases the quenching distance to values well in excess of 10 meters. This implies that the downstream position of the test section is not an important factor in the experimental design. Should the atom concentration not be satisfactory, the pressure or wall condition could be adjusted to remedy the situation.

The experimental apparatus as described above has been incorporated into the overall apparatus diagram in Figure 34.

### Conclusion

The design of a versatile hydrogen discharge apparatus has been presented, and two possible experiments have been described. Additional experiments which the system is capable of performing include rate studies of hydrogen atom-hydrocarbon reactions and discharges of gas mixtures. The apparatus serves as the nucleus of a system which could be capable of duplicating and extending any of the experiments on atomic hydrogen which have been performed in the last sixty years.

## RESULTS AND CONCLUSIONS

Although the primary purpose of this research was to develop the apparatus for an energy balance experiment around hydrogen atom generation, the research also fulfilled other purposes. The overall research will serve as part of the data base for research into plasmas and plasma chemistry now underway at Michigan State University. In particular, the review of hydrogen atom generation and detection techniques, since it is more complete than the summary included in the only review of hydrogen atom chemistry (95), will provide a useful background for research into the chemistry of hydrogen atoms.

The review of hydrogen atom generation methods established that, of the generation methods examined (shock tube, hot filament, direct photolysis, mercury photosensitization, electron pulse radiolysis, direct-current discharge, radiofrequency discharge, and microwave discharge), the microwave discharge is best able to dissociate a flowing stream of pure hydrogen at high pressures ( $>10$  torr) and with conversions greater than 10%. Although the other generation methods, notably mercury photosensitization and d.c. discharges, appear more frequently in the literature, these are more suitable for applications (such as kinetics experiments) where low pressures ( $<10$  torr) or low conversions ( $<10\%$ ) are acceptable. The conclusions of the generation technique review were:

1. All of the techniques except those involving thermal dissociation (shock tube or hot filament) are nonequilibrium in nature. For pressures above 0.5 torr, a gas temperature in excess of 2000 °K is required to achieve an equilibrium conversion greater than 10%.
2. The photolysis techniques produce low conversions (typically lower than 5%), and are generally used in static, rather than flowing, systems. Direct photolysis requires a light source, such as a helium flash lamp, capable of producing light with a wavelength less than 89 nm. Mercury photosensitization requires the presence of trace amounts of mercury vapor in the hydrogen, making it a difficult technique to use in a flowing system.
3. Thermal dissociation on a tungsten filament can produce the same amount of dissociation as is found in photolysis systems, but in a flowing system. The technique is equilibrium-limited to conversions below 10%.
4. Dissociation in a shock wave is used primarily for examining the high-temperature kinetics of free radicals and ions, including hydrogen atoms. The technique is also constrained in conversion by equilibrium, requires sophisticated data-collection systems, and cannot be used as a flowing system.
5. The d.c. discharge technique has been used to achieve conversions above 80% at pressures below 5.0 torr, but there is no evidence that the technique can produce measureable quantities of hydrogen atoms without the use of a water-containing (2-3%) hydrogen feed.
6. The a.c. discharge techniques (in particular, the microwave discharge) have been shown to produce conversions greater than 50% at a pressure of 1.0 torr in a flowing stream of pure hydrogen. Since these results were obtained at relatively low (~100 watts) power inputs, and since the conversion is expected to increase with power input, the use of high-power microwave discharges seem most suitable for the experiments which are presently planned.

The survey of hydrogen atom detection methods resulted in the selection of gas-phase titration and electron spin resonance spectroscopy as the techniques to be used in the proposed apparatus on the basis of their ease of calibration. The remaining methods (molecular

diffusion, catalytic probe, mass spectrometer, Lyman- $\alpha$  photometry) were eliminated from consideration because they weren't species-specific (catalytic probe, molecular diffusion), difficult to calibrate (Lyman- $\alpha$  photometry), or require difficult measurements (mass spectroscopy, molecular diffusion). The results of the detection systems review were:

1. The detection system capable of the greatest degree of accuracy for the measurement of hydrogen atom concentrations is the electron spin resonance spectrometer. Its ability to be calibrated using a molecular standard, rather than by comparison with another detection system, makes it unique among the free radical detection techniques.
2. Gas-phase titration is probably the easiest to use of the remaining detection techniques, since no calibration of the detection system is necessary. The difficulty involved with measuring the flowrates and pressures of the corrosive gases (NO, NO<sub>2</sub>, NOCl) used in the titration for hydrogen atoms introduces error into the measurement which isn't present when spectroscopic techniques are used.
3. The mass spectrometer is a useful tool for the analysis of complex reaction mixtures. However, the necessity of calibrating the detector with the free radical species and the proximity of the peaks of molecular and atomic hydrogen in the mass spectrum makes its use for the detection of atomic hydrogen quite difficult.
4. The Lyman- $\alpha$  technique is a simple, species-specific system which can be used to make fast measurements of hydrogen atom concentrations. The necessity for calibrating the detector with some other technique, however, results in a decrease in accuracy to the level which that technique is capable of.
5. As in the case with gas-phase titration, the detection methods using catalytic probes require no calibration. Well-designed systems, such as that used by Ham, Trainor, and Kaufman (38, 96), can be quite accurate and fairly easy to use. However, the use of catalytic probes for measuring hydrogen atom concentrations in complex systems results in significant errors, due to the presence of other recombining radicals which can add their energy to that produced by recombination of hydrogen atoms.

6. The Wrede-Harteck, or molecular diffusion, gauge is the least accurate of the methods reviewed in this report, primarily because of its dependence on a pressure measurement to determine the atom concentration. The technique is interesting primarily for its historic value as the first quantitative hydrogen atom detection technique.

After completion of the literature survey, the microwave discharge was modeled as a continuously-stirred tank reactor (CSTR) to provide general information about the discharge's behavior under various operating conditions. The simplicity with which the outlet conversion of a CSTR can be computed made it possible to examine the behavior of the discharge under a wide range of operating conditions. The conditions which were varied were the pressure, temperature, flow rate, electron density, tube diameter, recombination coefficient, and power input (using the discharge theory developed by Bell [12]). The results of the discharge modeling were:

1. The modeling of the hydrogen discharge showed that the most important parameters for maximizing the conversion of hydrogen molecules to atoms are the electron density, pressure, and flow rate.
  - a. Conversions higher than 50% can only be obtained readily when the pressure is less than 10 torr.
  - b. The effects of increasing the flow rate are most important at low pressures; at higher flow rates, the variation becomes less apparent.
  - c. The appearance of an electron density "threshold" in the conversion is an unforeseen result, and could explain why the conversion's calculated using Bell's discharge theory are much lower than would be expected, based on experience.
2. The wall recombination coefficient is not as important in the discharge as might be expected. Once its value falls below 0.001, subsequent changes in its value have

little effect on the conversion. At pressures above 10.0 torr, the increased importance of gas-phase recombination makes the outlet conversion virtually independent of the value of the wall recombination coefficient.

3. The effects of changes in the tube diameter on outlet conversion are dependent on the gas pressure. At pressures below 1.0 torr, where wall recombination predominates, the reactor with the smallest surface area (smallest diameter) produces the highest conversion. As the pressure increases, and gas-phase reactions become more important, the volume of the reactor available for the reactions producing the hydrogen atoms becomes the most important factor, and the larger tubes exhibit the highest conversion.
4. An increase in gas temperature in the discharge will result in an increase in conversion, with the increase being larger at low flow rates. This is a result of a decrease in the gas density and gas-phase recombination coefficients as the temperature decreases. A temperature increase from 300 °K to 1000 °K can result in a conversion increase from 20% to 200%, depending on the flow rate and pressure.

The final step in the research was to make certain, by modeling the region downstream from the discharge, that it was possible to transport hydrogen atoms to experimental sites separated by a few meters from the discharge. The downstream region was modeled as an isothermal plug-flow reactor (PFR), and the experimental conditions (temperature, pressure, tube diameter, and wall recombination coefficient) varied in order to determine the conditions which maximize the downstream "quenching distance" at which a threshold hydrogen atom concentration was reached. The results of this downstream modeling were:

1. The parameters having the strongest effect on the quenching distance are the gas pressure and the wall recombination coefficient:
  - a. When the wall recombination coefficient is lowered to values as low as  $10^{-6}$ , the quenching distance is essentially infinite. The quenching distance changes most rapidly with the flow rate when the wall recombination coefficient is in the range  $10^{-2}$  to  $10^{-4}$ .
  - b. When the gas pressure is decreased to 0.5 torr, the quenching distance becomes quite large (on the order of tens of meters). As the pressure decreases, the quenching distance decreases very rapidly. This effect isn't as severe as that found for the wall recombination coefficient, but it is still quite large.
2. The effects of changing the tube diameter can be explained by the increased velocity which the gas will have at a constant flow rate in tubes with differing cross-sectional areas. An decrease in tube diameter from 5.0 cm to 1.25 cm will increase the gas velocity by a factor of 16, which will, in turn, result in an increase in the quenching distance.
3. The effect increasing the gas temperature from 420 °K to 800 °K is only to increase the quenching distance by, at the lowest pressures, a maximum of 0.5 meters.

## RECOMMENDATIONS FOR RESEARCH

1. There is, at the present time, no literature in which the energy balance within an electrical discharge is examined. This balance could be used to create a highly efficient hydrogen atom generator for use in kinetics experiments or in practical applications. The lack of any data, outside of that obtained by Poole, eliminates the determination of which operating conditions allow the highest yields to be obtained. An experimental apparatus which can be used for such research has been presented.
2. The almost complete lack of any experimental data on the wall recombination coefficient for surfaces other than glass makes it impossible to determine the mechanism of the recombination reaction on other types of surfaces which are generally found in a discharge system, such as fused silica (quartz) or poisoned surfaces. An experiment to determine the value of the recombination coefficient on such surfaces would be extremely useful for developing the theory of surface recombination. In order to produce the most useful data, the apparatus should be capable of producing wall temperatures well below the boiling point of liquid nitrogen.
3. The kinetics of hydrogen atom recombination should be examined in order to determine improved values of the rate constant for the hydrogen-atom-stabilized gas-phase recombination reaction. Although the lack of agreement between the literature values indicates the difficulty of the experiment, more accurate values of the constant could be used to further develop theories of hydrogen atom recombination, and could also be used in subsequent attempts to model hydrogen discharges.
4. The demonstration in this report that the theory of r.f. discharges developed by Bell is inadequate for the purpose of modeling indicates a need for a more complete theory of such discharges. This theory should be primarily concerned with relating external variables, such as pressure and power input, with the parameters which determine the extent of dissociation in the discharge, especially the electron density. The modeling which has been done in this report clearly shows that an accurate knowledge of that parameter is perhaps the most important requirement for accurate modeling of the discharge.

**APPENDIX A:**

**THE COMPUTER PROGRAM USED TO  
MODEL THE DISCHARGE**

PROGRAM DISCH(INPUT,OUTPUT)

DISCH CALCULATES THE OUTLET CONVERSION FROM A MICROWAVE DISCHARGE FOR A NUMBER OF ELECTRON DENSITIES, PRESSURES, AND FLOW RATES. THE INPUT VARIABLE IS DT, THE TUBE REACTOR DIAMETER IN CENTIMETERS. THE MODEL EMPLOYED IS THAT OF A CSTR REACTOR.

NOMENCLATURE:

PRES(I) = PRESSURE DATA BASE  
 COEF(I) = RECOMBINATION COEFFICIENT DATA BASE  
 TEMP(I) = TEMPERATURE DATA BASE  
 FO(I) = FLOW RATE DATA BASE  
 XMAT(I,J) = OUTLET CONVERSION FOR PRES(I) AND FO(J)

T = CURRENT TEMPERATURE (FROM TEMP(I))  
 GAM = CURRENT RECOMBINATION COEFFICIENT (FROM COEF(I))  
 LD = DISCHARGE LENGTH, CM  
 VD = DISCHARGE VOLUME, CM\*\*3  
 LAM = REDUCED TUBE DIAMETER  
 K1 = RECOMBINATION RATE COEFFICIENT FOR M = H2  
 K2 = RECOMBINATION RATE COEFFICIENT FOR M = H  
 NE = ELECTRON DENSITY, CM\*\*-3  
 BETA = GAS DENSITY, MOLES/CM\*\*3  
 CBAR = AVERAGE MOLECULAR SPEED, CM/SEC  
 PO = PRESSURE CORRECTED TO T = 198 K  
 PLAM = PO X LAM; DISCHARGE PARAMETER  
 EEOP = EFFECTIVE FIELD STRENGTH/PRESSURE; DISCHARGE PARAMETER  
 KC = DISSOCIATION RATE CONSTANT, CM\*\*-3  
 A,B,C,D,E,C2,C3,CR = COEFFICIENTS

DIMENSION PRES(10),FO(10),XMAT(10,10)  
 DIMENSION COEF(3),TEMP(4)  
 REAL LAM,NE,LD,K1,K2,KD,GAM  
 DATA PRES /0.5,1.,2.,5.,10.,20.,50.,100.,500.,760./  
 DATA COEF /0.1,1.E-4,1.E-6/  
 DATA TEMP /300.,600.,800.,1000./  
 DATA FO /50.,75.,100.,200.,500.,1000.,1500.,2000.,  
 +5000.,10000./  
 DATA PI /3.141592654/, XMAT /100\*0.0/  
 READ 2,DT

ENTER TUBE DIAMETER

MAJOR LOOP CALCULATES FOR ALL TEMP AND COEF.

FORMAT (F10.0)  
 DC 9500 ITE = 1,4  
 DC 9500 ICO = 1,3  
 T = TEMP(ITE)  
 GAM = COEF(ICO)  
 CBAR = 14506.12 \* SQRT(T)

C  
C  
C  
CALCULATE CONSTANT AND TEMPERATURE-DEPENDENT PARAMETERS.

LD = 30.  
 VD = PI \* DT \* DT \* LD/4.  
 LAM = DT/4.81  
 K1 = 10.0 \*\* (15.243 - 1.95E-4 \* T)  
 K2 = 9.082E15 \* EXP(35.38/T)

C  
C  
C  
THIS LOOP VARIES THE ELECTRON DENSITY FROM 10\*\*10 TO  
 10\*\*20.

DC 9000 IK = 10,20,2  
 NE = 10.\*\*IK

C  
C  
C  
THIS LOOP VARIES THE PRESSURE THROUGH THE 10 VALUES  
 ALLOWED, AND THEN CALCULATES THE REMAINING  
 DISCHARGE PARAMETERS.

DC 9003 I = 1,10  
 BETA = PRES(I)/(62396.\*T)  
 P0 = 298.\*PRES(I)/T  
 PLAM = P0\*LAM  
 EEOP = 15.8304 \* PLAM\*\*(-0.3927)  
 KD = 2.7857E-15 \* EEOP\*\*4.0591

C  
C  
C  
NOW, THE FLOW RATE LOOP IS ENTERED. THE COEFFICIENTS  
 NECESSARY IN THE CALCULATION ARE CALCULATED.

DC 9001 K = 1,10  
 A = 2.\*F0(K)\*1.E-6  
 B = 2.\*VD\*KD\*NE\*BETA  
 C = 2.\*VD\*GAM\*CBAR\*BETA/DT  
 D = 8.\*K1\*VD\*BETA\*\*3  
 E = 16.\*K2\*VD\*BETA\*\*3  
 C2 = 3.\*A + B + C - D + E  
 C3 = 3.\*A + B + 2.\*C + D  
 C4 = A - B + C

```

C
C THIS IS THE BEGINNING OF THE NEWTON-RAPHSON SOLUTION
C TO THE FOURTH DEGREE POLYNOMIAL. THE INITIAL
C VALUE OF THE CONVERSION IS 0.5
C
      X = 0.5
8000  X0 = X
      X = X0 - (((A*X0+C2)*X0+C3)*X0+C4)*X0-B)/
      +(((4.*A*X0+3.*C2)*X0+2.*C3)*X0+C4)
      IF (ABS(X-X0)/X0 .GT. 1.E-5) GO TO 8000
9001  XMAT(I,K) = X
9003  CCNTINUE
      CALL PRINT (T,GAM,DT,XMAT,PRES,F0,NE)
C
C PRINT PRINTS OUT THE CONVERSION MATRIX
C
9000  CCNTINUE
9500  CONTINUE
      PRINT 3
3     FORMAT (*                      END DISCH*)
      END

      SUBROUTINE PRINT (T,GAM,DT,XMAT,PRES,F0,NE)
C
C SUBROUTINE PRINT PRINTS THE CONVERSIONS CALCULATED IN
C DISCH.
C
      DIMENSION XMAT(10,10),F0(10),PRES(10)
      REAL NE
      PRINT 1
1     FORMAT (* HYDROGEN REACTOR MODEL*)
      PRINT 2,DT,GAM,T
2     FORMAT (//* TUBE DIAMETER = *,20X,F5.2,*CM.*/
      +* WALL RECOMBINATION COEFFICIENT = *, E13.5,/
      +* DISCHARGE TEMPERATURE = *,12X,F5.1,* DEGREES K*/)
      PRINT 3,NE
3     FCRMAT (* ELECTRON DENSITY = *,E8.2,*CM-3*/)
      PRINT 4
4     FORMAT (* HYDROGEN CONVERSION VS. FLOW RATE*,
      +* AND PRESSURE*)
      PRINT 5
5     FORMAT (57X,*FLOW RATE, MICROMOLES/SEC*)
      PRINT 6,(F0(I),I=1,10)
6     FORMAT (* H2 PRESSURE*,/,6X,*TORR*,5X,10(4X,
      +F5.0,1X)/)
      DO 100 I = 1,10
100   PRINT 7,PRES(I),(XMAT(I,J),J=1,10)
7     FCRMAT (5X,F6.1,6X,10(2X,E10.4)/)
      RETURN

```

APPENDIX B:

THE COMPUTER PROGRAM USED TO  
MODEL THE DOWNSTREAM REGION

PROGRAM STREAM2(INPUT,OUTPUT)

STREAM2 IS A PROGRAM TO PERFORM AN EULER INTEGRATION OF THE MODELING EQUATION FOR THE REGION DOWNSTREAM FROM THE DISCHARGE.

NOMENCLATURE:

K1 = RECOMBINATION RATE COEFFICIENT FOR M = H2  
 K2 = RECOMBINATION RATE COEFFICIENT FOR M = H  
 XI = INITIAL CONVERSION  
 Y(I) = NUMBER DENSITY OF HYDROGEN ATOMS  
 QC(I) = QUENCHING DISTANCE  
 CBAR = AVERAGE MOLECULAR SPEED  
 FO(I) = FLOW RATE  
 BETA = GAS DENSITY  
 A,B,C,D = COEFFICIENTS IN RATE EQUATION  
 FX,FY = INTERCONVERSION FUNCTIONS BETWEEN MOLE FRACTION AND CONVERSION  
 DELZ = INTEGRATION STEP-SIZE

INITIALIZE...

DIMENSION QD(6),X(6),FO(6),Y(6)  
 REAL K1,K2  
 COMMON T,GAM,DT,PRES,DELZ  
 DATA AVN/6.023E23/,PI/3.141592654/,XI/0.5/  
 DATA FO/50.,100.,200.,500.,1000.,2000./  
 FY(X) = 2.\* X/(1.+X)  
 FX(Y) = Y/(2.-Y)

CALL INPUT SUBROUTINE TO INITIALIZE PARAMETERS

CALL INPUT(1)  
 CONTINUE

INITIALIZE TEMPERATURE-DEPENDENT PARAMETERS

K1 = 10.\*\* (15.243-1.95E-4\*T)  
 K2 = 9.082E15 \* EXP(35.38/T)  
 CBAR = 14506.12 \*SQRT(T)  
 BETA = PRES/62396./T

INITIALIZE COEFFICIENTS AND OTHER VARIABLES

A = PI \* DT \* DT \* DELZ \* 5.E5  
 B = 8. \* K1 \* BETA\*\*3  
 C = 16. \* K2 \* BETA\*\*3  
 D = 2.\*GAM\*CBAR\*BETA/DT  
 Z = 0.0  
 DO 2 J = 1,6  
 X(J) = XI  
 QC(J) = 0.0

BEGIN CALCULATION OF QD(I) --

COUNTS THE NUMBER OF QD'S SET -- IF IC = 6, THEN DENSITY IS LESS THAN 10\*\*8 FOR ALL FLOW RATES, AND CALCULATION ENDS. IF THE CALCULATED CONVERSION IS LESS THAN ZERO OR MORE THAN ONE, THEN INPUT IS ENTERED TO REDUCE STEP-SIZE, AND CALCULATION IS RESTARTED FROM THE BEGINNING.

```

7      IC = 0
      DC 3 I = 1,6
      IF (QD(I) .NE. 0.0) GO TO 5
      RHS = (A/F0(I))*(B*X(I)*X(I)*(1.-X(I))/(1.+X(I))**3
+      + C*(X(I)/(1.+X(I))**3 + D*X(I)/(1.+X(I)))
      X(I) = X(I) - RHS
      IF (X(I) .GT. 1. .OR. X(I) .LT. 0.) GO TO 500
      Y(I) = FY(X(I)) * BETA * AVN
      IF (Y(I) .GE. 1.E8) GO TO 4
      QD(I) = Z
5      IC = IC + 1
4      CCNTINUE
3      CONTINUE
      IF (IC .EQ. 6) GO TO 6
      Z = Z + DELZ
      GO TO 7
6      CONTINUE
C
C      PRINT RESULTS...
C
      PRINT 10
10     FORMAT (//4X,*FLOW RATE*,13X,*QUENCHING DISTANCE*,/
+* (MICROMOLES/SEC)*,12X,*CENTIMETERS*//)
      DC 8 I = 1,6
8      PRINT 11,F0(I),QD(I)
11     FORMAT (4X,F8.1,11X,F13.3)
C
C      RE-ENTER MODELING PARAMETERS
      PRINT 20
20     FORMAT (* ENTER OPTION NUMBER (1 TO 6, 0 TO QUIT) >*)
      READ *,J
      IF (J .EQ. 0) GO TO 999
      CALL INPUT(J)
      GO TO 1
C
C      ROUTINE TO ENTER NEW DELZ IF TOO LARGE
C
500    CCNTINUE
      PRINT 30
30     FORMAT (//* DELZ IS TOO LARGE -- PLEASE REENTER *)
      CALL INPUT(6)
      GO TO 1
999    CCNTINUE
      END

```

```

      SUBROUTINE INPUT(J)
C
C  SUBROUTINE INPUT IS USED AS THE INTERACTIVE
C  INTERFACE BETWEEN STREAM2 AND THE USER.
C
      COMMON T,GAM,DT,PRES,DELZ
      GO TO (1,2,3,4,5,6) J
1     PRINT 100
100   FCRMAT (* 1.  START*)
2     PRINT 200
200   FORMAT (* 2.  ENTER NEW TEMPERATURE> *)
      READ *,T
      IF (J .NE. 1) GO TO 700
3     PRINT 300
300   FORMAT (* 3.  ENTER NEW COEFFICIENT> *)
      READ 301,GAM
301   FORMAT (E20.0)
      IF (J .NE. 1) GO TO 700
4     PRINT 400
400   FCRMAT (* 4.  ENTER NEW TUBE DIAMETER> *)
      READ *,DT
      IF (J .NE. 1) GO TO 700
5     PRINT 500
500   FORMAT (* 5.  ENTER NEW PRESSURE> *)
      READ *,PRES
      IF (J .NE. 1) GO TO 700
6     PRINT 600
600   FORMAT (* 6.  ENTER NEW DELTA-Z> *)
      READ *,DELZ
700   PRINT 800,T,GAM,DT,PRES,DELZ
800   FORMAT (//,* FOR THIS RUN:*/
+4X,*TEMPERATURE = *,18X,F6.1,* DEGREES KELVIN*/
+4X,*RECOMBINATION COEFFICIENT = *, E9.3,/
+4X,*TUBE DIAMETER = *,16X,F5.2,* CM.*/
+4X,*PRESSURE = *,21X,F5.1,* TORR*/
+4X,*DELTAZ = *,22X,F7.5,* CM */)
      RETURN

```

## REFERENCES

## REFERENCES

1. Ahumada, J. J., and Michael, J. V. "Chemical kinetic effects of walls on active species. Results for hydrogen atoms." *J. Phys. Chem.* 78, 465 (1974).
2. Amdur, I., and Robinson, A. L. "The recombination of hydrogen atoms. I." *J. Amer. Chem. Soc.* 55, 1395 (1933).
3. Amdur, I., and Robinson, A. L. "The temperature coefficient of the recombination of hydrogen atoms." *J. Amer. Chem. Soc.* 55, 2615 (1933).
4. Amdur, I. "Viscosity and diffusion coefficients of atomic hydrogen and atomic deuterium." *J. Chem. Phys.* 4, 339 (1936).
5. Amdur, I. "Recombination of hydrogen atoms. III." *J. Amer. Chem. Soc.* 60, 2347 (1938).
6. Anderson, F. O., and Herr, H. N. "The formation of active hydrogen in the creepage corona discharge." *J. Amer. Chem. Soc.* 47, 2429 (1925).
7. Bach, A. "Active hydrogen." *Ber.* 58B, 1388 (1925); *Chem. Abstr.* 19, 2889 (1925).
8. Barker, J. R., and Michael, J. V., "Experimental estimate of the oscillator strength of the  $2P_{3/2} \rightarrow 2S_1$  transition of the hydrogen atom." *J. Opt. Soc. Am.* 58, 1615 (1968).
9. Barker, J. R., and Michael, J. V. "Reaction of hydrogen atoms with ethylene." *J. Chem. Phys.* 51, 850 (1969).
10. Barker, J. R.; Keil, D. G.; Michael, J. V.; and Osborne, D. T. "Reaction  $H + C_2H_4$ : Comparison of three experimental techniques." *J. Chem. Phys.* 52, 2079 (1970).
11. Bates, S. R., and Taylor, H. S. "Studies in photosensitization. I." *J. Amer. Chem. Soc.* 49, 2438 (1927).
12. Bell, A. T. "A model for the dissociation of hydrogen in an electric discharge." *Ind. Eng. Chem. Fundam.* 11, 209 (1972).

13. Bennett, J. E., and Blackmore, D. R. "The measurement of the rate of recombination of hydrogen atoms at room temperature by means of esr spectroscopy." Proc. Roy. Soc. (Lond.) A305, 553 (1968).
14. Bishop, W. P., and Dorfman, L. M. "Pulse radiolysis studies. XVI. Kinetics of the reaction of gaseous hydrogen atoms with molecular oxygen by fast Lyman- $\alpha$  absorption spectrophotometry." J. Chem. Phys. 52, 3210 (1970).
15. Brackman, R. T.; Fite, W. L.; and Hagen, K. E. "Iodine-vapor-filled ultraviolet photon counter." Rev. Sci. Instr. 29, 125 (1958).
16. Braun, W., and Lenzi, M. "Resonance fluorescence method for kinetics of atomic reactions. Reactions of atomic hydrogen with olefins." Discuss. Faraday Soc. 44, 252 (1967).
17. Brown, J. M.; Coates, P. B.; and Thrush, P. A. "The rate of the reaction between hydrogen atoms and ethylene." Chem. Comm. 1966, p. 843.
18. Brown, J. M., and Thrush, B. A. "E.S.R. studies of the reactions of atomic oxygen and hydrogen with simple hydrocarbons." Trans. Faraday Soc. 63, 630 (1967).
19. Chang, J. S., and Barker, J. R. "Reaction rate and products for the reaction  $O(^3P) + H_2CO$ ." J. Phys. Chem. 83, 3059 (1979).
20. Cheng, D. Y., and Blackshear, P. L. "Measurement of the viscosity of atomic hydrogen." J. Chem. Phys. 56, 213 (1972).
21. Clyne, M. A. A., and Thrush, B. A. "Reactions of hydrogen atoms with nitric oxide." Trans. Faraday Soc. 57, 1305 (1961).
22. Clyne, M. A. A., and Thrush, B. A. "Reaction of nitrogen dioxide with hydrogen atoms." Trans. Faraday Soc. 57, 2176 (1961).
23. Clyne, M. A. A., and Thrush, B. A. "Rates of elementary processes in the chain reaction between hydrogen and oxygen. II. Kinetics of the reaction of hydrogen atoms with molecular oxygen." Proc. Roy. Soc. (Lond.) A275, 559 (1963).
24. Clyne, M. A. A., and Stedman, D. H. "Reactions of atomic hydrogen with HCl and NOCl." Trans. Faraday Soc. 62, 2164 (1966).
25. Compton, K. T., and Duffendack, O. S. "Dissociation of hydrogen and nitrogen by mercury atoms excited in an arc." Phys. Rev. 23, 109 (1924).

26. Compton, K. T.; Turner, L. A.; and McCurdy, W. H. "Theory and experiments relating to the striated glow discharge in mercury vapor." *Phys. Rev.* 24, 597 (1924).
27. Cowfer, J. A.; Keil, D. G.; Michael, J. V.; and Yeh, C. "Absolute rate constants for the reactions of hydrogen atoms with olefins." *J. Phys. Chem.* 75, 1584 (1971).
28. Cyetanović, R. J., and Doyle, L. C. "Relative rates of reaction of hydrogen atoms with olefins." *J. Chem. Phys.* 50, 4705 (1969).
29. Dickinson, R. G. "The combination of hydrogen and oxygen in the presence of activated mercury." *Proc. Nat. Acad. Sci.* 10, 409 (1924).
30. Dingle, J. R., and Le Roy, D. J. "Kinetics of the reaction of H with  $C_2H_2$ ." *J. Chem. Phys.* 18, 1632 (1950).
31. Duffendack, O. S., and Compton, K. T. "Dissociation of hydrogen and nitrogen by excited mercury atoms." *Phys. Rev.* 23, 583 (1924).
32. Eyre, J. A.; Hikida, T.; and Dorfman, L. M. "High-pressure limiting rate constant for H-atom addition to ethylene." *J. Chem. Phys.* 53, 1281 (1970).
33. Fehsenfeld, F. C.; Evenson, K. M.; and Broida, H. P. "Microwave discharge cavities operating at 2450 MHz." *Rev. Sci. Instr.* 36, 294 (1965).
34. Gardiner, W. C., Jr. Reactions Under Plasma Conditions, Vol. II, H. Venugopalan, ed. Wiley-Interscience, New York, 1971.
35. Gelb, A., and Kim, S. K. "Theory of atomic recombination on surfaces." *J. Chem. Phys.* 55, 4935 (1971).
36. Griem, H. R. Spectral Line Broadening by Plasmas. Academic Press, New York, 1974.
37. Halstead, M. P.; Leathard, D. A.; Marshall, R. M.; and Purnell, J. H. "The reaction of hydrogen atoms with ethylene." *Proc. Roy. Soc. (Lond.)* A316, 575 (1970).
38. Ham, D. O.; Trainor, D. W.; and Kaufman, F. "Gas phase kinetics of  $H + H + H_2 \rightarrow 2H_2$ ." *J. Chem. Phys.* 53, 4395 (1970).
39. Harteck, P. "The viscosity of atomic hydrogen." *Z. physik. Chem., Abt. A*, 139, 98 (1928); *Chem. Abstr.* 23, 2613 (1929).

40. Herzberg, G. Spectra of Diatomic Molecules. Van Nostrand, Princeton, 1950.
41. Hulburt, E. O. "Phenomena in gases excited by radio-frequency currents." *Phys. Rev.* 20, 127 (1922).
42. Hurle, I. R.; Jones, A.; and Rosenfeld, J. L. J. "Shock-wave observation of rate constants for atomic hydrogen recombination from 2500 to 7000 °K: Collisional stabilization by exchange of hydrogen atoms." *Proc. Roy Soc. (Lond.)* A310, 253 (1969).
43. Jennings, K. R., and Cvetanović, R. J. "Relative rates of addition of hydrogen atoms to olefins." *J. Chem. Phys.* 35, 1233 (1961).
44. Kaufman, F., and Del Greco, F. P. "Formation, lifetime, and decay of OH radicals in discharge-flow systems." *J. Chem. Phys.* 35, 1895 (1961).
45. Keck, J. C. "Statistical theory of chemical reaction rates." *J. Chem. Phys.* 29, 440 (1958).
46. Kirkby, P. J. "Chemical effects of the electric discharge in rarified hydrogen and oxygen." *Phil. Mag.* 13, 289-312 (1906).
47. Koda, S.; Nakamura, K.; Hoshino, T.; and Hikita, T. "Reaction of hydrogen atoms with acrylaldehyde." *Bull. Chem. Soc. Jpn.* 51, 957 (1978).
48. Kretschmer, C. B., and Peterson, H. L. "Kinetics of three-body recombinations." *J. Chem. Phys.* 39, 1772 (1963).
49. Langmuir, I. "The dissociation of hydrogen into atoms." *J. Amer. Chem. Soc.* 34, 860 (1912).
50. Langmuir, I. "A chemically active modification of hydrogen." *J. Amer. Chem. Soc.* 34, 1310 (1912).
51. Langmuir, I., and Mackay, G. M. J. "Dissociation of hydrogen into atoms. I." *J. Amer. Chem. Soc.* 36, 1708 (1914).
52. Langmuir, I. "Dissociation of hydrogen into atoms. II." *J. Amer. Chem. Soc.* 37, 417 (1915).
53. Larkin, F. S., and Thrush, B. A. "Recombination of hydrogen atoms in the presence of atmospheric gases." *Discuss. Faraday Soc.* 39, 112 (1964).

54. Larkin, F. L. "Homogeneous rate of recombination of hydrogen atoms." *Can. J. Chem.* 46, 1005 (1968).
55. Lee, P. "Photodissociation and photoionization of oxygen ( $O_2$ ) as inferred from measured absorption coefficients." *J. Opt. Soc. Am.* 45, 703 (1955).
56. Lewis, B., and von Elbe, G. "Heat capacities and dissociation equilibria of gases." *J. Amer. Chem. Soc.* 57, 612 (1935).
57. Linnett, J. W., and Marsden, D. G. H. "The kinetics of the recombination of oxygen atoms at a glass surface." *Proc. Roy Soc. (Lond.)* A234, 489 (1956).
58. Mallard, W. G., and Owen, J. H. "Rate constant for  $H + H + Ar \rightleftharpoons H_2 + Ar$  from 1300 to 1700 K." *Int. J. Chem. Kinet.* 6, 753 (1974).
59. Mandl, A., and Salop, A. "Magnetic resonance spectrometer measurements of atomic hydrogen surface recombination." *J. Appl. Phys.* 44, 4776 (1973).
60. Marshall, A. L. "Mechanism of the photochemical reaction between hydrogen and chlorine." *J. Phys. Chem.* 29, 842 (1925).
61. Marshall, A. L. "Photosensitization by optically excited mercury atoms: The hydrogen oxygen reaction." *J. Phys. Chem.* 30, 34 (1926).
62. Marton, L. Methods of Experimental Physics, Vol. 13, Spectroscopy (D. Williams, ed.). Academic Press, New York, 1976.
63. McCarthy, R. C. "Chemical synthesis from free radicals produced in microwave fields." *J. Chem. Phys.* 22, 1360 (1954).
64. McQuarrie, D. A. *Statistical Mechanics*. Harper and Row, New York, 1976.
65. Mearns, A. M., and Ekinci, E. "Hydrogen dissociation in a microwave discharge." *J. Microwave Power* 12, 156 (1977).
66. Mentall, J. E., and Gentieu, E. P. "Lyman- $\alpha$  fluorescence from the photodissociation of  $H_2$ ." *J. Chem. Phys.* 52, 5641 (1970).
67. Mertz, S. F.; Asmussen, J.; and Hawley, M. C. "An experimental study of CO and  $H_2$  in a continuous flow microwave discharge reactor." *I.E.E.E. Trans. Plasma Science* PS-2(4), 297 (1974).
68. Mertz, S. F.; Hawley, M. C.; and Asmussen, J. "A kinetic model for the reactions of CO and  $H_2$  to  $CH_4$  and  $C_2H_2$  in a flow." *I.E.E.E. Trans. Plasma Science* PS-4(1), 11 (1976).

69. Michael, J. V., and Weston, R. E. "Determination of hydrogen atom concentrations by Lyman- $\alpha$  photometry. I. Oscillation strength of the hydrogen atom  $2P_{3/2} + 2S_{1/2}$  transition. II. Kinetics of the reaction of hydrogen atoms with acetylene and ethylene." *J. Chem. Phys.* 45, 3632 (1966).
70. Michael, J. V., and Osborne, D. T. "Time-resolved Lyman- $\alpha$  photometry in a chemical kinetic investigation of H + C<sub>2</sub>H<sub>4</sub>." *Chem. Phys. Lett.* 3, 402 (1969).
71. Mitchell, A. C. G. "Activation of hydrogen by excited mercury atoms." *Proc. Nat. Acad. Sci.* 11, 458 (1925).
72. Myerson, A. L.; Thompson, H. M.; and Joseph, P. J. "Resonance absorption spectrophotometry of the hydrogen atom behind shock waves." *J. Chem. Phys.* 42, 3331 (1965).
73. Myerson, A. L., and Watt, W. S. "Atom formation rates behind shock waves in hydrogen and the effect of added oxygen." *J. Chem. Phys.* 49, 425 (1968).
74. Noyes, W. A. "Photochemical studies. III. The reaction between nitrogen and hydrogen in the presence of mercury vapor, and the resonance radiation of mercury." *J. Amer. Chem. Soc.* 47, 1003 (1925).
75. Perry, R. H., and Chilton, C. H., eds. Chemical Engineers' Handbook, 5th ed. McGraw-Hill, New York, 1973.
76. Poole, H. G. "Atomic hydrogen. I. Calorimetry of hydrogen atoms." *Proc. Roy Soc. (Lond.)* A163, 404 (1937).
77. Poole, H. G. "Atomic hydrogen. II. Surface effects in the discharge tube." *Proc. Roy Soc. (Lond.)* A163, 415 (1937).
78. Poole, H. G. "Atomic hydrogen. III. The energy efficiency of atom production in a glow discharge." *Proc. Roy Soc. (Lond.)* A163, 424 (1937).
79. Rony, P. R., and Hanson, D. N. "Effect of oxygen, nitrogen, and water in low pressure hydrogen discharges." *J. Chem. Phys.* 44, 2536 (1966).
80. Rose, D. J., and Brown, Sanborn C. "High frequency gas discharge plasma in hydrogen." *Phys. Rev.* 98, 310 (1955).
81. Rosser, W. A., and Wise, H. "The rate of reaction of hydrogen with nitrogen dioxide." *J. Phys. Chem.* 65, 532 (1961).

82. Salop, A., and Mandl, A. "A magnetic resonance spectrometer for studying the recombination decay of atomic hydrogen concentrations using a sampling technique." *J. Phys. E.* 4, 645 (1971).
83. Sauer, M. C., and Ward, B. "The reactions of hydrogen atoms with benzene and toluene studied by pulsed radiolysis: Reaction rate constants and transient spectra in the gas phase and aqueous solution." *J. Phys. Chem.* 71, 3971 (1967).
84. Shaw, T. M. "Dissociation of hydrogen in a microwave discharge." *J. Chem. Phys.* 30, 1366 (1959).
85. Shui, V. H.; Appleton, J. P.; and Keck, J. C. "Three-body recombination and dissociation of nitrogen: A comparison between theory and experiment." *J. Chem. Phys.* 53, 2547 (1970).
86. Shui, V. H. "Thermal dissociation and recombination of hydrogen according to the reactions  $H_2 + H \rightleftharpoons H + H + H$ ." *J. Chem. Phys.* 58, 4868 (1973).
87. Smallwood, H. M. "The rate of recombination of atomic hydrogen." *J. Amer. Chem. Soc.* 51, 1985 (1929).
88. Smallwood, H. M. "The rate of recombination of atomic hydrogen. II." *J. Amer. Chem. Soc.* 56, 1542 (1934).
89. Smith, W. V. "The surface recombination of H atoms and OH radicals." *J. Chem. Phys.* 11, 110 (1943).
90. Steiner, W. "The recombination of hydrogen atoms." *Trans. Faraday Soc.* 31, 623 (1935).
91. Strausz, O. P., and Gunning, H. E. "Reactions of hydrogen atoms with nitric oxide." *Trans. Faraday Soc.* 60, 347 (1964).
92. Tanaka, I., and McNesby, J. R. "Photosensitized reaction between hydrogen ( $^2P$ ) atoms and molecular nitrogen." *J. Chem. Phys.* 36, 3170 (1962).
93. Taylor, H. S., and Marshall, A. L. "The reactions of hydrogen activated by excited mercury atoms." *J. Phys. Chem.* 29, 1140 (1925).
94. Taylor, H. S.; Marshall, A. L.; and Bates, J. R. "Chemical effects produced by resonance radiation." *Nature* 117, 267 (1926).
95. Thrush, B. A. "Reactions of hydrogen atoms in the gas phase." *Progr. Reaction Kin.* 3, 63 (1965).

96. Trainor, D. W.; Ham, D. O.; and Kaufman, F. "Gas phase recombination of hydrogen and deuterium atoms." *J. Chem. Phys.* 58, 4599 (1973).
97. Varnerin, L. J., Jr., and Brown, S. C. "Microwave determinations of average electron energies and the first Townsend coefficient in hydrogen." *Phys. Rev.* 79, 946 (1950).
98. Venkatarmiah, Y. "The activation of hydrogen by the silent electric discharge." *Chem. News* 124, 323 (1922).
99. Venkatarmiah, Y. "The preparation of active hydrogen." *J. Amer. Chem. Soc.* 45, 261 (1923).
100. Venkatarmiah, Y., and Raghara, S. V. Bh. "Active hydrogen by electrolysis." *Nature* 112, 57 (1923).
101. Wendt, G. L. "Active hydrogen and nitrogen." *Nature* 109, 749 (1922).
102. Westenberg, A. A., and de Haas, N. "Quantitative measurements of gas phase O and N atom concentration by ESR." *J. Chem. Phys.* 40, 3087 (1964).
103. Westenberg, A. A. "Intensity relations for determining gas-phase OH, Cl, Br, I, and free-electron concentrations by quantitative ESR." *J. Chem. Phys.* 43, 1544 (1965).
104. Westenberg, A. A., and de Haas, N. "Quantitative ESR measurements of gas-phase H and OH concentrations in the H-NO<sub>2</sub> reaction." *J. Chem. Phys.* 43, 1550 (1965).
105. Westenberg, A. A., and de Haas, N. "Atom-molecule kinetics at high temperature using ESR detection. Technique and results for O + H<sub>2</sub>, O + CH<sub>4</sub>, and O + C<sub>2</sub>H<sub>6</sub>." *J. Chem. Phys.* 46, 490 (1967).
106. Westenberg, A. A., and de Haas, N. "Atom-molecule kinetics using ESR detection. II. Results for D + H<sub>2</sub> → HD + H and H + D<sub>2</sub> → HD + D." *J. Chem. Phys.* 47, 1393 (1967).
107. Westenberg, A. A., and de Haas, N. "Atom-molecule kinetics using ESR detection. III. Results for O + D<sub>2</sub> → OD + D and theoretical comparison with O + H<sub>2</sub> → OH + H." *J. Chem. Phys.* 47, 4241 (1967).
108. Westenberg, A. A., and de Haas, N. "Atom-molecule kinetics using ESR detection. IV. Results for Cl + H<sub>2</sub> ⇌ HCl + H in both directions." *J. Chem. Phys.* 48, 4405 (1968).

109. Westenberg, A. A., and de Haas, N. "Atom-molecule kinetics using ESR detection. V. Results for  $O + OCS$ ,  $O + CS_2$ ,  $O + NO_2$ , and  $H + C_2H_4$ ." *J. Chem. Phys.* 50, 707 (1969).
110. Whitlock, P. A.; Muckerman, J. T.; and Roberts, R. E. "Classical mechanics of recombination via the resonance complex mechanism:  $H + H + M \rightarrow H_2 + M$  for  $M = H, H_2, He, \text{ and } Ar$ ." *J. Chem. Phys.* 60, 3658 (1974).
111. Wittke, J. P., and Dicke, R. H. "Redetermination of the hyperfine splitting in the ground state of atomic hydrogen." *Phys. Rev.* 103, 620 (1956).
112. Wood, B. J., and Wise, H. "Kinetics of hydrogen atom recombination on surfaces." *J. Phys. Chem.* 65, 1976 (1961).
113. Wood, B. J., and Wise, H. "The kinetics of hydrogen atom recombination on pyrex glass and fused quartz." *J. Phys. Chem.* 66, 1049 (1962).
114. Wood, R. W. "Hydrogen spectra from long vacuum tubes." *Phil. Mag.* 42, 729 (1921).
115. Wood, R. W. "Atomic hydrogen and the Balmer series spectra." *Phil. Mag.* 44, 538 (1922).
116. Wood, R. W. "Spontaneous incandescence of substances in atomic hydrogen gas." *Proc. Roy Soc. (Lond.)* A102, 1 (1922).
117. Woolley, G. R., and Cvetanović, R. J. "Production of hydrogen atoms by photolysis of  $H_2S$  and the rates of their addition to olefins." *J. Chem. Phys.* 50, 4697 (1969).
118. Wrede, E. "Monatomic hydrogen, oxygen, and nitrogen." *Z. Physik* 54, 53 (1929); *Chem. Abstr.* 23, 2886 (1929).
119. Zemansky, M. W. "The quenching of mercury resonance radiation by foreign gases." *Phys. Rev.* 31, 812 (1928).

MICHIGAN STATE UNIV. LIBRARIES



31293010684219